U.S. Department of Commerce
National Bureau of Standards

NBS MEASUREMENT SERVICES

Special Publication 250–32

A Calibration Service for 30 MHz Attenuation and Phase Shift

Robert T. Adair and David H. Russell

INTRODUCING THE CENTER FOR ELECTRONICS AND ELECTRICAL ENGINEERING

The Center for Electronics and Electrical Engineering (CEEE) is the component of the National Bureau of Standards charged with providing Bureau activities and services supporting electrotechnology. In response to identified and anticipated needs, Center programs provide national reference standards, measurement methods, supporting theory and data, and traceability to national standards. Beneficiaries are U.S. industry, other Government organizations, the academic community, and society at large. In fiscal year 1987, the Center calibrated nearly a thousand transfer standards for some 200 customers.

The Center is organized into four technical divisions, with the Electrosystems and Semiconductor Electronics Divisions at Gaithersburg, Maryland and the Electromagnetic Fields and Electromagnetic Technology Divisions at Boulder, Colorado. The Center provides **measurement research and services** for:

- Conducted electrical signals and energy in the Electrosystems Division:
  - dielectrics for advanced power systems
  - conducted electromagnetic interference
  - waveform synthesis
  - signal acquisition and processing
  - automatic test equipment
  - calibration/testing strategies

- Radiofrequency signals and interference in the Electromagnetic Fields Division:
  - radiofrequency to millimeter-wave electromagnetic fields and signals
  - general microwave and millimeter-wave instruments, components
  - microwave and millimeter-wave noise
  - microwave and millimeter-wave antenna systems
  - radiated electromagnetic interference; electromagnetic compatibility
  - monolithic microwave/millimeter-wave integrated circuits
  - materials properties measurements at high frequencies

- Lightwaves, cryogenics, and magnetics in the Electromagnetic Technology Division:
  - optical fibers; integrated electro-optics
  - superconducting materials
  - superconducting electronics
  - magnetic materials

- Semiconductor electronics, in the Semiconductor Electronics Division:
  - semiconductor materials, such as silicon and gallium arsenide
  - semiconductor materials modification
  - semiconductor devices
  - integrated-circuit test structures for rapid process assessment

For information, contact the Center at 1-301-975-2220 or write to: The Center for Electronics and Electrical Engineering, Metrology Building Room B-358, National Bureau of Standards, Gaithersburg, MD 20899.

NBS MEASUREMENT SERVICES:
A Calibration Service for 30 MHz Attenuation and Phase Shift

Robert T. Adair and David H. Russell

Electromagnetic Fields Division
Center for Electronics and Electrical Engineering
National Engineering Laboratory
National Bureau of Standards
Boulder, CO 80303

April 1988

U.S. DEPARTMENT OF COMMERCE, C. William Verity, Secretary
NATIONAL BUREAU OF STANDARDS, Ernest Ambler, Director

Library of Congress Catalog Card Number: 88-600527

National Bureau of Standards Special Publication 250-32
Natl. Bur. Stand. (U.S.), Spec. Publ. 250-32, 184 pages (Apr. 1988)
CODEN: XNBSAV

U.S. GOVERNMENT PRINTING OFFICE
WASHINGTON: 1988

For sale by the Superintendent of Documents, U.S. Government Printing Office, Washington, DC 20402-9325

PREFACE

Calibrations and related measurement services of the National Bureau of Standards (NBS) provide the means for industry, government agencies, academia, and others to relate the measurements they make to national standards and, by extension, to the measurement systems of other countries throughout the world. It is of crucial importance to improving U.S. productivity, efficiency, and quality -- in short our competitive stance -- that measurements of appropriate accuracy can be made at all stages of product development, production, and marketing and that it is possible to refer the results of these measurements to each other in a meaningful way. NBS services provide essential support for satisfying these needs, as well as measurement needs arising from societal concerns such as health, safety, natural resources, and defense. The requirements of NBS clientele range from the highest levels of accuracy realizable from advanced science and technology to the practical levels of accuracy needed to support routine production. A reference-level measurement may be the result of days of painstaking individual effort or may be provided by a semi-automatic measuring system in minutes. The variation in customer needs and hence in NBS services responsive to those needs is great.

The more than 300 different calibration services, measurement assurance services, and special tests that are offered by NBS are described in NBS Special Publication 250, NBS Calibration Services Users Guide. The Guide provides essential technical details of NBS calibration and related measurement services, such as levels of accuracy provided by NBS and the requirements to be met by customers' transfer standards. It also provides information needed for placing orders for these services and identifies technical and administrative contacts for each service.

Technical descriptions in the Users Guide are intended to be restricted to the material needed by a potential customer to decide if a given service will meet that customer's needs. Frequently, a customer may be interested in more detailed and extensive information, such as the way in which the errors associated with a measurement are assessed. Beginning in 1987, NBS established a Special Publication 250 series which supplements the Guide. Each publication in this series provides a detailed technical description of a specific NBS calibration service, or closely related set of services, and includes:

- specifications for the service
- design philosophy and theory
- description of NBS measurement system used to provide service
- NBS operational procedures
- measurement uncertainty assessment, including error budget, identification of systematic and random errors
- NBS internal quality control procedures

Special Publication 250-32, **A Calibration Service for 30 MHz Attenuation and Phase Shift**, describes service offered primarily under NBS Test Numbers 61215C (attenuation) and 61410C (phase shift) and the reference basis for related service under NBS Test Numbers 61211C and 61230S. These services are provided by the Microwave Metrology Group in the Electromagnetic Fields Division as part of a series of services offered by the Division in support of microwave and millimeter-wave technology.

CONTENTS

CONTENTS (cont.)

CONTENTS (cont.)

CONTENTS (cont.)

CONTENTS (cont.)

FIGURES

FIGURES (cont.)

FIGURES (cont.)

TABLES

A CALIBRATION SERVICE

FOR

30 MHz ATTENUATION & PHASE SHIFT

A calibration service currently being offered by NBS for attenuation and phase shift at 30 MHz is described. The service offers measurements on coaxial attenuators that are either fixed (standard attenuation) or variable for incremental (step) attenuation. Waveguide-below-cutoff variable attenuators with coaxial connectors are also calibrated for incremental attenuation. Ranges of capabilities and estimated limits of systematic and random uncertainty are presented.

Calibration of phase shifters which provide fixed (insertion) phase shift and those with variable phase shift (phase shift difference) is described. Ranges of phase shift and estimated limits of uncertainty are given in degrees. However, a smaller portion of this document is devoted to this calibration service since it is requested only infrequently.

Definitions, capabilities of the system and techniques of calibration are given. The standards, measurement uncertainties, results from intercomparisons, quality assurance and statistical control of the system are discussed and analyzed. Representative reports of calibration are also included.

Key words: attenuation ; calibration ; coaxial; incremental; phase shift ; standard; step; uncertainty ; waveguide-below-cutoff.

1.0 Introduction

The accurate measurement of the attenuation and phase shift of energy in coaxial and waveguide transmission lines is a fundamental requirement in the design, development and operation of most electronic systems. Attenuators which decrease rf energy in a precisely known way and devices to change rf phase accurately must be calibrated by comparison with reference standards maintained by or traceable to the National Bureau of Standards (NBS). For both technical and historical reasons, many rf, microwave and millimeter wave measurements over the entire frequency spectrum are ultimately referenced to 30 MHz calibrations.

The NBS 30 MHz attenuation and phase shift calibration service has been operating for many years. However, the current service is the result of continuing improvements both in techniques and quality control. System capabilities and accuracies are presented and definitions of these parameters and techniques of measurement are described. The NBS 30 MHz dual-channel rf null system for attenuation and phase measurement is documented, including theory of operation and discussion of uncertainties of the standard piston attenuator and the precision phase shifter. Procedures for calibrating an NBS Model VII piston attenuator and a commercial variable phase shifter are presented, as typical examples, with tabulated data and calibration results. Sample reports of calibration for each are included. NBS system measurement uncertainties, quality assurance procedures and multi-year measurement trends are presented. Intercomparisons of attenuation calibration data with other systems such as the NBS SQUID and six-port systems, and with those of international laboratories, are discussed and summarized. Conclusions are given that indicate these results are proof of the validity of the published accuracies of the calibration service at NBS and that the system is in statistical control.

This report is a condensation of several of the many available published documents on rf attenuation and phase shift calibration. It deals almost entirely with the calibration systems which are presently being operated by the Microwave Metrology Group of the Electromagnetic Fields Division at the Boulder Laboratories of the National Bureau of Standards. The laboratory approach is stressed herein and the reader desiring the formal theoretical approach is urged to consult the listed references as well as the other available material on this subject matter.

1.1 Present Capabilities at NBS

A complete listing of the measurements available from the Microwave Metrology Group (including 30 MHz Attenuation and Phase Shift Calibrations) is listed in a publication entitled, "NBS Calibration Services Users Guide 1986-88" [1]. This publication describes capabilities, accuracy and acceptable standards plus relevant fee schedules in an appendix which is published every six months [2]. Tables 1.1 and 1.2 present the general capabilities and accuracies of the 30 MHz attenuation calibration service in decibels (dB) and phase calibration service in degrees (deg).

TABLE 1.1

Capabilities and Accuracies of 30 MHz Attenuation Calibrations

1. Coaxial Fixed Attenuators (Standard Attenuation)

Frequency MHz	Attenuation Range dB	Estimated Limits of Uncertainty ± dB
30	0 to 100	0.02 to 0.0005 A*

2. Coaxial Variable (or Step) Attenuators (Incremental Attenuation)

Frequency MHz	Attenuation Range dB	Estimated Limits of Uncertainty ± dB
30	0 to 100	0.01 to 0.0005 A*

3. Waveguide Below-Cutoff Attenuators with Coaxial Connectors (Incremental Attenuation)

Frequency MHz	Attenuation Range including initial insertion loss dB	Estimated Limits of Uncertainty ± dB
30	0 to 140	0.003 + 0.0003 A*

*A = the measured value of attenuation

TABLE 1.2

Capabilities and Accuracies of 30 MHz Phase Calibrations

Fixed Phase Shifters with Coaxial Connectors (Insertion Phase Shift)

and

Variable Phase Shifters with Coaxial Connectors (Phase Shift Difference)

Frequency MHz	Range of Phase Shift deg	Estimated Limits of Uncertainty ± deg
30	0 to 360°	0.1 to 0.5

* A = measured value of attenuation

1.2 System Overview

1.2.1 System Uncertainty

The limits of uncertainty stated in Tables 1.1 and 1.2 are the sums of estimated systematic, random, and mismatch uncertainties. Their relative values are dependent upon the particular standard under calibration. Fixed and variable coaxial attenuators, and fixed and variable phase shifters are normally measured in a system having a characteristic impedance of 50 ohms. Because measurement limits of uncertainty are degraded by any deviation from this characteristic impedance, the types of allowable connectors are limited. Connectors with a known plane of reference, such as the sexless precision connectors or Type N and similar connectors which meet military standard MIL-C-39012, are acceptable. Limits of uncertainty also depend upon the VSWR of the individual instrument, quality of the connector, and the magnitude of the attenuation and phase [3].

1.2.2 Device Under Test Requirements. All measurements on fixed coaxial attenuators are made by the substitution method, which requires asexual connectors, or an attenuator with a male connector at one port and a female connector at the other. If an adapter is required to comply with the foregoing, it must be supplied with the attenuator. The combination is calibrated as one unit.

Since the only change in insertion loss is measured on coaxial variable attenuators, both ports may have identical connectors. The zero setting of the variable attenuator, or some other setting if specified, is used as the reference during calibration. Variable attenuators and incremental (step) attenuators must have a repeatability of 0.01 dB or better.

1.3 Definitions

1.3.1 Insertion Loss. The 1959 IRE standard [4] gives two definitions of insertion loss, one in which system mismatch is not specified, the other in which the system is nonreflecting. The definitions contradict each other since the insertion loss of an attenuator will be different for each case. The measurement procedure for both definitions is to open the system, insert the attenuator, and note the relative power absorbed by the load (or detecting device) before and after insertion. The insertion loss in dB is computed from these two values. If the attenuator is variable and remains in the system, the initial and final powers absorbed by the load for two settings are used. This determination is more properly called "Change in Insertion Loss."

Either definition is entirely adequate for a single, unique system, but if the loss (or gain) measurement is to be transferred from one laboratory to another, more must be specified about system conditions.

1.3.2 Attenuation. This is defined as the insertion loss in a nonreflecting system ($\Gamma_G = \Gamma_L = 0$).[1] These impedance matching conditions cannot be achieved exactly because of imperfections in connectors or adapters and the inability to ascertain when a system is precisely matched. Since attenuation cannot be measured exactly, the more practical term "standard attenuation" has come into more general use.

---

[1] Γ_G and Γ_L are defined as the reflection coefficients of the generator and load respectively.

1.3.3 Standard Attenuation. This is defined as the insertion loss of a linear two-port device in an essentially nonreflecting system which is initially connected together at the insertion point by a standard connector[2] pair or waveguide joint. The nonreflecting condition is obtained in the standard coaxial or waveguide sections to which the standard connectors or waveguide joints are attached. The standard attenuation is the ratio expressed in dB of the power absorbed by the load before and after insertion of the two-port device being calibrated.

1.3.4 Incremental Attenuation. Incremental attenuation is the change in attenuation of a variable attenuator between a reference setting (usually zero) and any other setting. The same restraints on system conditions apply here as those for attenuation and standard attenuation. The term "differential attenuation" is sometimes applied to this case and usually refers to two non-zero settings.

1.3.5 Characteristic Insertion Loss. This quantity, as defined in IEEE Standard 474-1973, Specifications and Test Methods for Fixed and Variable Attenuators, Dc to 40 GHz [5], most closely describes the attenuation calibrations as performed by NBS. An excerpt from this standard is included as Appendix A of this document. The reader is encouraged to review the complete standard as needed.

---

[2]A "standard connector" is one which is made precisely to standard specifications for the particular type of connector under consideration. Standard connector pairs usually have low but measurable loss and reflections [3,6,7].

1.3.6 Insertion Phase Shift is the phase change of a wave incident upon the load before and after insertion of a two-port device between the generator and load of a stable nonreflecting system.

1.3.7 Phase Shift Difference is the phase change of a wave incident upon the load, from an initial to a final condition, resulting from inserting a two-port device between the generator and load of a stable nonreflecting system.

Note: The following conditions apply: (1) The frequency, the load impedance, and the generator characteristics (internal impedance and available power) have the same values before and after the device is inserted or changed; (2) the joining devices (connectors or adapters) belonging to the system conform to standard specifications (the same specifications must be used by different laboratories, if measurements are to agree precisely); and (3) nonreflecting conditions must be obtained in the uniform, standard sections of transmission line on the system sides of the connectors at the place of insertion.

1.3.8 Decibel. The decibel is one tenth of a bel[3] and is defined fundamentally in terms of a power ratio:

$$\text{dB} = \text{number of decibels} = 10 \log \frac{P_1}{P_2}, \tag{1}$$

where P_1 is the incident power from an impedance matched source and P_2 is the net power into an impedance matched load after a device is inserted between the source and load. If the powers P_1 and P_2 are associated with equal

---

[3]Named in honor of Alexander Graham Bell.

impedances, this power ratio can be expressed as the square of either the voltage or current ratio.

Hence: Number of decibels $= 20 \log \left| \frac{E_1}{E_2} \right| = 20 \log \left| \frac{I_1}{I_2} \right|$. (2)

1.3.9 dBm. This term indicates a power level with respect to one milliwatt.

Thus, power level in dBm $= 10 \log \frac{P}{0.001}$ (3)

where P = power level in watts.

Similarly, power level in dBm $= 10 \log \frac{E^2/R}{0.001}$ (4)

where E is in volts

and R is in ohms.

1.3.10 Neper. A unit used to express the scalar ratio of two currents or two voltages, where the number of nepers is the natural logarithm of the ratio.

Hence, nepers of attenuation $= N = \ln \left| \frac{E_1}{E_2} \right| = \ln \left| \frac{I_1}{I_2} \right|$. (5)

If the power ratio is the square of the above voltage or current ratio, then (5) can be expressed as:

$$N = \frac{1}{2} \ln \frac{P_1}{P_2} \text{ nepers} \qquad (6)$$

1.3.11 Conversion from Nepers to Decibels.

One neper - 8.686 decibels.

1.3.12 Propagation Constant. The propagation constant, γ, is defined as

$$\gamma = \sqrt{YZ} = \sqrt{(R + j\omega L)(G + j\omega C)} \qquad (7)$$

where the ac series impedance of a transmission line is $Z = R + j\omega L$ in ohms per unit length

and the ac shunt admittance of a transmission line is $Y = G + j\omega C$ in ohms per unit length.

From (7) it is seen that the propagation constant γ will, in general, have a real part and an imaginary part.

Hence, $\gamma = \alpha + j\beta$ (8)

where, α = attenuation constant in nepers per unit length

and, β = phase constant in radians per unit length.

The voltage, E, propagates along the line a distance, ℓ, as

$$E = A_1 e^{j\omega t - \gamma\ell} \text{ volts} \qquad (9)$$

2.0 Dual Channel Rf Null System for Attenuation and Phase Calibration

Attenuation measurements are frequently performed below 1 GHz using intermediate frequency (IF) or audio frequency (AF) substitution techniques. These techniques have a number of sources of uncertainty since it is necessary to convert from one frequency to another [8]. For this reason they are not preferred and will not be presented in this document. The direct substitution technique, whereby the standard attenuator and the attenuator under calibration operate at the same frequency, is a simpler approach with fewer sources of uncertainty.

A basic block diagram of the unmodulated two-channel system employed by NBS at 30 MHz is presented in figure 2.1 [9]. A two-channel nulled system has fewer problems of level instability in the source and gain instability of the monitor, and has high sensitivity. However, phase and magnitude adjustments must both be made and the system is more complex than a single channel system. A range of attenuation measurement in excess of 100 dB can be attained with this system by placing the device under test (DUT) in the insertion point shown in figure 2.1. The resolution is very high for large signal amplitudes. Better resolution can be maintained at small signal amplitudes by using quadrature detection rather than a simple nulling approach. Thus to obtain a successful system, a precision phase shifter of constant amplitude or one with precisely known losses is required to achieve the null or quadrature phasing of the two channels.

A complete block diagram of the present 30 MHz NBS attenuation and phase calibration system is presented in figure 2.2.

ATTENUATION - PHASE CALIBRATION SYSTEM

DUAL-CHANNEL RF NULL

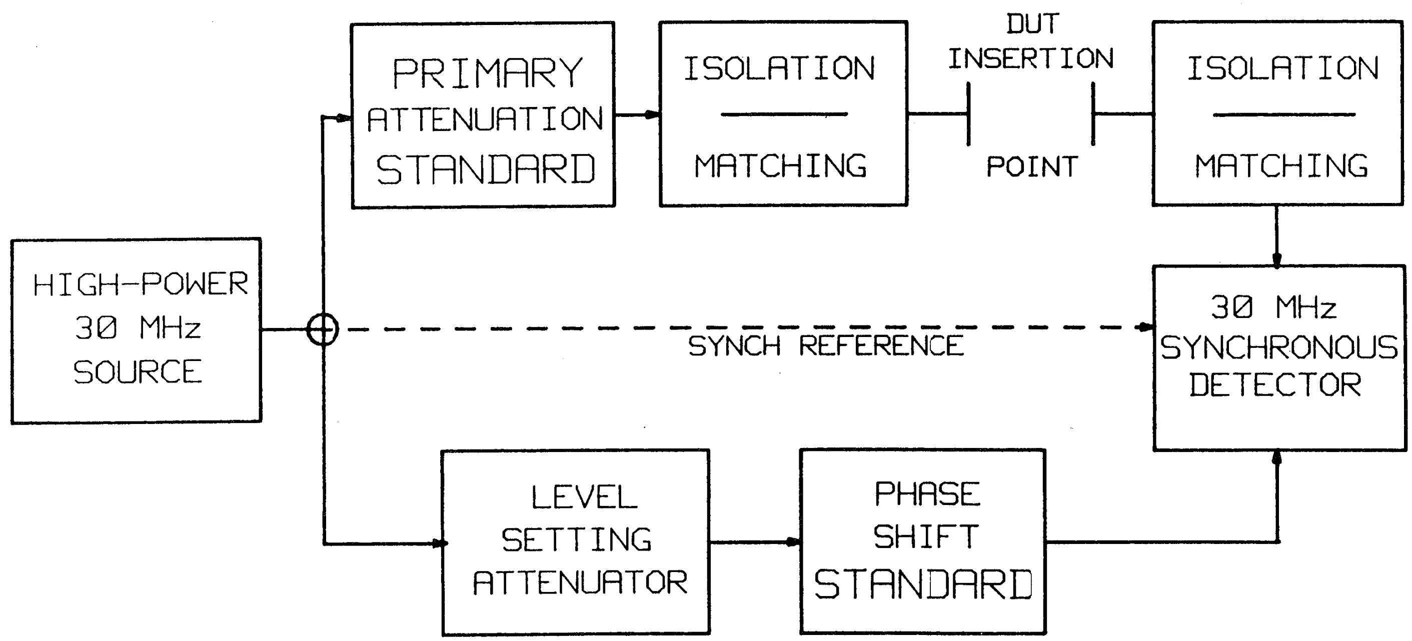

Fig. 2.1 Basic block diagram of dual-channel RF null attenuation and phase calibration system

30 MHZ DUAL-CHANNEL ATTENUATION/PHASE MEASUREMENT SYSTEM BLOCK DIAGRAM

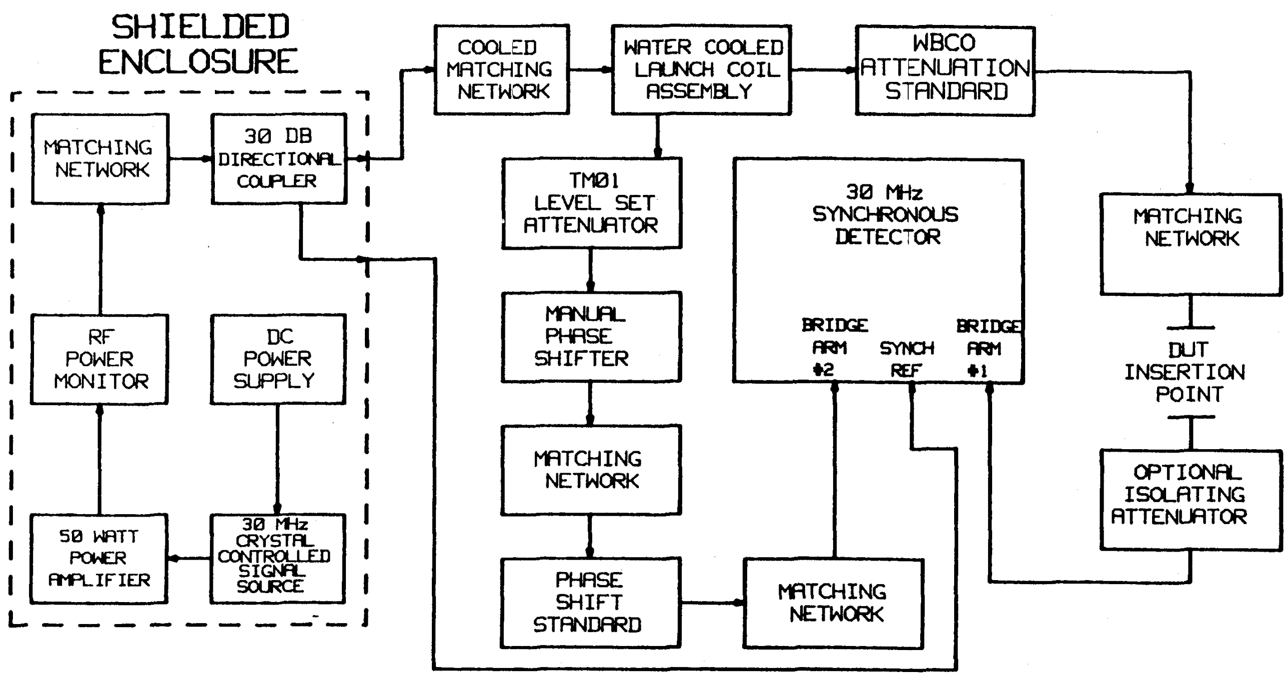

Fig. 2.2 Complete block diagram of 30 MHz dual channel RF null attenuation and phase calibration system

2.1 Description of 30 MHz Calibration System

2.1.1 30 MHz Standard Piston Attenuator

This standard is a circular waveguide-below-cutoff (WBCO) attenuator which is a standard with a continuously variable attenuation, commonly called a piston attenuator. The complete mechanical assembly is shown in figures 2.3 and 2.4. Figure 2.5 shows the drive and readout in more detail including an earlier version of the signal launching assembly.

2.1.1.1 Theory

The incremental attenuation of this type of standard can be accurately predicted from only a knowledge of its dimensions. Thus a major advantage of this standard is the determination of the attenuation (except for secondary effects) by the fundamental units of length and time (frequency). When the waveguide section is uniform and excited in only one mode by a sinusoidal signal below the cutoff frequency, the field will decay exponentially along the guide. More specifically, electromagnetic fields existing in a uniform perfectly conducting waveguide can be expressed as a linear combination of terms called modes. The electromagnetic field components for each mode are proportional to the term $e^{-\gamma \ell + j\omega t}$, where γ, the propagation constant, (see equation 10) is determined completely by the waveguide dimensions and frequency [10]. Thus, below the cutoff frequency, γ becomes an entirely real component and the fields decay exponentially at a rate dependent on the mode of propagation. The mode with the smallest decay rate is used to ensure mode purity at the high attenuation levels.

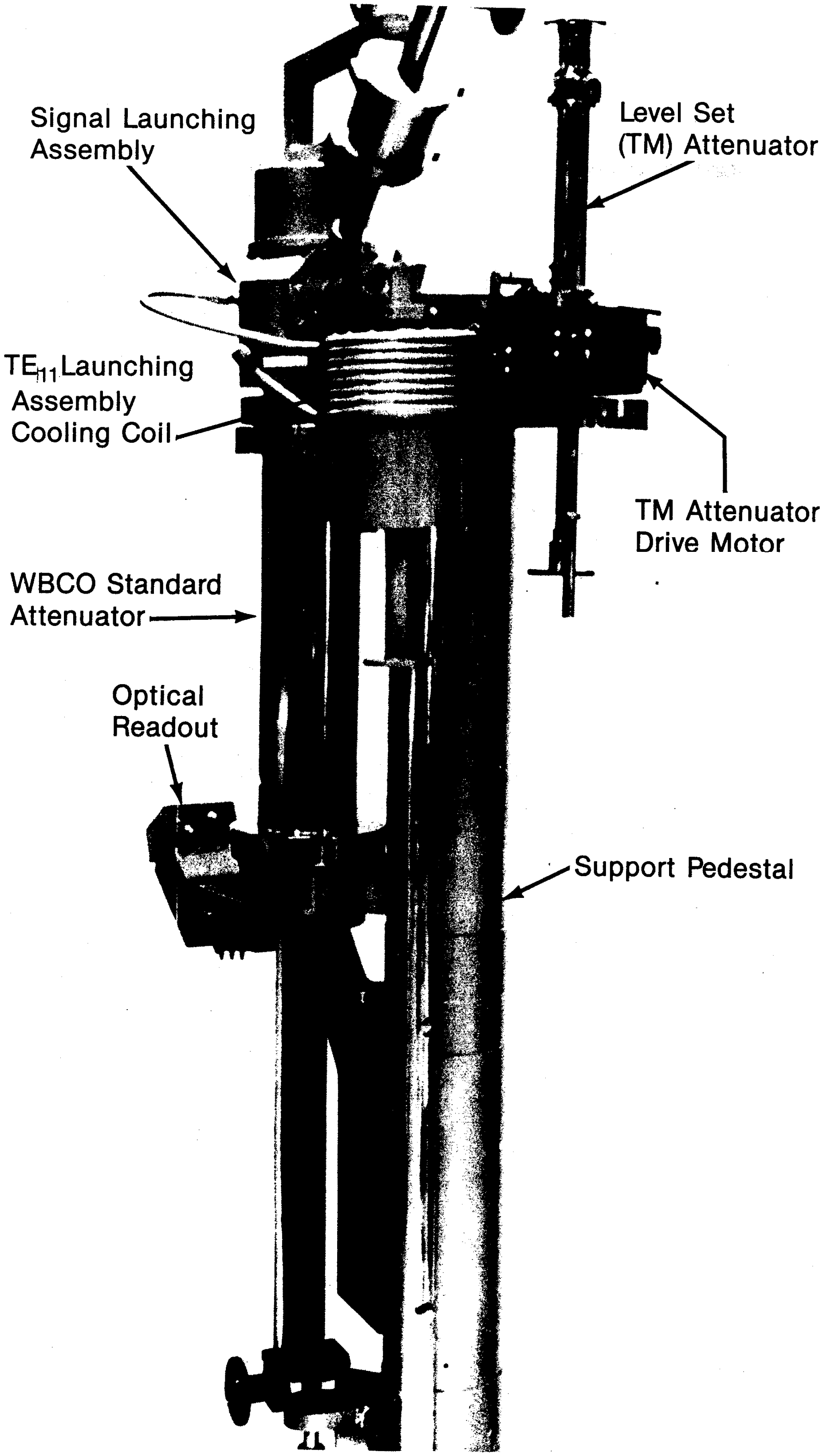

Figure 2.3. View of upper portion of 30 MHz standard attenuator assembly showing the level set attenuator, the WBCO standard and the signal launching assembly.

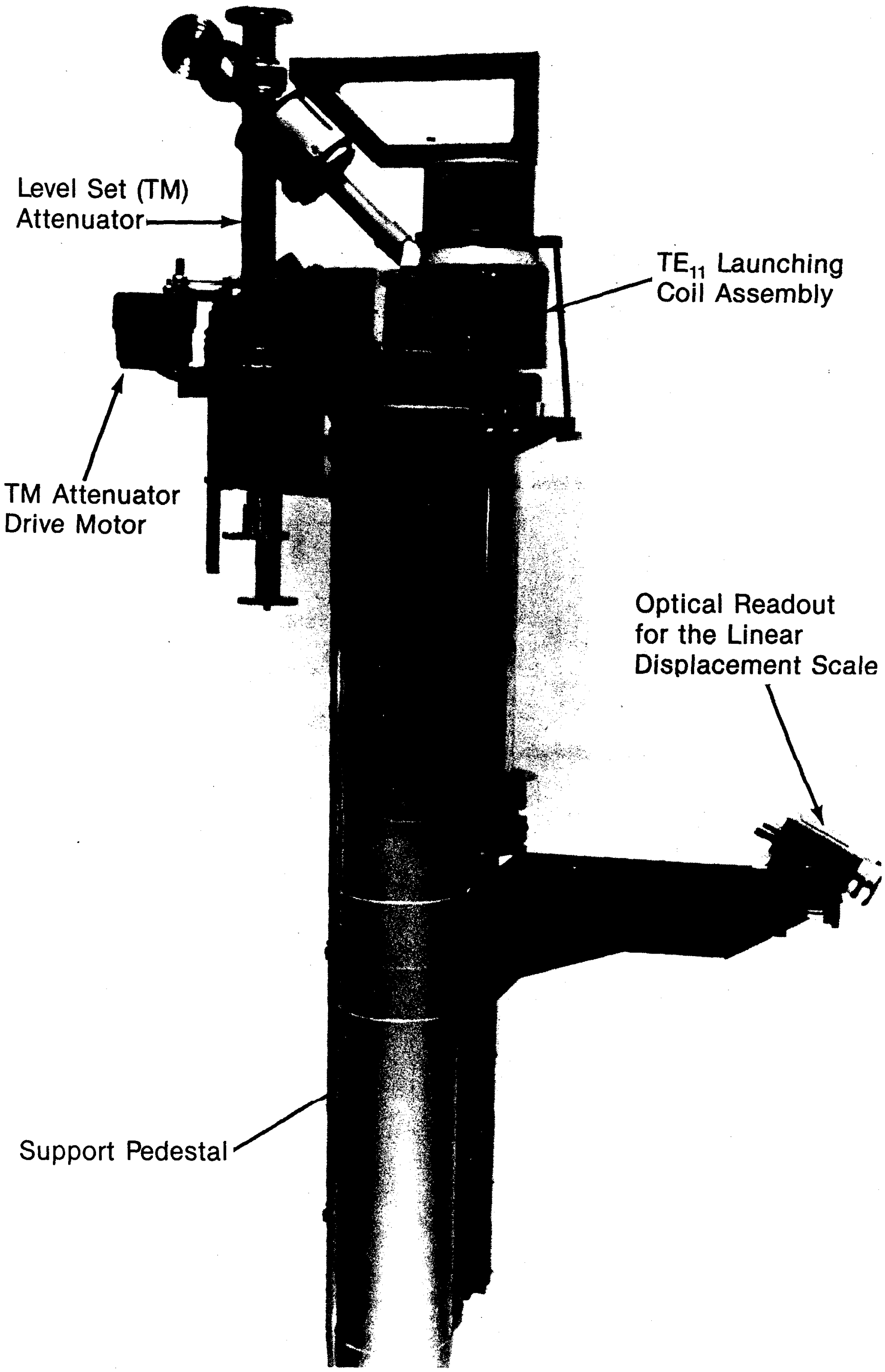

Figure 2.4. View of upper portion of the 30 MHz standard attenuator assembly showing the optical readout for the linear displacement scale.

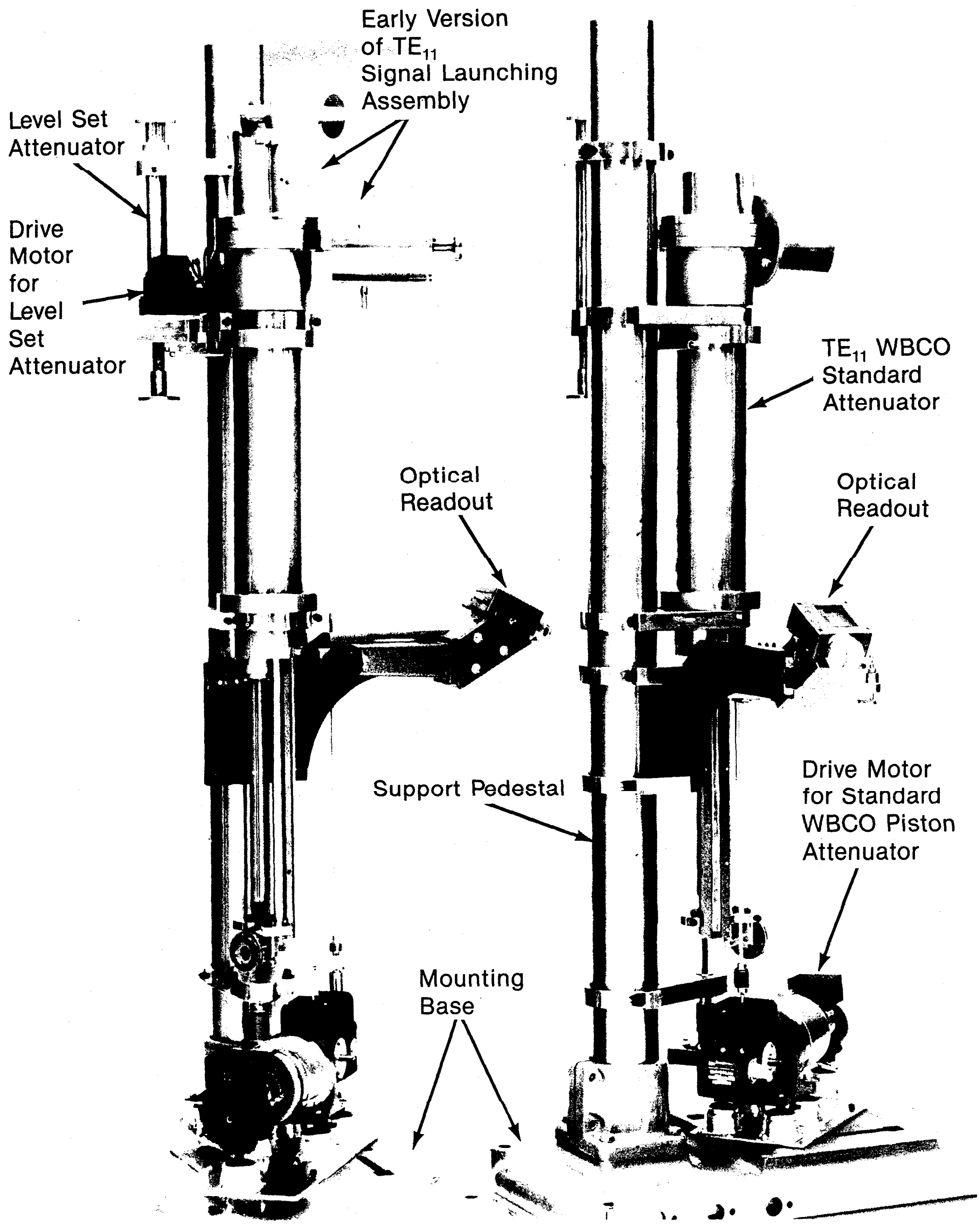

Figure 2.5. 30 MHz standard attenuator assembly.

The primary disadvantage of this WBCO standard attenuator occurs because it is a nondissipative device and therefore varying amounts of energy are reflected rather than absorbed as the attenuation is varied. This results in the need for a high minimum insertion loss (approximately 30 dB) to reach the highly linear attenuation range of operation. Also the terminal networks must contain reactances which are frequency-dependent.

2.1.1.2 Description

This WBCO attenuator has a launching coil and a moving probe or pick-up coil to sample the decaying field and an indicating readout to correlate the probe position with the attenuation level change. The coupling coils in the attenuator must be sufficiently separated at all times to prevent mutual coupling and loading effects from excessively affecting the excited mode. This is the reason for the high initial insertion loss of WBCO attenuators. A circular waveguide is chosen for ease of precise fabrication and because excitation symmetry is not critical. The desired excited field in this WBCO attenuator consists of the transverse electric $(TE)_{11}$ mode which unfortunately is not far in frequency from some higher modes. The transverse magnetic $(TM)_{01}$ mode has the greatest probability of causing difficulty since its attenuation rate is closest to the rate of the TE_{11} mode. Mode filters with metallic strips are constructed to suppress the TM modes by over 60 dB while reducing the TE_{11} mode by less than 0.5 dB.

A close approximation for the propagation constant, γ, (in nepers per meter) in the TE_{11} mode is given by [10]:

$$\gamma = \frac{S_{11}}{r}\left[\sqrt{1 - \left(\frac{2\pi r f\sqrt{\varepsilon}}{S_{11}C}\right)^2} - \frac{1}{r\sqrt{\pi\mu f\sigma}}\right]$$

$$\cdot \left[1 + j \left(1 - \frac{1}{1 - \dfrac{1}{r \left\{ 2 - \left(\dfrac{2\pi r f \sqrt{\varepsilon}}{S_{11}\, C} \right)^2 \right\} \sqrt{\pi \mu f \sigma}}} \right) \right] \tag{10}$$

Where $S_{11} \approx 1.8411838$ = first root of the first derivative of the first-order Bessel function of the first kind,

r = radius of the waveguide cylinder,

f = frequency of operation in hertz,

ε = relative dielectric constant of the medium inside the waveguide,

$v \approx 2.997925 \times 10^8$ m/s = velocity of light,

μ = permeability of guide wall (relative, usually taken to be 1.00000),

$\sigma = 1.35 \times 10^7$ mhos/meter = conductivity of the brass waveguide wall.

Equation (10) illustrates that the most important quantities other than the radius are the frequency and conductivity. Brown [11] shows that the quantity in square brackets contributes a very small and usually negligible phase shift at IF frequencies in waveguides constructed of good conducting materials. The actual phase shift for the NBS attenuator is less than one degree (deg) in 100 dB of attenuation.

The displacement of the receiving coil relative to the launching coil is measured with a steel ruled scale and optical projector. The scale is accurate to 2.54 μm (0.0001 inch) within any 15.24 cm (six inches) length. The thermal coefficients of expansion of the stainless steel scale and the brass waveguide are nearly the same. For a 2.222°C (4°F) temperature change, the difference in the temperature coefficients would contribute a calculated error of only 0.0001 dB per 10 dB attenuation change.

The brass waveguide has an outer diameter of 9.906 cm (3.9 inches) and a length of 56.64 cm (22.3 inches). The internal diameter of the waveguide (approximately 8.128 cm (3.2 inches)) is chosen to give an attenuation rate of 10 dB/2.54 cm (1 inch) of travel. For a perfectly conducting waveguide of circular cross section of radius, r, in cm, and having TE_{11} mode cutoff frequency, f_c, the attenuation rate, α, when operating at frequency, f, below cutoff is:

$$\alpha = \frac{15.99}{r} \sqrt{1 - \left(\frac{f}{f_c}\right)^2} \text{ dB/cm} \qquad (11)$$

where $f_c = \frac{55.20}{2\pi r}$ GHz [3]. (12)

The inside wall of the waveguide is coated with 0.127 µm to 0.254 µm (5 to 10 microinches) of rhodium. This presents a hard surface to the sliding silver contacts of the piston and prevents corrosion of the brass guide without significantly affecting the conductivity of the waveguide surface.

Dimensional tolerances on the guide and the resolution and accuracy with which the displacement between the exciting and receiving coils can be measured are very important. The guide diameter must remain constant and be perfectly circular. Any ellipticity in the guide will cause the propagation constant to differ from the circular case, thereby possibly exciting degenerate modes of propagation. Angular variations along the major axis will produce undesirable variations in the exponential decay of the field within the waveguide.

2.1.1.3 Uncertainties

Table 2.1 presents the uncertainties of the 30 MHz WBCO piston attenuator as measured and calculated by Allred and Cook [10].

TABLE 2.1

Uncertainties in the NBS 30 MHz Standard Piston Attenuator

Systematic Uncertainties	
Coaxial waveguide diameter	0.0003 dB/10 dB
Linear displacement of receiving coil	0.001 dB/10 dB
Velocity of electromagnetic waves in medium inside guide	Negligible for air
Rf conductivity of guide	0.00026 dB/10 dB
Rf permeability of guide	Negligible for brass
Total Systematic Uncertainty	0.00156 dB/10 dB
Random Uncertainty	Negligible in controlled environment
Total Uncertainty	0.00156 dB/10 dB

2.1.2 30 MHz TE_{11} Launching Assembly

The input system on the piston attenuator is a major determining factor in the measurement range of the total system.

A system is needed which launches the single TE_{11} mode with an intensity independent of the position of the receiving coil, and/or a system which launches the desired mode so efficiently that the receiving coil never has to be positioned near the input coil.

The following describes the approach used at NBS. A current sheet with spatial TE_{11} mode electric field distribution (two-dimensional polar coordinates) in the transverse plane of the waveguide is established as nearly ideal as possible. This mode is launched in both directions from the current sheet. If such a constant current sheet is obtainable and is independent of the fields reflected from the pickup coil, the undesirable effect of interaction between coils will not create errors.

These conditions are approached by constructing the launching assembly as illustrated in figures 2.6 and 2.7. The constant current sheet is initially obtained by sampling the launching current and keeping it constant by using negative feedback to the rf source. In the present system the feedback loop is not actuated because the pickup and receiving coils are not allowed to approach each other closely enough to interact and a more stable solid state rf source has replaced the original source. This reduces the overall dynamic range of the system by approximately 10 dB, however, for normal calibrations. The resulting range of 140 dB is still adequate. In the event of special needs for higher ranges, the feedback system can be reactivated.

The attenuator waveguide was extended behind the launching coil in order to terminate the field propagated from the back side of the launching coil. Since the pickup coil absorbs some energy, it produces a reflected field which passes through the launching coil with very little interaction and is terminated by the same waveguide extension.

The launching assembly is constructed of small stainless steel tubing through which water is passed to prevent excessive heating of the waveguide which would otherwise change its dimensions. Mode filters are used to eliminate the axial electric fields (higher modes) caused by the reactive impedance of the launching unit.

The resistive component of the launching coil is estimated to be between 0.01 and 0.1 ohm which is difficult to match to the 50-ohm rf source. An impedance match is obtained by using a capacitive type impedance matching

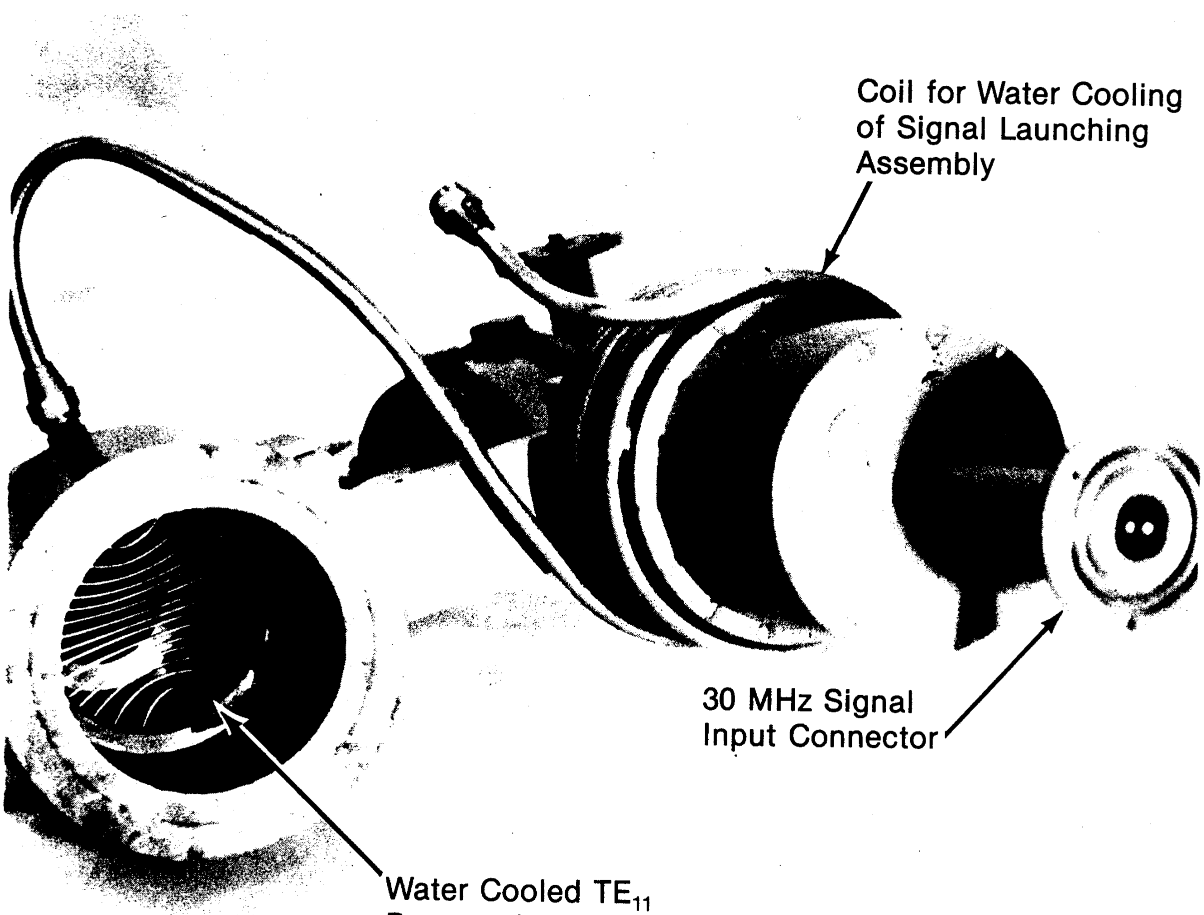

Figure 2.6. 30 MHz TE_{11} launching assembly.

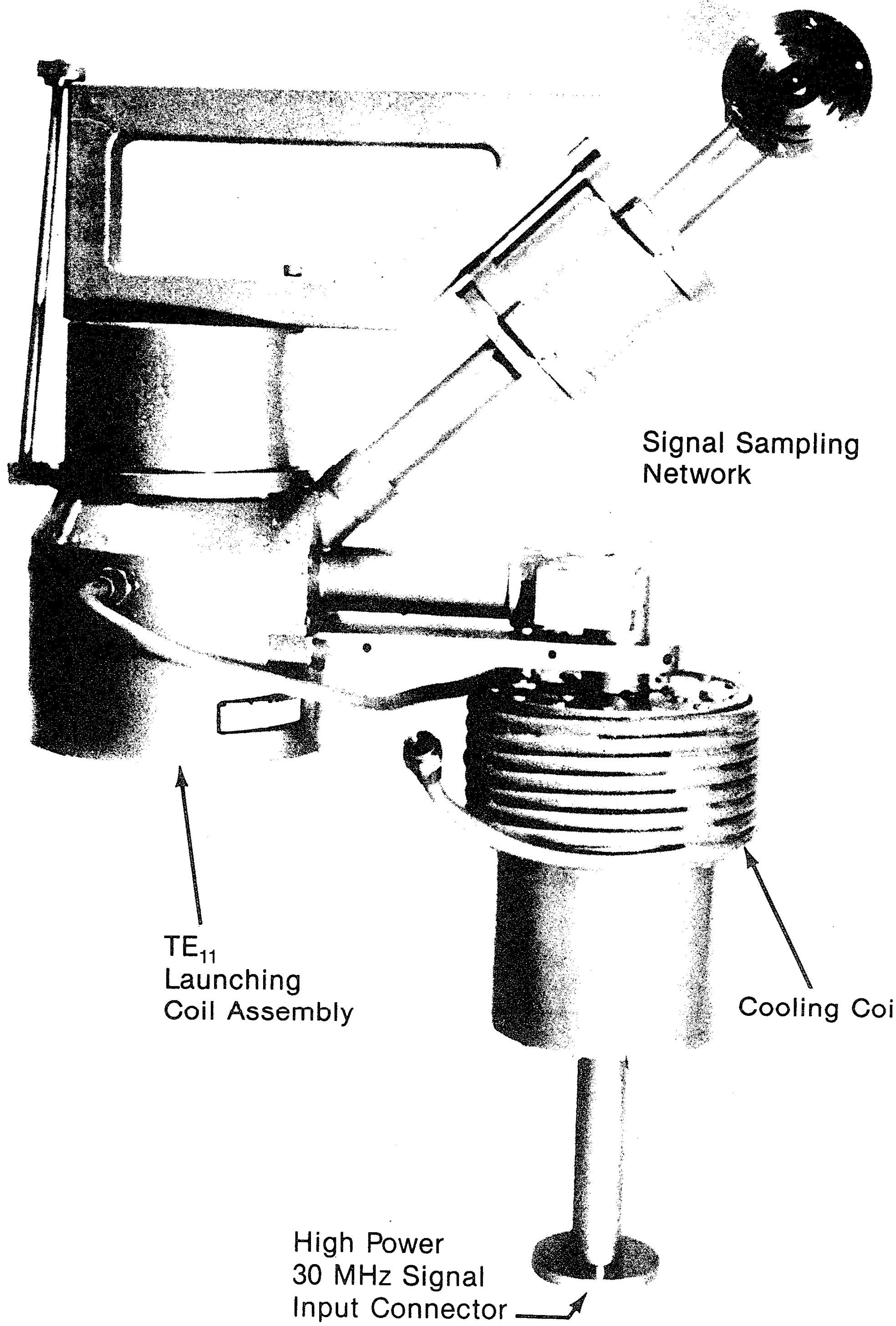

Figure 2.7. 30 MHz launching assembly with matching and sampling networks.

network with a maximum rating of 200 watts. A 10-watt input to the matching network produces an rf launching coil current of approximately 1.1 amperes. The sub-assembly is shown mounted in figure 2.7.

2.1.3 30 MHz Precision Phase Shifter

2.1.3.1 Description

The constant amplitude precision phase shifter used at NBS consists of a sliding airline trombone configuration as shown in figure 2.8. Non-constant impedance construction is used since this system operates only at one single frequency. The attenuation level variations are held to a minimum by terminating the precision fixed line sections in their characteristic impedance. This can be accomplished only at a single frequency since the sliding section has a lower characteristic impedance than the fixed sections of line. The fixed line sections are terminated properly by placing a pi matching network on each side of a 10-dB attenuator and installing this complete configuration in the center of the moving section of line. This then provides the desired characteristic impedance at the sliding junction to properly terminate the precision fixed sections of line. Additional attenuators and matching networks terminate other two ends of the precision phase shifter.

The outer conductors of the precision section of the phase shifter are precision machined brass cylinders with 1.27.cm (0.5-inch) thick walls. The inside walls are heavily plated with burnished silver, with a thin coating of rhodium. The center conductors are brass rods with silver plate and rhodium coating similar to that used on the outer conductors. The maximum deviation of the critical diameters from the mean value is 8.89 μm (0.00035 inch) which could produce a calculated maximum characteristic impedance variation of slightly less than 0.04 percent.

The four terminating impedance matching networks are adjusted until a maximum change in phase range produces less than 0.01 ohm total impedance change, measured on a sensitive rf impedance bridge.

Over the total range of the phase shifter (38 deg or 101.6 cm (40 inches) of travel), the change in level is less than 0.0005 dB. This range is adequate when calibrating attenuators since piston attenuators normally have negligible amounts of phase shift. The phase shift in dissipative attenuators approximates their physical length, which is a small fraction of the phase shifter travel.

As stated above, the trombone phase shifter has a range of travel in excess of 101.6 cm (40 inches) which yields a phase shift of slightly over 38 degrees. The readouts of the devices under test are given in deg, and therefore the results are computed and stated in deg, rather than in the SI units of radians. A mechanical counter is connected to the phase shifter to indicate precisely the travel of the shifter. One count on the counter corresponds to a phase shift of 0.01142 deg.

2.1.3.2 Uncertainties

Table 2.2 presents the sources and magnitudes of the uncertainties in the 30 MHz precision phase shifter [10].

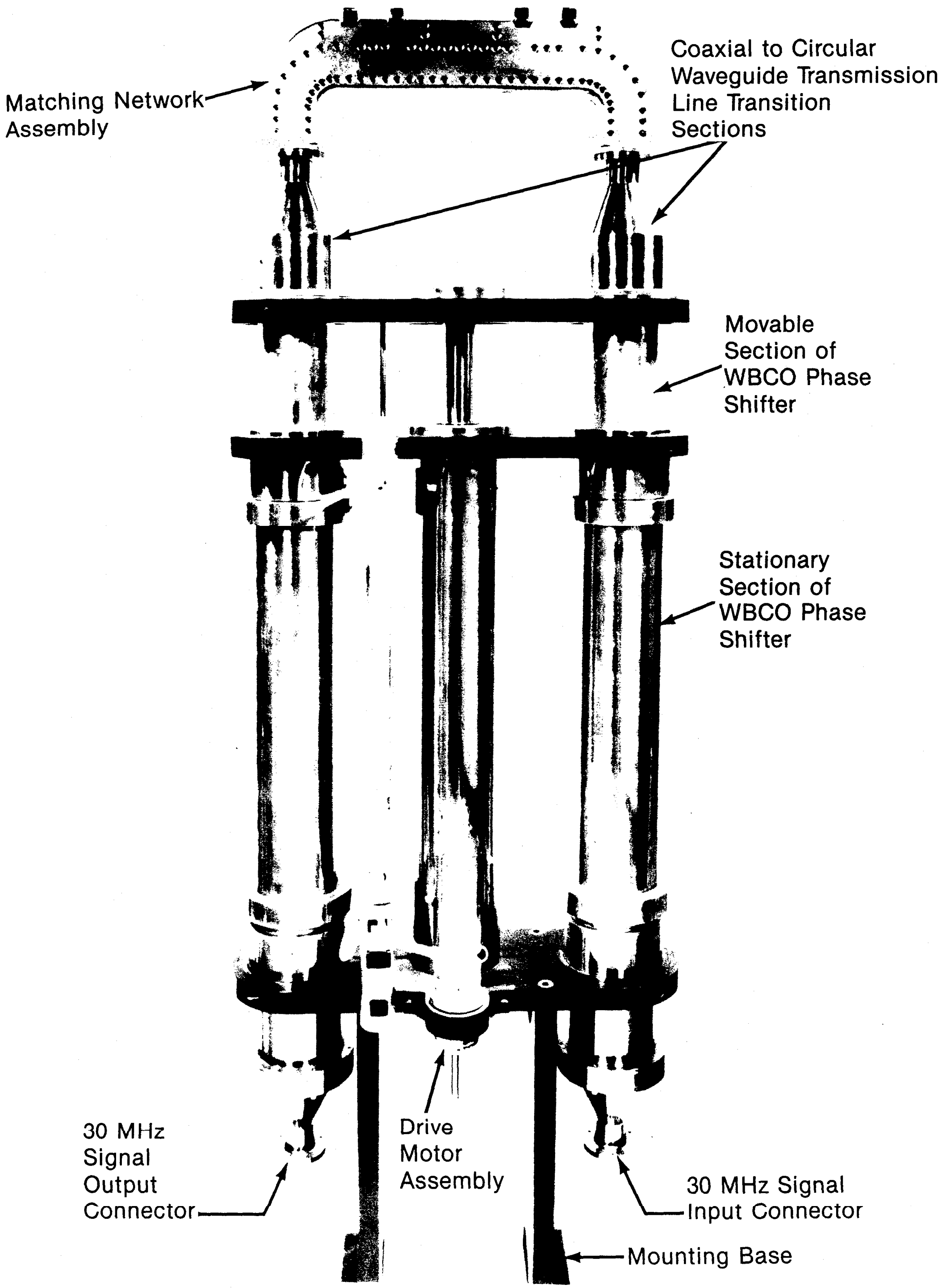

Figure 2.8. 30 MHz precision phase shifter.

TABLE 2.2

Uncertainties in the NBS 30 MHz Precision Phase Shifter (for a 36 degree measurement)

Systematic Uncertainty	
Mismatch uncertainty in the sliding sections	0.012 deg
Measurement of linear displacement and Uniformity of diameter	0.048 deg
Losses in trombone for 30 degree increment	0.018 deg
Resolution of readout	0.06 deg
Random Uncertainty	Negligible
Total Uncertainty	0.138 deg/36 deg

2.1.4 30 MHz Coarse Phase Shifter

This manually operated phase shifter consists of two commercial phase shifters connected in series. These phase shifters have been modified by adding high resolution manual-drive mechanisms with which to adjust them. Refer to the block diagram in figure 2.2 for its location in the circuit. These phase shifters have a characteristic impedance of 50 ohms and an insertion loss of approximately one dB each. Each of these phase shifters provides a shift of 0 to 180 deg and is driven by gears. The gear ratios are chosen so that one of the phase shifters acts as a coarse adjustment while the other functions as a medium adjustment. This arrangement provides a fast and convenient means of initially adjusting the phase leg to null the dual channel system. The large 30 MHz trombone precision phase shifter provides the system with the final complete rf null.

The coarse phase shift unit is necessary to calibrate a phase shifter over a range greater than 30 deg since the precision phase shifter has a range of only approximately 40 deg. The coarse phase shifter unit is then used to change the phase shift reference (from 0 to 360 deg) so that the precision phase shift standard can be used (bootstrapped) over a 360 deg range in steps of 30 deg.

2.1.5 Level Set Attenuator

The rf power level adjusting attenuator is shown in figure 2.9 with its associated fast and slow speed drive motors. It is a TM mode WBCO piston attenuator. It consists of a variable capacitor formed by mating hemispherical electrodes inside a cylindrical waveguide. One of the electrodes is motor-driven so that the spacing between them can be varied, thus changing the value of attenuation within the waveguide. This particular design is chosen for this attenuator because it produces no significant phase shift. (This mode has no significant skin depth correction, and hence very small phase shifts are associated with its level changes.) It has an attenuation constant of 20.9 dB/radius. The radius of the inside of the waveguide is approximately 1.27 cm (one-half inch) which gives an attenuation rate of slightly more than 15.74 dB/cm (40 dB/inch) of travel. Hence, this level set attenuator does not introduce undesirable phase changes in the system and does not have to travel very far to yield a significant change in attenuation. It is located in the phase leg of the dual channel system as shown in figure 2.2. The amount of rf signal propagation in this leg of the system is predetermined by the setting of the TM mode level set attenuator. Optimum sensitivity of the entire system may be maintained by pre-positioning this attenuator regardless of which attenuator is under calibration (within the capabilities of the system).

Refer back to figures 2.3, 2.4 and 2.5 to observe the installed position of the level set attenuator with respect to the standard 30 MHz piston attenuator.

2.1.6 Rf Null Detection System

The rf null detector is a double-conversion frequency-locked receiver. The 30 MHz null detection system consists of an rf null detector Model NBS/SND which is a synchronous detector designed, developed, and constructed at NBS with a 30 MHz frequency plug-in unit (Model SND/PI-30A), [12]. This instrument is designed for extremely high sensitivity consistent with simplicity of operation. The detector is frequency-locked to the signal to be examined and thus requires a synchronous reference voltage to achieve its high sensitivity. A single gain control adjusts the sensitivity. The null signal is indicated by two front panel center-indicating meters. A continuously-variable phase control enables in-phase and quadrature components of the null signal to be displayed individually on separate meters. The 30 MHz detector has a gain of approximately 150 dB, a bandwidth of ±20 kHz, a 2-dB noise figure, and a 360-deg continuously-variable phase control. The input impedances of the two signal input ports and the reference signal input port are nominally 50 ohms. The receiver has a dynamic sensitivity range of 90 dB without saturation which allows the operator to locate the system null easily. The gain control on the receiver also assists the operator to find the null rapidly and efficiently.

This null detector system is constructed of separately-shielded modules which minimize the adverse effects of signal leakage and interference.

The maximum sensitivity of this 30 MHz detection system is approximately 1 nanovolt. The calibration range of the complete system is

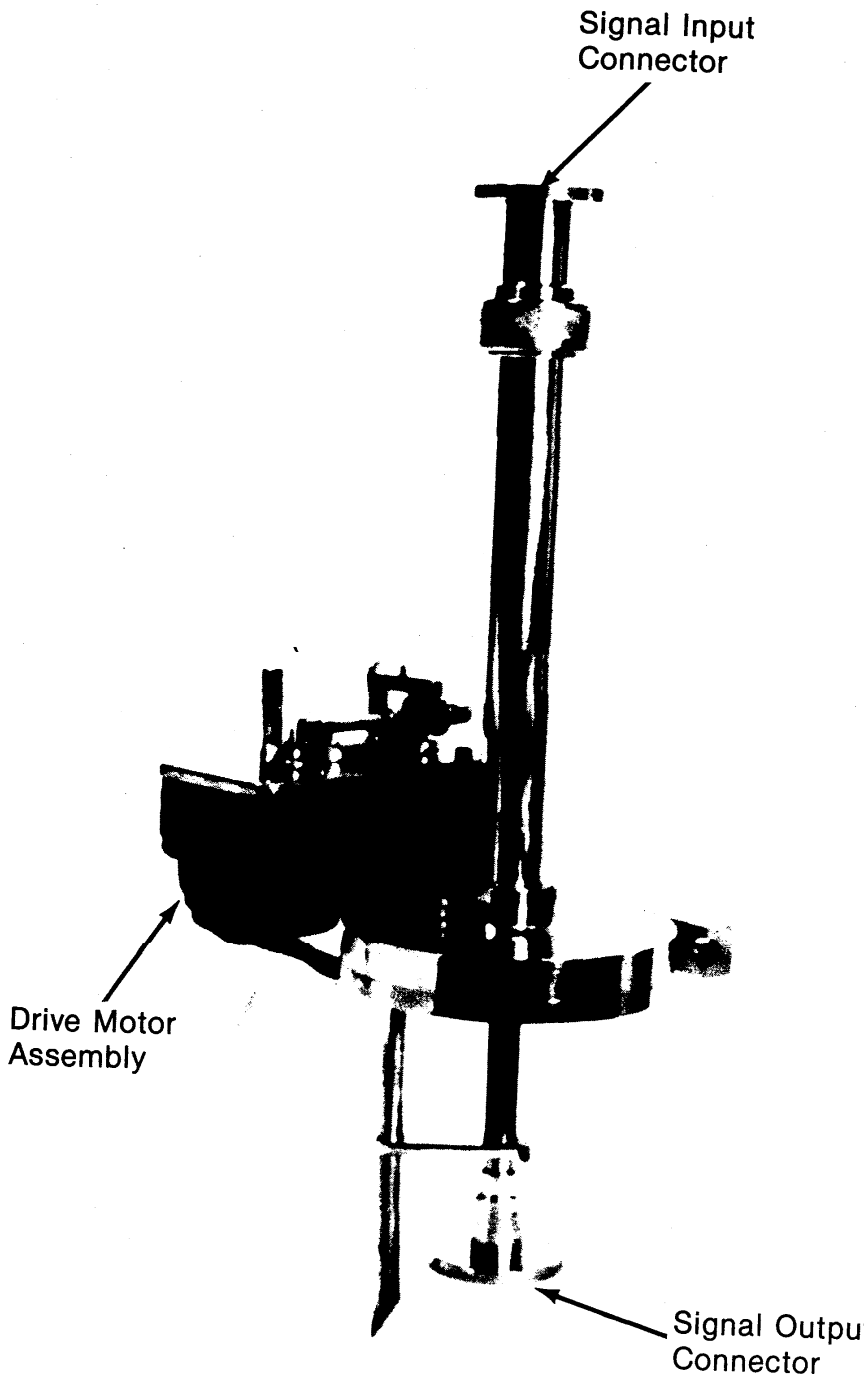

Figure 2.9. 30 MHz level set (TM) attenuator with drive motors.

approximately 150 dB including the initial insertion loss of the attenuator under calibration (20 to 30 dB in the case of a variable WBCO attenuator).

The resolution of the system (primarily due to the readout) is 0.001 dB when measuring a 100-dB change in attenuation on a piston attenuator (with an initial insertion loss of 30 dB). Thus, the detection system has an attenuation resolution of better than 0.001 dB at 130 dB below the maximum (practical) 50 milliwatt (mW) output from the standard attenuator.

Similarly, the system has a phase shift resolution of better than 0.01 degree at similar rf signal levels.

2.1.7 RF Source and Associated Circuitry

The 30 MHz fixed frequency rf source which provides the signal for this dual-channel attenuation and phase calibration system is represented in figure 2.2. It consists of a 30 MHz ultra-stable, crystal-controlled, continuous wave (CW) source and 50-watt linear amplifier which delivers approximately 10 watts (W) of rf power to the attenuator launching system. The frequency of this source is stable within 1 part in 10^6.

The output power level of the rf source and power amplifier combination is sufficiently stable so that no external level circuitry is required. This signal source arrangement is adequate to produce the nearly constant current sheet in the TE_{11} launching assembly as mentioned in section 2.1.2 of this document.

The key to adequate stability is the sampling of the reference channel (phase shifter leg) at the launching coil of the standard attenuator. Minor level variations are equally reflected in each channel and thus contribute negligible error as long as adequate separation of the launching and receiving coils is maintained.

2.1.8 The Insertion Point

The insertion point in a system is the point at which the system is opened in order to insert the instrument being calibrated. The insertion point is a very important portion of the attenuation and phase calibration system. It must permit physical motion, be well shielded and must not adversely effect the rest of the system in any way. These requirements are met at the NBS Boulder Laboratories by using a combination of semirigid, coaxial cable and double-shielded, flexible, coaxial cable. The semirigid cables are brought to the front panel of the calibration console where they are connected to precision 14-mm connectors. At this point, short lengths of double-shielded, coaxial, flexible cables are connected. This double-shielded cable has only one electrical shield since both layers of shielding braid are lying against each other. A third separate shield is stretched over the outside of these flexible, coaxial cables and clamped securely to the connector at each end of each cable. This then produces flexible, coaxial cables for the insertion point which are truly double-shielded cables that reduce rf signal leakage to insignificant levels.

2.2 Uncertainty Analysis

2.2.1 30 MHz Attenuation Calibration Uncertainties

Table 2.3 presents the sources and magnitudes of the uncertainties in the 30 MHz attenuation calibration system [10, 12].

TABLE 2.3

30 MHz Attenuation Calibration Uncertainties

Systematic Uncertainties

Reference Standard Piston Attenuator (from Table 2.1)	0.0016 dB/10 dB
Resolution of Detecting System	0.0004 dB/10 dB
Maximum Rf Leakage (measured by field strength meter) and reference channel variation due to standard phase shifter.	0.001 dB/10 dB
Total Systematic Uncertainty	0.003 dB/10 dB + mismatch uncertainty
Random Uncertainty ($3S_{\bar{X}}$ value)	0.001 dB/10 dB
Total Uncertainty	0.004 dB/10 dB
Typical Maximum Mismatch Uncertainty	0.001 dB/10 dB
Typical Total Uncertainty (including mismatch)	0.005 dB/10 dB

The total uncertainty quoted to a customer depends upon the resettability and repeatability of the standard being measured.

The uncertainty due to impedance mismatches when calibrating attenuators on this system has been calculated using the VSWR's of the system and the attenuator being calibrated. The VSWR of this system is approximately 1.01. Therefore calculations are based on the assumption of a maximum VSWR of 1.02. Variable attenuators which are calibrated on this system have a similar VSWR; thus a mismatch error of 0.001 dB is typical. The above generalized mismatch uncertainty figure is verified with a substantial sampling of the VSWR's of variable attenuators under calibration. Note that the added mismatch uncertainty only affects attenuation increments referenced to a zero setting on the variable attenuator. An increment referenced to a higher starting point such as 20 dB is not affected significantly by mismatch since a reflected signal is 40 dB below the incident signal level.

During the calibration of fixed resistive attenuators at 30 MHz, the actual VSWR is measured at both terminals of the properly terminated attenuator so any uncertainty in the attenuation measurement due to impedance mismatch can be calculated and taken into account.

The uncertainties due to rf leakage are difficult to measure precisely. The entire calibration system is extremely well shielded in order to prevent problems caused by rf leakage. The rf power source is housed in a solid-copper, shielded room; all interconnecting cables are made of semirigid coax; NBS Type W flanged connectors are used at every interface except the insertion point; all the coaxial connections are painted with conducting paint to prevent rf radiation; and the null detection system is housed in a double screened enclosure. This greatly reduces the possibility of significant rf leakage. Thus the portion of the total uncertainty of the system due to rf leakage as presented in table 2.3 is a conservative figure, particularly for measured attenuation values below 60 decibels.

The uncertainty of calibration is usually not stated in a calibration report as 0.005 dB/10 dB as listed in table 2.3. A more specific statement is needed to better define the uncertainty of the measurement at attenuation values which are not at even 10-dB intervals. For a precision variable attenuator which is calibrated at 30 MHz, a general uncertainty statement may read as follows: "The estimated uncertainty of the measured values at the indicated points is 0.003 decibel plus 0.03 percent of the indicated change in insertion loss in decibels." However, as a service to the calibration customers, the actual uncertainty associated with each attenuation increment is calculated and tabulated in the calibration report. The report lists separate values for systematic and random uncertainties plus a total uncertainty for each point measured. (See sample calibration report following table 2.5.) The previous general uncertainty statement, however, is useful in describing NBS capability in response to inquiries and in technical publications.

2.2.2 30 MHz Phase Shift Calibration Uncertainties

Table 2.4 presents the sources and magnitudes of the uncertainties in the 30 MHz phase calibration system [10].

TABLE 2.4

30 MHz Phase Shift Calibration Uncertainties

Systematic Uncertainty

Reference standard trombone phase shifter (from table 2.2)	0.138 deg per 36 deg
Mismatch uncertainty	0 to 0.2 deg
Frequency stability (for 360° phase shift)	0.00036 deg
Phase shift in standard attenuator	0.01 deg
Resolution of coarse phase shifter	0.02 to 0.13 deg

Total Systematic Uncertainty	0.168 to 0.478 deg per 36 deg
Random Uncertainty (typical $3S_{\bar{X}}$ values)	0.01 deg
Total Uncertainty (nominal values)	≈ 0.2 to 0.5 deg per 36 deg

2.3 Procedure for Calibrating an NBS Model VII 30 MHz Attenuator

Figure 2.10 shows an operator calibrating an NBS Model VII WBCO piston attenuator at 30 MHz. This calibration is performed in the following manner.

2.3.1 Calibration Procedure for NBS Model VII Attenuators

1. Connect a standards-quality, 50-ohm, 10-dB attenuator on the output end of the attenuator under calibration. This is necessary to isolate the device under test (DUT) to insure proper a impedance match when operating the Model VII at its low attenuation values. (The 10-dB isolating attenuator can be removed when calibrating the DUT at values above 20 dB).
2. Connect this combination into the insertion point with the input of the Model VII connected to the output of the standard 30 MHz attenuator impedance matching network as shown in figure 2.2.
3. Set the attenuation of the Model VII attenuator so that the counter reads 00000 and dial reads 0. This must be done in a manner which will remove the adverse effect of the backlash in the drive mechanisms. The conventional procedure is always to approach the desired setting of the attenuator from a lower value

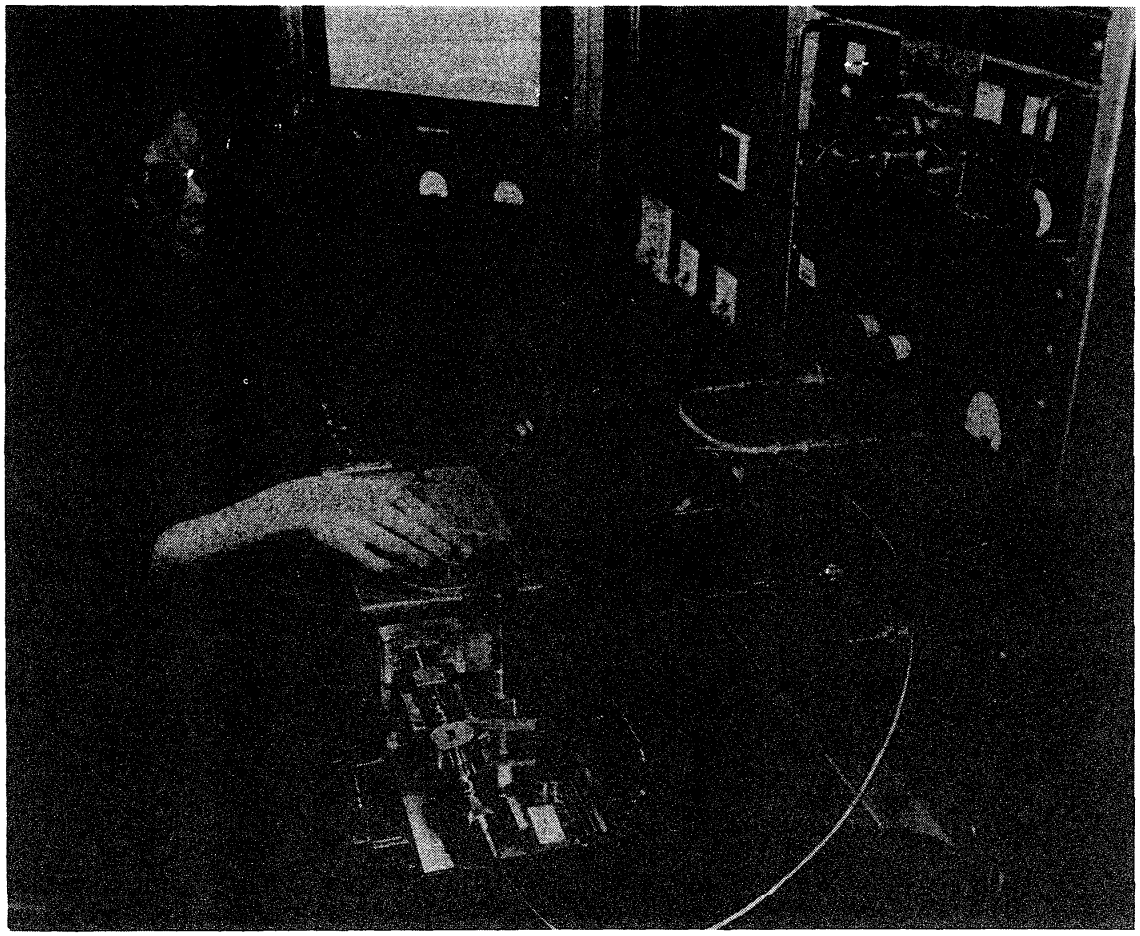

Fig. 2.10 Operator calibrating an NBS Model VII piston attenuator at 30 MHz

of attenuation setting. This technique allows the very precise setting of the desired attenuation value.

4. Adjust the receiver sensitivity to a low value by adjusting the gain control.

5. Adjust the external phase and magnitude controls on the synchronous detector so that the meter needles are at mid-scale.

6. Follow the detailed instructions for operating the null detector as stated in [11].

7. Adjust the coarse (manual) phase shifters until a null condition exists (with the precision phase shifter approximately in the center of its range).

8. Adjust the standard piston attenuator until a deeper null is reached. This can best be done by passing through the null point several times in order to determine the position of the true null point on the null indicator. The standard attenuator is operated on fast speed until the approximate null is reached; then the drive is switched to slow speed so the operator can stop the movement of the standard exactly at the null point.

9. The precision phase shifter is adjusted until the phase is nulled. This standard phase shifter also has both fast and slow speed drive motors.

10. Renull both the standard attenuator and the standard phase shifter to be certain the true system null has been found. (This may necessitate changing the null indicator sensitivity to keep the needle on scale).

11. Check the system sensitivity by changing the Model VII attenuator by 0.001 dB. The null indicator reading should change significantly if the system sensitivity is sufficient. The sensitivity can be changed by changing the power into the attenuator under calibration via the level set attenuator and by readjusting the sensitivity controls of the null detector.

    Set the attenuator under test back to the 0-dB position as explained in Step 3 above and again null the system.

12. Record the standard attenuator setting as read in the optical projector. This is the 0-dB reference setting.

13. Remove the Model VII attenuator from the insertion point leaving the 10 dB attenuator attached to the flexible cable.

14. Connect the insertion point together and renull the system as in Steps 4 through 10 above.

15. Record this value from the scale on the standard attenuator's optical projector. This value is the initial insertion loss reference setting.

16. Subtract the value obtained in Step 12 from the value obtained in Step 15. This is the insertion loss of the NBS Model VII attenuator at the 0-dB setting (approximately 30 dB).

17. Repeat this procedure two or three more times and average the results. This average attenuation value is the insertion loss of the attenuator being calibrated when it is set at 0 dB. If this insertion loss is not approximately 30 dB or if it has changed appreciably from the previous calibration, the attenuator under calibration should be suspected and checked for possible damage.

18. Repeat Steps 1 through 12 above to obtain a new 0-dB reference reading. This eliminates the possibility of erroneous readings due to drift in the calibration system, and varying impedance effects.

19. Set the attenuator under test at exactly 1.000 dB, (the desired calibration point).

20. Null the system as in Steps 4, 5, 6, 8, 9, and 10, and record the attenuation value as seen in the optical readout on the standard attenuator.

21. Repeat Step 19 and set the attenuator under test at 2.000 dB.

22. Repeat Step 20.

23. Continue this process until measurements are recorded for settings up to 10.000 dB on the attenuator under test.

24. Return this attenuator to its 0.000 dB setting and obtain the 0-dB reference setting as in Steps 3 through 12. This value should be within a few thousandths of a dB of the value obtained in the original Step 12.

25. The above procedure must be repeated to obtain readings at 15, 20, 25, 30, 35, 40, 45, 50, and 60 dB.

26. The 10-dB fixed resistive coaxial attenuator should be removed from the output end of the NBS Model VII attenuator and the cable connected directly to the Model VII output connector. This 10-dB fixed attenuator may be removed since it is not needed for matching when the attenuator under calibration is operated at levels such as 50 or 60 dB and above. The removal of this 10-dB fixed

attenuator increases the system sensitivity by 10 dB without changing the power input to the standard under test.

27. The attenuator under calibration should be set at 60.000 dB and the system nulled as in Steps 4, 5, 6 8, 9, and 10.
28. Record this value of attenuation as read from the standard attenuator optical readout. This is then used as the reference reading for the 70 and 80 dB calibration levels.
29. Calibrate the NBS Model VII attenuator at 70 and 80 dB in a manner similar to the lower dB settings. If the system sensitivity is not sufficient the power into the attenuator under calibration can be increased by changing the position of the level set attenuator as necessary.
30. This entire calibration process is repeated at least two more times so that the instrument is calibrated completely a minimum of three separate times. These results are averaged and entered into a complete calibration report.

2.3.2 Attenuator Calibration Data Reduction

The attenuation calibration data are reduced in the following manner. (Refer to table 2.5 for a typical data sheet).

1. The attenuation value for each setting of the attenuator under calibration as read from the standard attenuator is subtracted from its respective reference reading and recorded in table 2.5.

2. The average of the three columns of calibration results (change in insertion loss) is calculated to the nearest 0.001 dB and recorded.

3. This column of averaged data ($\bar{\bar{X}}$) is then used along with the three columns of data from Step 2 to compute the random uncertainty (3 times the standard deviation (SD) of the mean ($S_{\bar{\bar{X}}}$)) of the measurements. These computed values are recorded in table 2.5 and entered in the calibration report.

4. The average insertion loss (with the attenuator under test set at exactly 0 dB) is computed and rounded to the nearest 0.1 dB to be entered in the calibration report. This 0-dB insertion loss is measured by inserting and removing the Device Under Test (DUT), with the same procedure as that used for calibration of fixed attenuator. This approximate value is useful only for general information and is not considered part of the precise calibration results, and therefore does not include a reported uncertainty.

2.3.3 Tabulated Data and Calibration Results

Table 2.5 presents the tabulated calibration data on a typical NBS Model VII 30 MHz WBCO piston attenuator.

2.3.4 Typical Report of Calibration for 30 MHz WBCO Variable Attenuators

Immediately following table 2.5 is a typical complete Report of Calibration issued on the 30 MHz attenuator whose calibration data appear in table 2.5.

TABLE 2.5

OBSERVATION SHEET NBS 366

TABULATED CALIBRATION DATA ON NBS MODEL VII 30 MHz WBCO PISTON ATTENUATOR

DATE 2/6/87
SHEET NO. 1
OBSERVER clf

KIND OF MEASUREMENT Attenuation

INSTRUMENT TESTED NBS Model VII, Typical Example TEST NO. Sample No.

FREQUENCY 30 MHz ROOM TEMPERATURE 23 °C. HUMIDITY 40 %. BAROMETER — MM.

Individual Measurement Results

	Run No. 1		Run No. 2		Run No. 3			
Attn Setting	Counter Reading	Change in count decibels X_1	Counter Reading	Change in count decibels X_2	Counter Reading	Change in count decibels X_3	Computed Average of Readings $\overline{X}$	Computed $3S_{\bar{x}}$
0	67047		67049		67046			
1	66047	1.000	66047	1.002	66045	1.001	1.001	0.002
2	65045	2.002	65046	2.003	65045	2.001	2.002	0.002
3	64050	2.997	64049	3.000	64048	2.998	2.998	0.003
4	63047	4.000	63047	4.002	63046	4.000	4.001	0.002
5	62048	4.999	62047	5.002	62047	4.999	5.000	0.003
6	61050	5.997	61049	6.000	61047	5.999	5.999	0.003
7	60044	7.003	60047	7.002	60046	7.000	7.002	0.003
8	59048	7.999	59047	8.002	59045	8.001	8.001	0.003
9	58049	8.998	58047	9.002	58046	9.000	9.000	0.003
10	57046	10.001	57046	10.003	57046	10.000	10.001	0.003
		Reset						
0	67163		67160		67159			
15	52164	14.999	52163	14.997	52162	14.997	14.998	0.002
20	47161	20.002	47160	20.000	47160	19.999	20.000	0.003
25	42162	25.001	42160	25.000	42161	24.998	25.000	0.003
30	37164	29.999	37163	29.997	37163	29.996	29.997	0.003
		Reset						
30	57029		57029		57028			
35	52026	5.003	52028	5.001	52026	5.002	5.002	0.002
40	47027	10.002	47028	10.001	47028	10.000	10.001	0.002
45	42028	15.001	42029	15.000	42029	14.999	15.000	0.002
50	37025	20.004	37026	20.003	37026	20.002	20.003	0.002

OBSERVATION SHEET
NBS 266

TABLE 2.5 (CONTINUED)

DATE 2/6/87
SHEET NO. 2
OBSERVER cdt

KIND OF MEASUREMENT Attenuation
INSTRUMENT TESTED NBS Model VII, Typical Example TEST NO. Sample No. 1
FREQUENCY 30 MHz ROOM TEMPERATURE 23 °C HUMIDITY 40 % BAROMETER — MM.

Individual Measurement Results

U.S. GOVERNMENT PRINTING OFFICE

Attn. Setting	Run No. 1 Counter Reading	Change in Count Decibels X_1	Run No. 2 Counter Reading	Change in Count Decibels X_2	Run No. 3 Counter Reading	Change in Count Decibels X_3	Computed Average of Readings $\bar{X}$	Computed $3S_{\bar{X}}$
		Remove Pads + Reset						
50	66045		66048		66051			
60	56047	9.998	56051	9.997	56055	9.996	9.997	0.002
70	46046	19.999	46051	19.997	46057	19.994	19.997	0.004
80	36050	29.995	36056	29.992	36060	29.991	29.993	0.004
	Measured Insertion Loss at 0 dB = 30.752 dB							
OUT	80450		80461		80469			
IN	49693	30.757	49701	30.760	49730	30.739	30.752	.020

XBG 266

TABLE 2.5 (CONTINUED)

DATE 2/6/87
SHEET NO. 3
OBSERVER clt

KIND OF MEASUREMENT Attenuation
INSTRUMENT TESTED N B S Model VII, Typical Examples TEST NO. Sample No. 1
FREQUENCY 30 MHz ROOM TEMPERATURE 23 °C. HUMIDITY 40 %. BAROMETER — MM.
Measurement Results to be Reported

U.S. GOVERNMENT PRINTING OFFICE

Counter Setting	Dial Setting	Insertion Loss	Systematic Uncertainty	Computed $3S_{\bar{x}}$	Computed Random Uncertainty		Total Uncertainty
00010	0.000	1.001	0.003	.002	0.002		0.005
00020	↓	2.002	0.003	.002	0.002		0.005
00030		2.998	0.003	.003	0.003		0.006
00040		4.001	0.003	.002	0.002		0.005
00050		5.000	0.003	.003	0.003		0.006
00060		5.999	0.003	.003	0.003		0.006
00070		7.002	0.003	.003	0.003		0.006
00080		8.001	0.003	.003	0.003		0.006
00090		9.000	0.003	.003	0.003		0.006
00100		10.001	0.003	.003	0.003		0.006
00150		14.998	0.005	.002	0.002		0.007
00200		20.000	0.006	.003	0.003		0.009
00250		25.000	0.008	.003	0.003		0.011
00300		29.997	0.009	.003	0.003		0.012
00350		34.999	0.011	.002	0.004		0.015
00400		39.998	0.012	.002	0.004		0.016
00450		44.997	0.014	.002	0.004		0.018
00500		50.000	0.015	.002	0.004		0.019
00600		59.997	0.018	.002	0.004		0.022
00700		69.997	0.021	.004	0.005		0.026
00800	↓	79.993	0.024	.004	0.005		0.029
—	—	—	—		—		—

Measured Insertion Loss at 0 dB = 30.8 dB

U.S. DEPARTMENT OF COMMERCE
NATIONAL BUREAU OF STANDARDS
NATIONAL ENGINEERING LABORATORY
Boulder, Colorado 80303

REPORT OF CALIBRATION

VARIABLE WAVEGUIDE BELOW-CUTOFF ATTENUATOR, COAXIAL CONNECTORS
National Bureau of Standards
Model VII, Typical Example

Submitted by:

National Bureau of Standards
Division 723.01
Boulder, Colorado 80303

The measurements on this attenuator were performed under ambient conditions of approximately 23° ± 2° C and 40 ± 5 percent relative humidity. The power presented to the attenuator during the calibration was less than 300 milliwatts. The attenuator was terminated at each end in approximately 50 ± j0 ohms. The calibration frequency of 30 MHz was accurate to one part in 10^6. The measured change in insertion loss when the counter is increased from a 00000 reference setting and the dial is increased from a 0.000 reference setting is indicated in the attached table.

The measured value of the "0 dB insertion loss" of the attenuator with the counter set at 00000 and the dial set at 0.000 was determined to be approximately 30.8 decibels.

Test No. Sample No. 1
Date of Calibration: February 6, 1987

Variable Waveguide Below-Cutoff Attenuator,
Coaxial Connectors
National Bureau of Standards
Model VII, Typical Example

Counter Setting	Dial Setting	Measured Change in Insertion Loss dB	Systematic Uncertainty dB	Random Uncertainty dB	Total Uncertainty dB
00010	0.000	1.001	0.003	0.002	0.005
00020	0.000	2.002	0.003	0.002	0.005
00030	0.000	2.998	0.003	0.003	0.006
00040	0.000	4.001	0.003	0.002	0.005
00050	0.000	5.000	0.003	0.003	0.006
00060	0.000	5.999	0.003	0.003	0.006
00070	0.000	7.002	0.003	0.003	0.006
00080	0.000	8.001	0.003	0.003	0.006
00090	0.000	9.000	0.003	0.003	0.006
00100	0.000	10.001	0.003	0.003	0.005
00150	0.000	14.998	0.005	0.002	0.007
00200	0.000	20.000	0.006	0.003	0.009
00250	0.000	25.000	0.008	0.003	0.011
00300	0.000	29.997	0.009	0.003	0.012
00350	0.000	34.999	0.011	0.004	0.015
00400	0.000	39.998	0.012	0.004	0.016
00450	0.000	44.997	0.014	0.004	0.018
00500	0.000	50.000	0.015	0.004	0.019
00600	0.000	59.997	0.018	0.004	0.022
00700	0.000	69.997	0.021	0.005	0.026
00800	0.000	79.993	0.024	0.005	0.029

This calibration data is valid only when the attenuator is set by approaching the indicated value from a lower value of attenuation.

Page 2 of 3
Test No. Sample No. 1
Date of Calibration: February 6, 1987

Variable Waveguide Below-Cutoff Attenuator,
Coaxial Connectors
National Bureau of Standards
Model VII, Typical Example

Three measurements were made at each attenuator setting to find the mean value of "Measured Change in Insertion Loss" and to estimate the standard deviation (S.D.) of this mean. The total uncertainty is the sum of the systematic uncertainty and the random uncertainty where the latter is defined as three times the estimate of the S.D. of the mean.

For convenience, usually one or more intermediate reference settings are used during calibration. To determine the estimate of the S.D. of the mean for a specific insertion loss setting which was measured with respect to an intermediate setting, the S.D. of the intermediate setting and the S.D. of the specific setting were combined by taking the root-sum-of-the-squares of the respective S.D. values.

Calibration performed by:
Connie L. True

Connie L. True, (303)497-3524

For the Director,
National Engineering Laboratory

Robert T. Adair

Robert T. Adair, Sr. Project Leader
Microwave Metrology Group
Electromagnetic Fields Division

Verified by:
L. Saulsbery

Leon F. Saulsbery

Page 3 of 3
Test No. Sample No. 1
Date of Calibration: February 6, 1987
Reference: RTA

It should be noted that the spread in the three different columns of data is no more than a few thousandths of a dB. This attests to the stability, repeatability, and resettability of the entire dual channel calibration system as well as the NBS piston attenuator being calibrated.

The dial on the NBS Model VII attenuator can be read to a smaller value than 0.0005 dB which, along with its repeatability and stability, provides greater calibration accuracy than most 30 MHz attenuators which are calibrated at NBS.

2.4 Procedure for Calibrating a 30 MHz Phase Shifter

The units of this procedure are not given in SI units. The readout of the device under test is given in degrees, and therefore the results are computed and stated in degrees.

A phase shifter may be calibrated over a 360-deg range at 30 MHz using the same system shown in figure 2.10 with the phase shifter inserted in the system instead of the attenuator under test. This calibration is performed in the following manner.

2.4.1 Calibration procedure for 30 MHz Phase Shifter

1. Connect a standards-quality, 50-ohm, 20-dB fixed resistive attenuator on the output of the phase shifter. This 20-dB attenuator insures proper impedance matching of phase shifter and system.
2. Adjust the 30 MHz receiver to low sensitivity by adjusting the gain control.

3. Connect this combination into the insertion point with the input of the phase shifter connected to the output of the 30 MHz standard attenuator matching network as shown in figure 2.2.
4. Set the phase shifter under calibration to 0 degree. This must be done by approaching this setting from a setting below the one desired to eliminate the undesirable effects of any backlash which might exist in the phase shifter drive mechanism.
5. Adjust the position of the 30 MHz standard phase shifter to a counter setting of approximately 3000 which will allow a phase shift of slightly more than 30 deg since one count equals 0.01142 deg.
6. Adjust the external phase and magnitude controls on the synchronous detector so the meter needles are at mid-scale.
7. Follow the detailed instructions for operating the null detector as stated in [12].
8. Adjust the coarse (manual) phase shifters until a null is reached.
9. Adjust the standard attenuator until a deeper null is reached. This will necessitate increasing the sensitivity of the null indicator to keep the needle on a readable portion of the scale. This standard can be moved toward the null position with the fast speed drive motor until the null is passed. Then the slow speed drive motor can be used to adjust the standard attenuator to the position of final null.
10. The precision phase shifter is next adjusted until a deeper null is found. This phase shifter also has fast and slow speed drive motors.

11. Renull both the standard attenuator and the precision standard phase shifter to be certain the true null of the system has been found. This may require readjusting the system sensitivity for more optimum use of the null indicator.

12. Check the system sensitivity by changing the setting of the phase shifter under test to 0.01 degree. The null indicator reading should change significantly if the system sensitivity is sufficient. The system sensitivity can be changed if necessary by readjusting the power input to the phase shifter under test via the level set attenuator and by readjustment of the sensitivity controls of the differential amplifier and the null indicator.

13. Set the phase shifter under test to 0 deg as explained in step 4 above and again null the system.

14. Record the standard attenuator setting and the standard phase shifter counter setting. These values are the 0 deg reference values shown in table 2.6 which follows section 2.4.2.

15. Remove the phase shifter from the insertion point leaving the 20 dB fixed attenuator attached to the flexible cable of the insertion point.

16. Reconnect the insertion point and renull the system as in steps 5 through 11 above.

17. Record the value from the standard attenuator's optical projector. This value is the initial insertion loss reference reading.

18. Subtract the value of attenuation obtained in step 14 from the value obtained in step 17. This result is the insertion loss of the phase shifter being calibrated at its 0 degree setting.

19. Repeat this procedure two or three more times and average the results to obtain the report value of the insertion loss of the phase shifter when it is set at 0 degree. If this value of insertion loss is not approximately the same as the manufacturers nominal value or if it has changed appreciably from the last time it was calibrated, the phase shifter under calibration should be suspected and checked for possible damage.

20. Repeat steps 1 through 14 above to obtain new 0-deg reference readings. This greatly reduces the possibility of erroneous readings due to drift in the calibration system.

21. Switch the null indicator out of the circuit and set the phase shifter under test to exactly 30 deg. For illustrative purposes the hypothetical calibration of this phase shifter will be performed at 30-deg intervals to reduce the amount of data to be handled.

22. Run the standard phase shifter with the fast speed drive motor until its counter reads approximately 200.

23. Switch the null indicator back into the circuit and renull the system as in steps 5, 6, 7, 9, 10 and 11.

24. Record the values as read from the standard attenuator and the standard phase shifter.

25. Adjust the setting of the standard phase shifter back to a counter reading of approximately 3000. Notice that the phase shifter under test is still set at exactly 30 deg.

26. Repeat steps 5 through 11 above.

27. Record the standard attenuator and standard phase shifter readings. These are the 30-deg reference readings.

28. Switch the null indicator out of the circuit and set the phase shifter under test to exactly 60-deg.

29. Repeat steps 5, 6, 7, 9, 10 and 11.

30. Record the standard attenuator and the standard phase shifter readings.

31. Repeat step 25 but notice the phase shifter under test remains set at 60 deg.

32. Repeat steps 5 through 11.

33. Record the standard attenuator and standard phase shifter readings. These values are the 60-deg reference readings.

    Since this precision phase shifter has a range of approximately only 40 deg each successive 30-deg setting on the phase shifter under test is used as a reference instead of a 0-deg reference. This allows the operator to step from 0 to 360 deg in increments of 30 deg. This makes it possible to calibrate a phase shifter all the way from 0 to 360 deg even though the standard phase shifter has a capability of approximately 40 deg.

34. Continue this process until the phase shifter is calibrated from 0 to 360 deg.

35. This entire calibration process must be repeated a minimum of two more times so that the instrument is calibrated completely at least three separate times. These results are averaged and form a complete calibration report.

2.4.2 Phase Shifter Calibration Data Reduction

The phase shift calibration data are reduced in the following manner. (Refer to table 2.6 following this section for a typical data sheet).

1. The standard phase shifter counter reading for each setting of the phase shifter under test is subtracted from its respective reference reading.
2. This is done for each of the three separate calibration runs, and the three results for each setting of the phase shifter under test are averaged.
3. These averages are then multiplied by 0.01142 deg per count to convert the number of counts per interval to the number of deg per interval.
4. These averages are successively added to obtain the total phase shift for each setting of the phase shifter under test.
5. Notice that the phase shift for the 360-deg setting is slightly less than 360 deg. This occurs since the operator must successively step the setting from 0 to 360 deg in intervals of 30 deg. To correct for this a technique known as "closing the data" is employed.
6. Closing the data is accomplished by subtracting the actual 360-deg measured value from 360.000 deg and dividing this number by the number of intervals measured between 0 and 360 deg. This resultant angle, which is extremely small, is the correction which must be added to the value of phase shift measured for the first interval (the 30-deg reading in this case). Two times this correction must be added to the second interval (the 60-deg reading) and

so on. The total correction which is added to the 360-deg data should correct that measured value to 360.000 deg.

7. The attenuation value for each setting of the phase shifter under calibration is subtracted from its respective reference reading.
8. These attenuation values are successively added algebraically to obtain the amount of attenuation which is present in the phase shifter at each setting of phase angle with respect to the original 0-deg insertion loss.
9. These three columns of data are averaged to obtain the values which appear in the calibration report.
10. The column of averaged phase shift data is rounded to the nearest 0.01 deg and entered in the calibration report.
11. The column of data of average attenuation change is rounded to the nearest 0.001 dB and entered in the calibration report to the nearest 0.01 dB.
12. The average initial insertion loss data are computed and rounded to the nearest 0.1 dB and entered in the calibration report.

2.4.3 Tabulated Data and Calibration Results for 30 MHz Phase Shifter

Table 2.6 presents the tabulated calibration data on a commercial 30 MHz phase shifter. These data are the averages of three separate calibration runs on this particular device.

2.4.4 Typical Report of Calibration for 30 MHz Phase Shifters

Immediately following table 2.6 is a typical complete report of calibration issued on the 30 MHz phase shifter whose data appear in table 2.6.

TABLE 2.6

TABULATED CALIBRATION DATA ON
A COMMERCIAL PHASE SHIFTER

OBSERVATION SHEET
NBS 866

DATE 2/9/87
SHEET NO. 1
OBSERVER CDT

KIND OF MEASUREMENT Phase Shift
INSTRUMENT TESTED Merrimac Type R-30, Typical Exp. TEST NO. Sample No.
FREQUENCY 30 MHz ROOM TEMPERATURE 23 °C. HUMIDITY 40 % BAROMETER — MM.

Individual Measurement Results

U.S. GOVERNMENT PRINTING OFFICE

SETTING DEGREES	Run No. 1 Counter Reading	Change in Count / Degrees X_1	Run No. 2 Counter Reading	Change in Count / Degrees X_2	Run No. 3 Counter Reading	Change in Count / Degrees X_3	Change in Attenuation Reading	Average Counts From Reference $\bar{X}$
0	430		425		433		75081	
30	3055	2625	3055	2630	3056	2623	75061	2626
		29.98		30.03		29.95	+.020	
30	430		423		426		75126	
60	3054	2624	3052	2629	3053	2627	75089	2627
		29.97		30.02		30.00	+.037	
60	430		432		429		75198	
90	3107	2677	3093	2661	3097	2668	75188	2669
		30.57		30.39		30.47	+.010	
90	429		434		439		75273	
120	3074	2645	3076	2642	3083	2641	75382	2643
		30.21		30.17		30.16	−.109	
120	430		422		421		75372	
150	2992	2562	2995	2573	3002	2581	75405	2572
		29.26		29.38		29.48	−.033	
150	430		421		426		75316	
180	3034	2604	3034	2613	3032	2606	75259	2608
		29.74		29.84		29.76	+.057	
180	429		430		428		75135	
210	3064	2635	3061	2631	3062	2634	75119	2633
		30.09		30.05		30.08	+.016	

OBSERVATION SHEET
NBS 344

TABLE 2.6 (CONTINUED)

DATE 2/9/87
SHEET NO. 2
OBSERVER clt

KIND OF MEASUREMENT Phase Shift
INSTRUMENT TESTED Merrimac Type R-30, Typical Example TEST NO. Sample No.
FREQUENCY 30MHz ROOM TEMPERATURE 23 °C. HUMIDITY 40 %. BAROMETER — MM.

Individual Measurement Results

U.S. GOVERNMENT PRINTING OFFICE

Setting Degrees	Run No. 1 Counter Reading	Run No. 1 Change in Count/Degrees X_1	Run No. 2 Counter Reading	Run No. 2 Change in Count/Degrees X_2	Run No. 3 Counter Reading	Run No. 3 Change in Count/Degrees X_3	Change in Attenuation Reading	Average Counts From Reference $\bar{X}$
210	430		429		424		75140	
240	3057	2627	3051	2622	3052	2628	75105	2626
		30.00		29.94		30.01	+.035	
240	431		431		435		75188	
270	3097	2666	3098	2667	3097	2662	75180	2665
		30.45		30.46		30.40	+.008	
270	431		432		438		75281	
300	3060	2629	3060	2628	3066	2628	75382	2628
		30.02		30.01		30.01	-.101	
300	438		436		429		75472	
330	2990	2552	2990	2554	2993	2564	75497	2557
		29.14		29.17		29.28	-.025	
330	430		426		429		75533	
360	3033	2603	3030	2604	3036	2607	75470	2605
		29.73		29.74		29.77	+.063	

Measured Insertion Loss at Ø Degrees = 35.9 dB

OUT	79801	—	79836					
IN	43898	35.903	44028	35.808				35.856

OBSERVATION SHEET
NBS 555

TABLE 2.6 (CONTINUED)

DATE 2/9/87
SHEET NO. 3
OBSERVER cAt

KIND OF MEASUREMENT Phase Shift
INSTRUMENT TESTED Mississ Type R-30 Typical Example TEST NO. Sample No. 2
FREQUENCY 30MHZ ROOM TEMPERATURE 23 °C. HUMIDITY 40 %. BAROMETER — MM.
Averages of Measurement Results

U.S. GOVERNMENT PRINTING OFFICE

SETTING DEGREES	AVERAGE COUNTER READING $\bar{X}$	(x).01142 DEGREES	(+) ϕ CLOSING CORRECTION	CORRECTED VALUE	ACCUMULATED VALUE	COMPUTED $3S_{\bar{X}}$	Δ ATTENUATION dB
30	2626	29.99	.063	30.05	30.05	0.07	+0.02
60	2627	30.00	↓	30.06	60.11	0.04	+0.04
90	2669	30.48		30.54	90.65	0.16	+0.01
120	2643	30.18		30.24	120.89	0.05	−0.11
150	2572	29.37		29.43	150.32	0.19	−0.03
180	2608	29.78		29.84	180.16	0.09	+0.06
210	2633	30.07		30.13	210.29	0.04	+0.02
240	2626	29.99		30.05	240.34	0.07	+0.04
270	2665	30.43		30.49	270.83	0.06	+0.01
300	2628	30.01		30.07	300.90	0.01	−0.10
330	2557	29.20		29.26	330.16	0.13	−0.03
360	2605	29.75	↓	29.81	359.97	0.04	+0.06
		359.25					

Measured Insertion Loss at ϕ degrees = 35.9 dB

OBSERVATION SHEET
NBS 266

TABLE 2.6 (CONTINUED)

DATE 2/9/87
SHEET NO. 4
OBSERVER CAH

KIND OF MEASUREMENT Phase Shift
INSTRUMENT TESTED Merrimac Type R-30, Typical Example TEST NO. Sample No. 2
FREQUENCY 30 MHz ROOM TEMPERATURE 23 °C. HUMIDITY 40 %. BAROMETER ——— MM.

Measurement Results to be Reported

U.S. GOVERNMENT PRINTING OFFICE

Dial Setting (Degrees)	Change in Phase (Degrees)	Insertion Loss (Decibels)	Random Uncertainty (Degrees)
30	30.05	0.02	0.07
60	60.11	0.04	0.04
90	90.65	0.01	0.16
120	120.89	-0.11	0.05
150	150.32	-0.03	0.19
180	180.16	0.06	0.09
210	210.29	0.02	0.04
240	240.34	0.04	0.07
270	270.83	0.01	0.06
300	300.90	-0.10	0.01
330	330.16	-0.03	0.13
360	359.97	0.06	0.04

Measured Insertion Loss at 0 degrees = 35.9 dB

U.S. DEPARTMENT OF COMMERCE
NATIONAL BUREAU OF STANDARDS
NATIONAL ENGINEERING LABORATORY
Boulder, Colorado 80303

REPORT OF CALIBRATION

VARIABLE COAXIAL PHASE SHIFTER
Merrimac Research and Development, Incorporated
Type R-30, Typical Example

Submitted by:

National Bureau of Standards
Division 723.01
Boulder, Colorado 80303

The measurements on this phase shifter were performed under ambient conditions of approximately 23° ± 2° C and 40 ± 5 percent relative humidity. The power presented to the phase shifter was less than 1.0 milliwatt. The VSWR presented to each terminal of the phase shifter was less than 1.05. The calibration frequency of 30 MHz was accurate to one part in 10^6.

The measured value of the initial insertion loss of the phase shifter with the dial set at 0.0 was determined to be approximately 35.9 decibels.

The change in phase when the dial is increased from a 0.0 reference setting is indicated in the following table. The change in insertion loss column represents an incremental change in total insertion loss of the phase shifter corresponding to the 30 degree dial setting increments. A negative value indicates a decrease in insertion loss from the preceding calibration point.

Dial Setting degrees	Measured Phase-Shift Difference electrical degrees	Change in Insertion Loss decibels	Random Uncertainty degrees
30	30.05	0.02	0.07
60	60.11	0.04	0.04
90	90.65	0.01	0.16
120	120.89	-0.11	0.05
150	150.32	-0.03	0.19
180	180.16	0.06	0.09
210	210.29	0.02	0.04
240	240.34	0.04	0.07
270	270.83	0.01	0.06
300	300.90	-0.10	0.01
330	330.16	-0.03	0.13
360	359.97	0.06	0.04

Page 1 of 2
Test No. Sample No. 2
Date of Calibration: February 9, 1987

Variable Coaxial Phase Shifter
Merrimac Research and Development, Incorporated
Type R-30, Typical Example

The "Measured Phase-Shift Difference" in electrical degrees is the mean of three separate readings taken during the measurement at the given dial setting.

The random uncertainty of the measured values is equal to three times the calculated standard deviation of the mean of the three separate determinations at each dial setting.

The systematic uncertainties are ± 0.1 degree and ± 0.01 decibel respectively for each 30 degree increment. The total uncertainty for each phase shift increment is given as the sum of the systematic uncertainty and the random uncertainty. These incremental uncertainties are not accumulative since closure within 0.01 degree was achieved at the 360 degree (0) setting. Closure was similarly achieved for insertion loss variation.

Calibration performed by:
Connie L. True
Connie L. True, (303)497-3524

For the Director,
National Engineering Laboratory

Robert T. Adair
Robert T. Adair, Sr. Project Leader
Microwave Metrology Group
Electromagnetic Fields Division

Verified by:
L. Saulsbery
Leon F. Saulsbery

Test No. Sample No. 2
Date of Calibration: February 9, 1987
Reference: RTA

2.5 Conclusions - Dual-Channel Rf Null Technique

The basic direct substitution technique (as illustrated in figure 2.1) has many advantages over a single-channel system as was mentioned previously. Briefly this dual-channel unmodulated technique provides extremely high resolution, large calibration-range attenuation, minimal effects of signal source amplitude instabilities, and avoids the complexity and errors due to modulation. A constant insertion loss phase shifter is necessary, however, and allows the system to be used for precise phase shift calibrations.

A satisfactory dual-channel rf null attenuation and phase calibration system similar to the NBS 30 MHz system can be constructed in nearly any well-equipped standards laboratory with existing or available equipment.

3.0 Measurement Uncertainty and Quality Assurance

3.1 NBS System Measurement Uncertainty

3.1.1 30 MHz Standard Piston Attenuator

The components of the uncertainty budget for the 30 MHz standard piston attenuator are listed in table 2.1. The key values are repeated here for convenience.

A. Uncertainty due to variation in the attenuator waveguide diameter: 0.0003 dB/10 dB.

B. Uncertainty in measuring piston displacement. This is governed by the accuracy of the ruled steel scale and optical readout: 0.001 dB/10 dB.

C. Uncertainty in estimation of the rf conductivity of the waveguide walls. This is the same order of magnitude as the machining tolerances on the waveguide itself: 0.00026 dB/10 dB.

This yields a total systematic uncertainty budget for the attenuation standard of 0.00156 dB per 10 dB increment. Total maximum systematic uncertainty of the attenuator: 0.0016 dB/10 dB. It would be possible to reduce this by one half by replacing the scale with a laser interferometer displacement measuring system. This technique has been implemented in the United Kingdom at NPL, and at CSIRO in Australia as well as by a commercial manufacturer in the U.S. NBS plans to implement this improvement in the near future as resources permit. Until recently the total systematic uncertainty of the NBS attenuator calibration service has been adequate to meet defense and industry requirements.

3.1.2 30 MHz Standard Phase Shifter

The components of the uncertainty budget for the 30 MHz standard trombone phase shifter are listed in table 2.2. The total uncertainty over its 36-deg measurement range does not exceed 0.138 deg.

A second key value related to this reference standard is its deviation from constant amplitude of less than 0.0005 dB over a range of 30 deg. This value is critical to assess uncertainties in measuring attenuation since it affects the reference arm of the null system.

Systematic uncertainty of phase shifter: 0.138 deg/36 deg.

Level variation over 30 deg: 0.0005 dB.

3.1.3 Measurement Uncertainty for Attenuation

The uncertainty budget for attenuation measurement is given in table 2.3. The key components of uncertainty are repeated below for convenience.

A.	Uncertainty of standard attenuator:	0.0016 dB/10 dB
B.	System leakage and reference channel variation due to standard phase shifter:	0.001 dB/10 dB
C.	Resolution of detection system:	0.0004 dB/10 dB
	Total systematic uncertainty	0.003 dB/10 dB
D.	Typical random uncertainty ($3S_{\bar{x}}$ value)[4]	0.001 dB/10 dB
	Total uncertainty	0.004 dB/10 dB

[4]The $3S_{\bar{x}}$ value is 3 times the computed standard error for the mean.

There are additional uncertainties in calibration if mismatch uncertainty is significant. Normally the uncertainty is between 0.001 and 0.002 dB which leads to a typical calibration uncertainty of 0.005 dB for a 10 dB fixed attenuator. This uncertainty is not applicable to WBCO attenuators where the large value of their minimum insertion loss renders them insensitive to terminating impedances.

3.1.3.1 Uncertainties Associated with Typical Attenuators

A. International comparisons and primary standards lab quality devices:	0.003 dB/10 dB
B. Good quality calibration standards with low rf leakage:	0.004 dB/10 dB
C. Average quality variable attenuators and fixed devices with mismatch uncertainties:	0.005 dB/10 dB

3.1.4 Measurement Uncertainties for Incremental Phase Shift

The uncertainty budget for phase shift measurement is given in table 2.4. The key components of uncertainty are repeated below for convenience.

A. Uncertainty of standard phase shifter (36 deg range):	0.138 deg/36 deg
B. Miscellaneous (standard attenuator, frequency stability, and coarse phase shifter resolution):	0.030 deg/36 deg
Total systematic uncertainty over 36 deg:	0.168 deg

C. Typical random uncertainty ($3S_{\bar{X}}$ value) on

any increment: 0.01 deg

Minimum total reported uncertainty: 0.2 deg/36 deg

The uncertainty due to impedance mismatches can be neglected because any variable phase shifter is isolated from the rest of the system by isolating attenuators whose VSWR is less than 1.01. The resultant phase shifter uncertainty (incremental) is less than 0.01 deg due to impedance mismatches and can be safely ignored.

3.2 Typical NBS System Attenuation Calibration Results

The following graphs are arranged in basic groups by type of attenuation standard.

3.2.1 Calibration of the NBS Model SA-1, 10-dB Step Attenuator. (Figure 3.1).

The Model SA-1 step attenuator was designed and constructed by NBS for several primary calibration laboratories and is based on the WBCO principle. It is a device which produces a highly repeatable 10-dB step attenuation measured by two gage blocks whose differential length is determined by an electronic null indicating system. The repeatability of setting is 0.001 dB and the calculated uncertainty of the 10-dB increment is 0.004 dB.

Calibration of this device provides both an independent check of the NBS primary standard absolute value and a measure of long-term stability of the NBS measurement system.

Figure 3.1 is a plot of the calibration results of five independent SA-1 attenuators have been measured over a 12-year time span. All device values lie within the assigned NBS uncertainty bounds except for one on test 951911 performed in 1972. Since the measured value of this unit returned to an expected value within limits in 1978 and values for the other units did not shift unidirectionally in 1972, we can assume a minor mechanical defect was exhibited by test 951911. This could have been caused by foreign material lodged on a gage pin which was subsequently dislodged or removed by recommended cleaning procedures.

3.2.1.1 Conclusions:

1. The assigned uncertainty limits are valid, and
2. The calibration system is in statistical control.

3.2.2 Calibration of NBS-Designed WBCO attenuators (Figures 3.2 through 3.9)

These NBS designed attenuators were calibrated over a working range of 80 decibels and results have been plotted for each 10-dB increment. As is the case with the Model SA-1, all of these devices are calculable standards based on dimensional measurements. The individual models are only slightly different from each other in mechanical details, and share a common waveguide diameter and thus have approximately the same calculated uncertainty of 0.005 to 0.008 dB per 10-dB increment.

A careful examination of the eight individual plots indicates that in over 22 years of calibration history for these devices using the same measurement system, there are only eleven values outside the assigned NBS uncertainty limits. Ten of these measurement values were obtained between 1963 and 1966, primarily for higher values of attenuation where rf leakage can cause significant uncertainty. In all of these cases the particular attenuators were refurbished by NBS to reduce leakage which solved the problem. The remaining out-

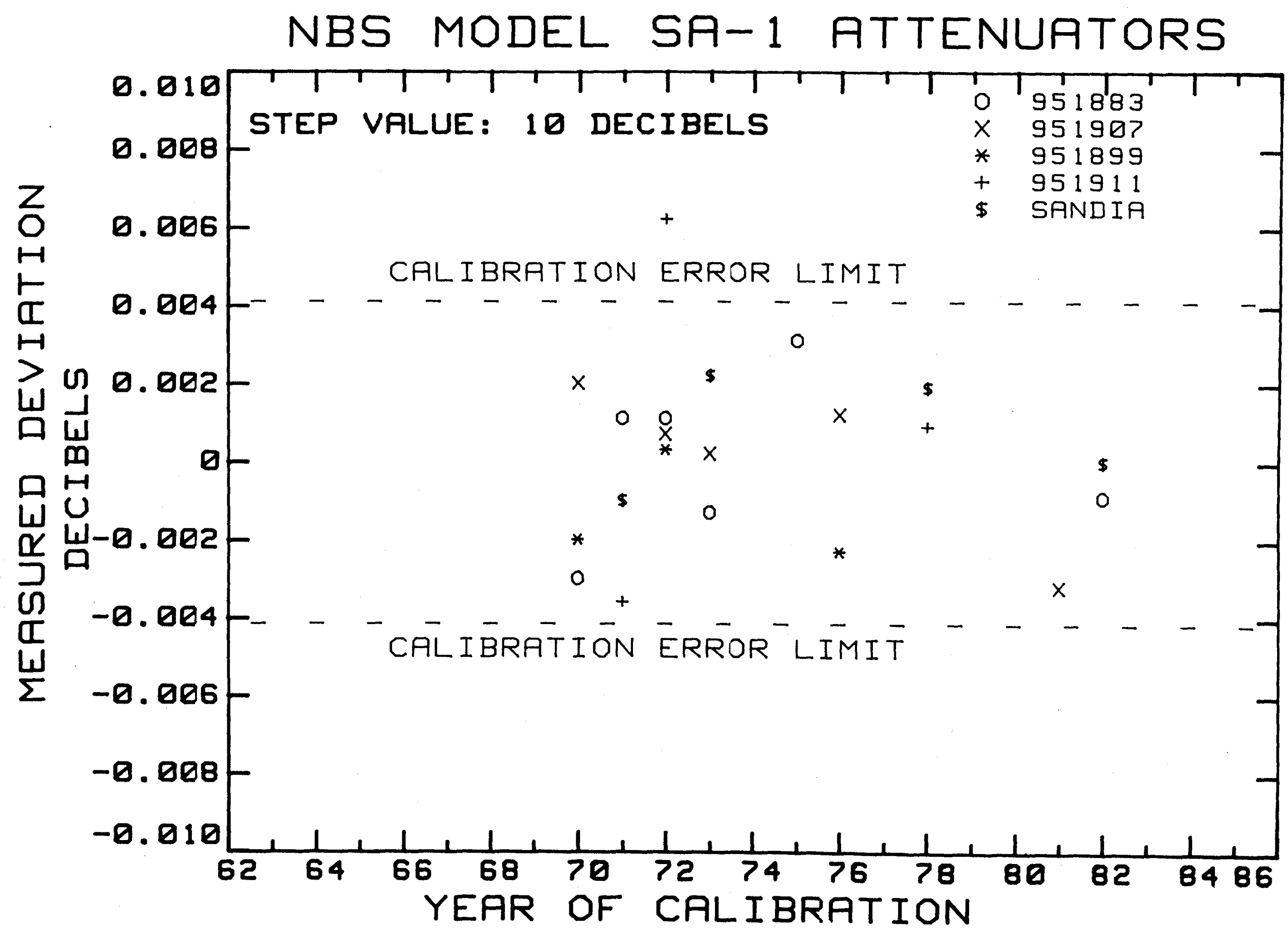

Figure 3.1 Calibration Results for NBS Model SA-1 10 dB Step Attenuators, 1970 to 1982.

lier in 1971 for test 950729 at 70 dB is not clearly explained. A recalibration in 1972 showed that this 70-dB value was again within limits. This attenuator had shown greater year-to-year variation than normal in the past and has not been resubmitted since 1972. Apparently it has been retired from service.

3.2.2.1 Conclusions:

1. The assigned uncertainty limits are valid and additionally verified by comparison with independently calculable attenuators.
2. The system has remained in statistical control over a 22-year time span. These results were achieved, even though during this time period the system was rebuilt twice. The system was modified by adding a new trombone phase shifter, replacing the null detection system and upgrading the rf source three times.

3.2.3 Calibration of Commercial WBCO Attenuators

(Figures 3.10 through 3.19). This group of plots tracks the values of 14 separate attenuators over a 20-year time span (individual attenuators have values for up to 19 years).

Since these attenuators were not designed by NBS, their calculated values cannot be used to validate the absolute values of the NBS system. Their mechanical dimensions and waveguide material differ from NBS designs and thus require different correction factors. The theory remains valid however, and

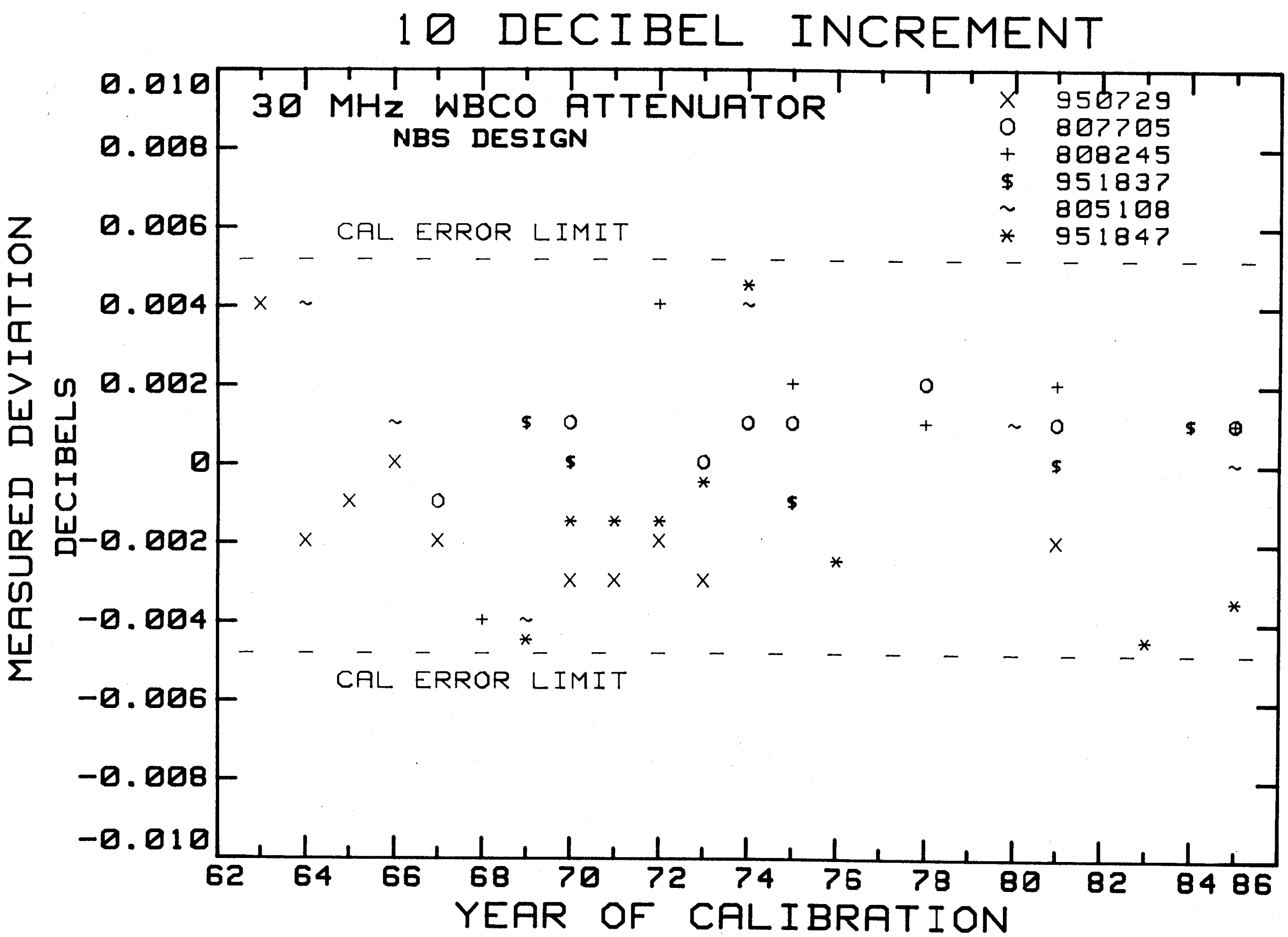

Figure 3.2. Calibration Results for NBS Design Variable WBCO Attenuators (10-dB increment), 1963 to 1985.

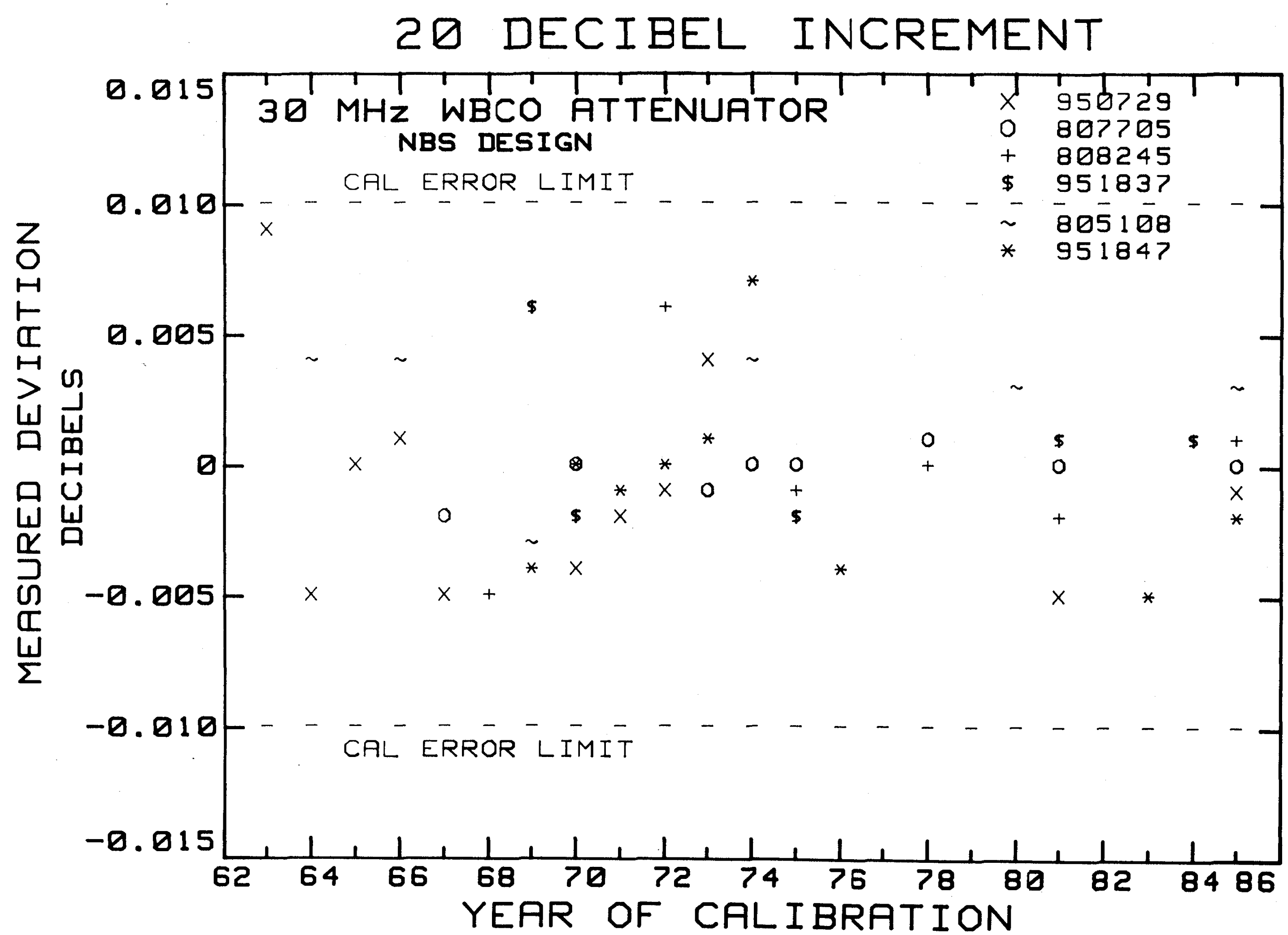

Figure 3.3. Calibration Results for NBS Design Variable WBCO Attenuators (20-dB increment), 1963 to 1985.

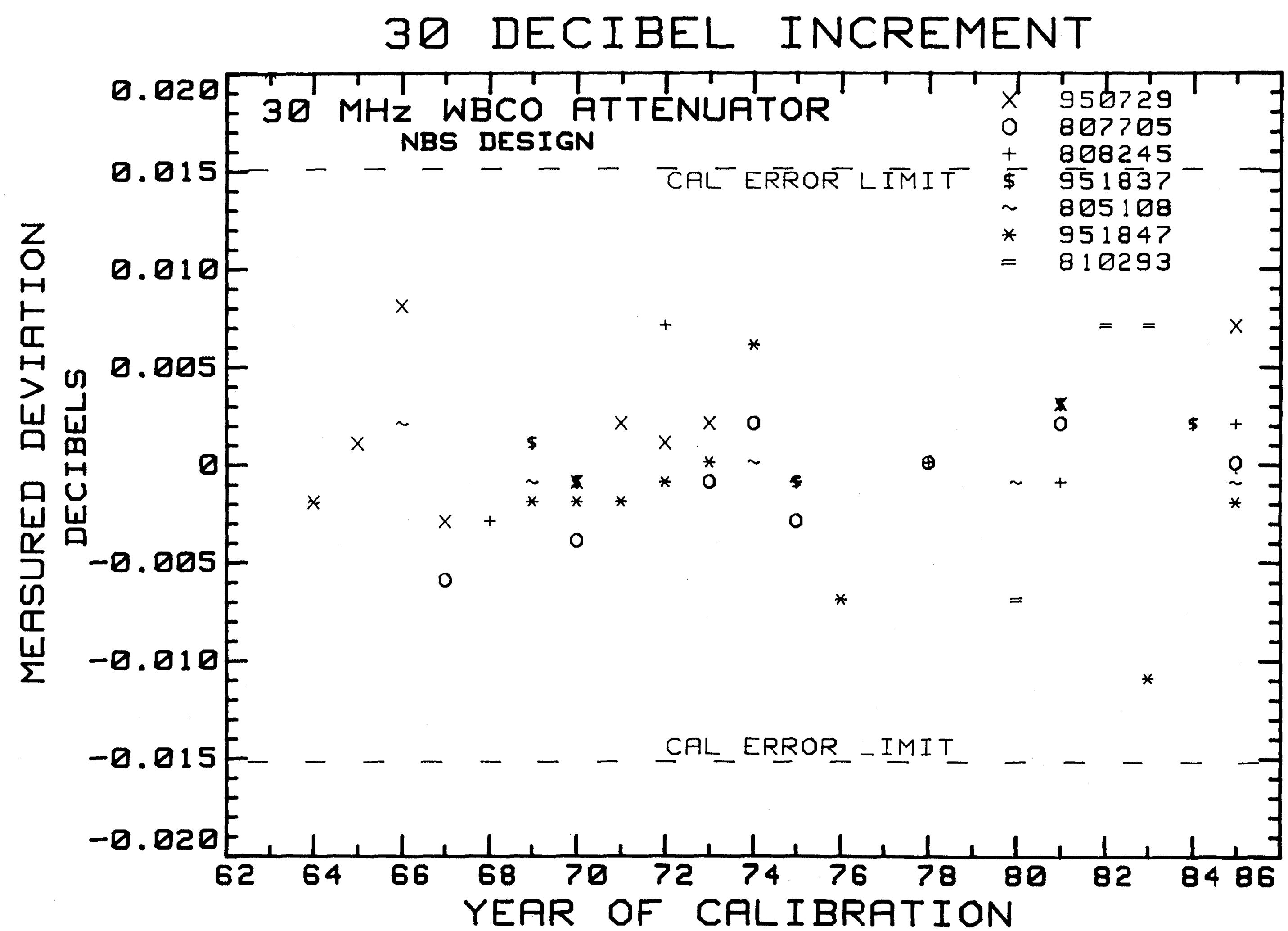

Figure 3.4. Calibration Results for NBS Design Variable WBCO Attenuators (30-dB increment), 1963 to 1985.

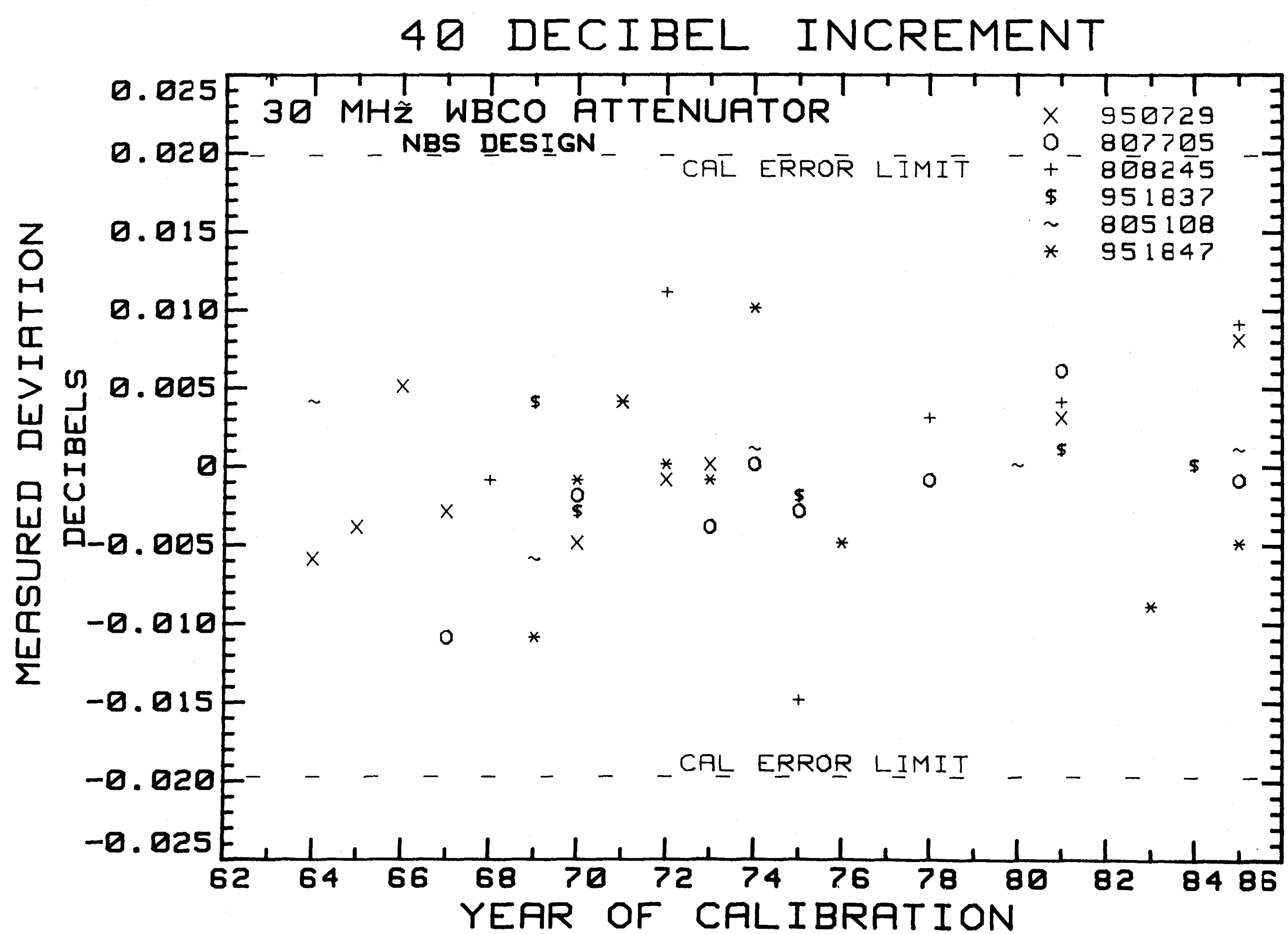

Figure 3.5. Calibration Results for NBS Design Variable WBCO Attenuators (40-dB increment), 1963 to 1985.

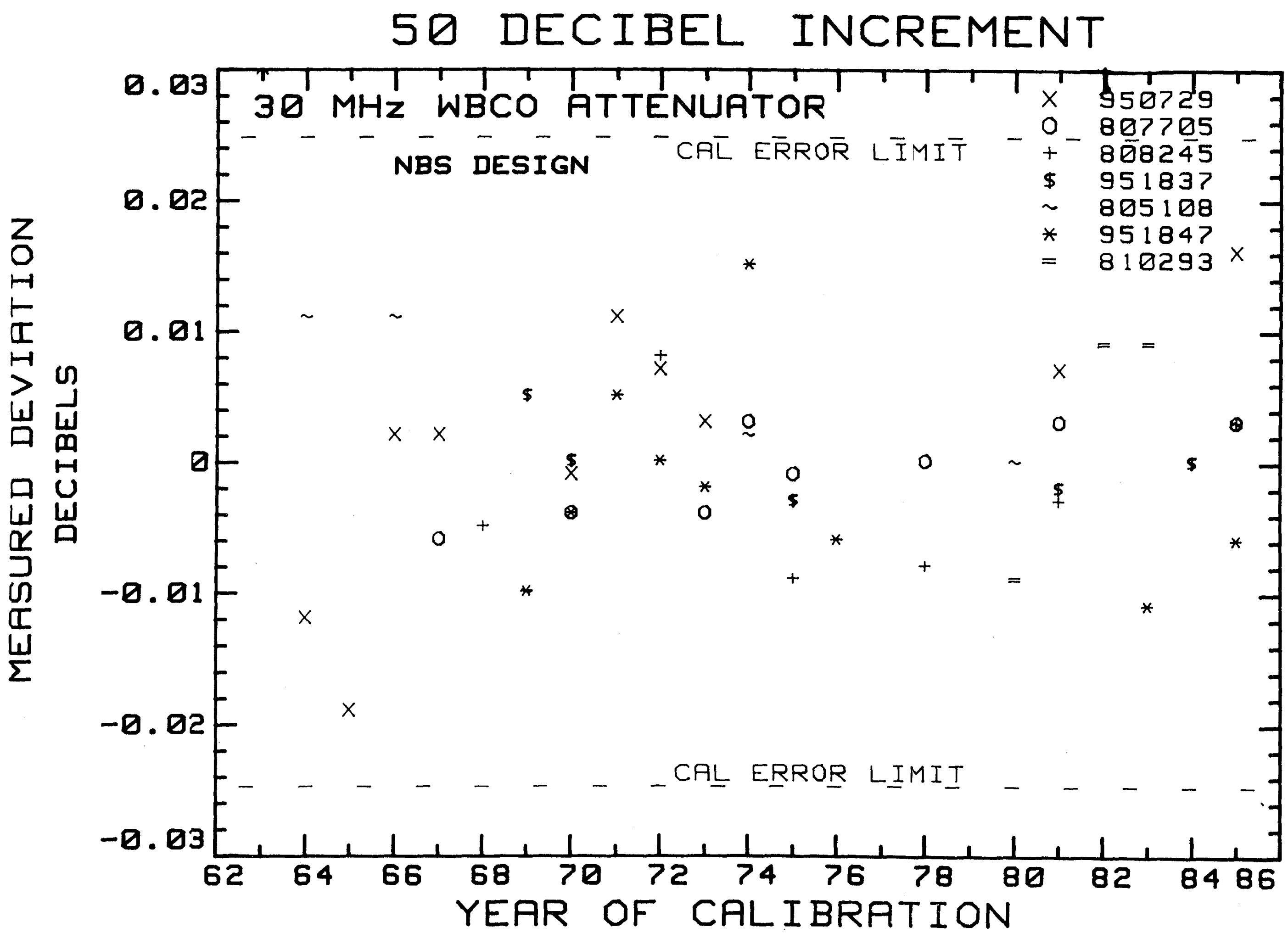

Figure 3.6. Calibration Results for NBS Design Variable WBCO Attenuators (50-dB increment), 1963 to 1985.

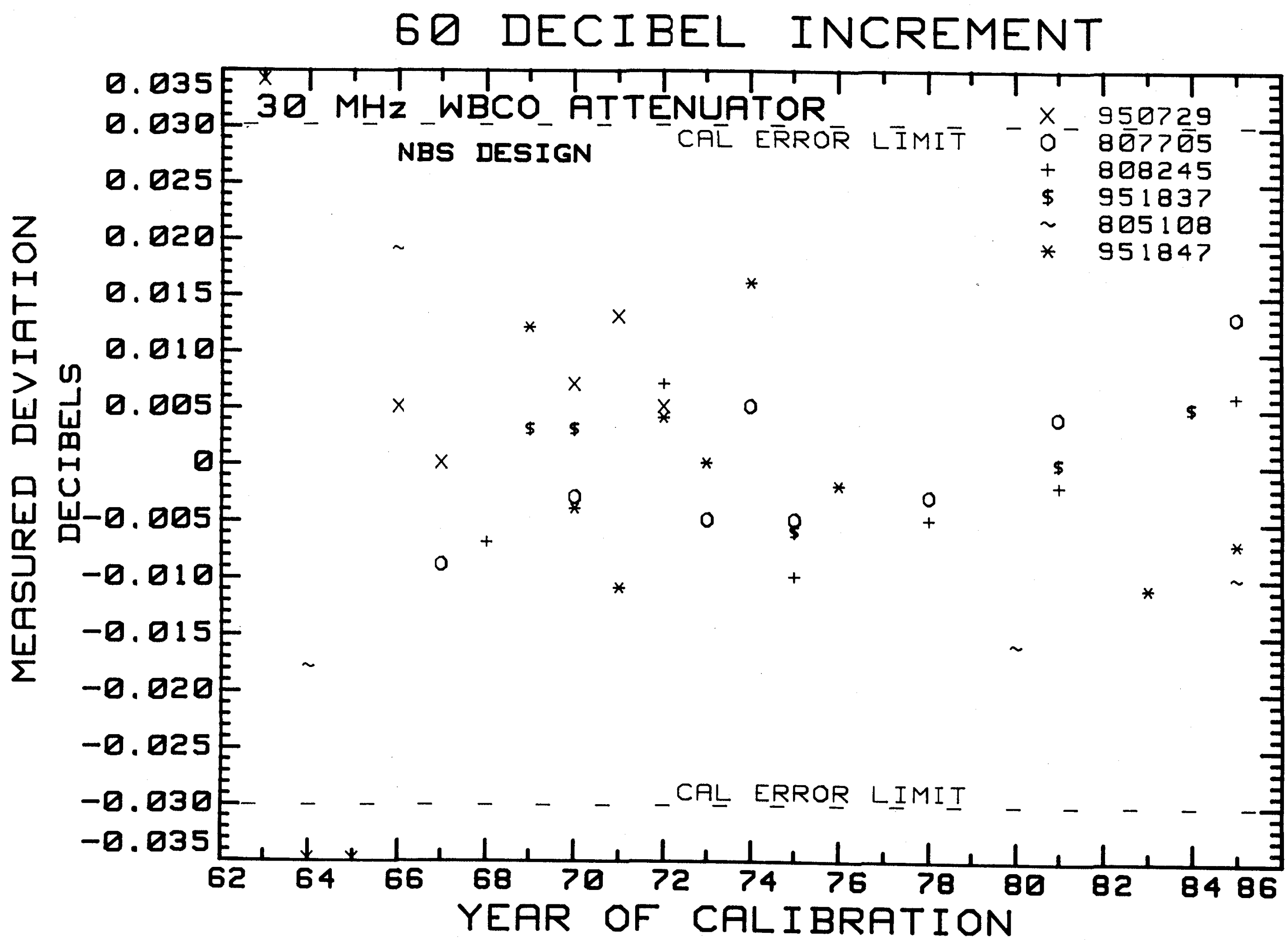

Figure 3.7. Calibration Results for NBS Design Variable WBCO Attenuators (60-dB increment), 1963 to 1985.

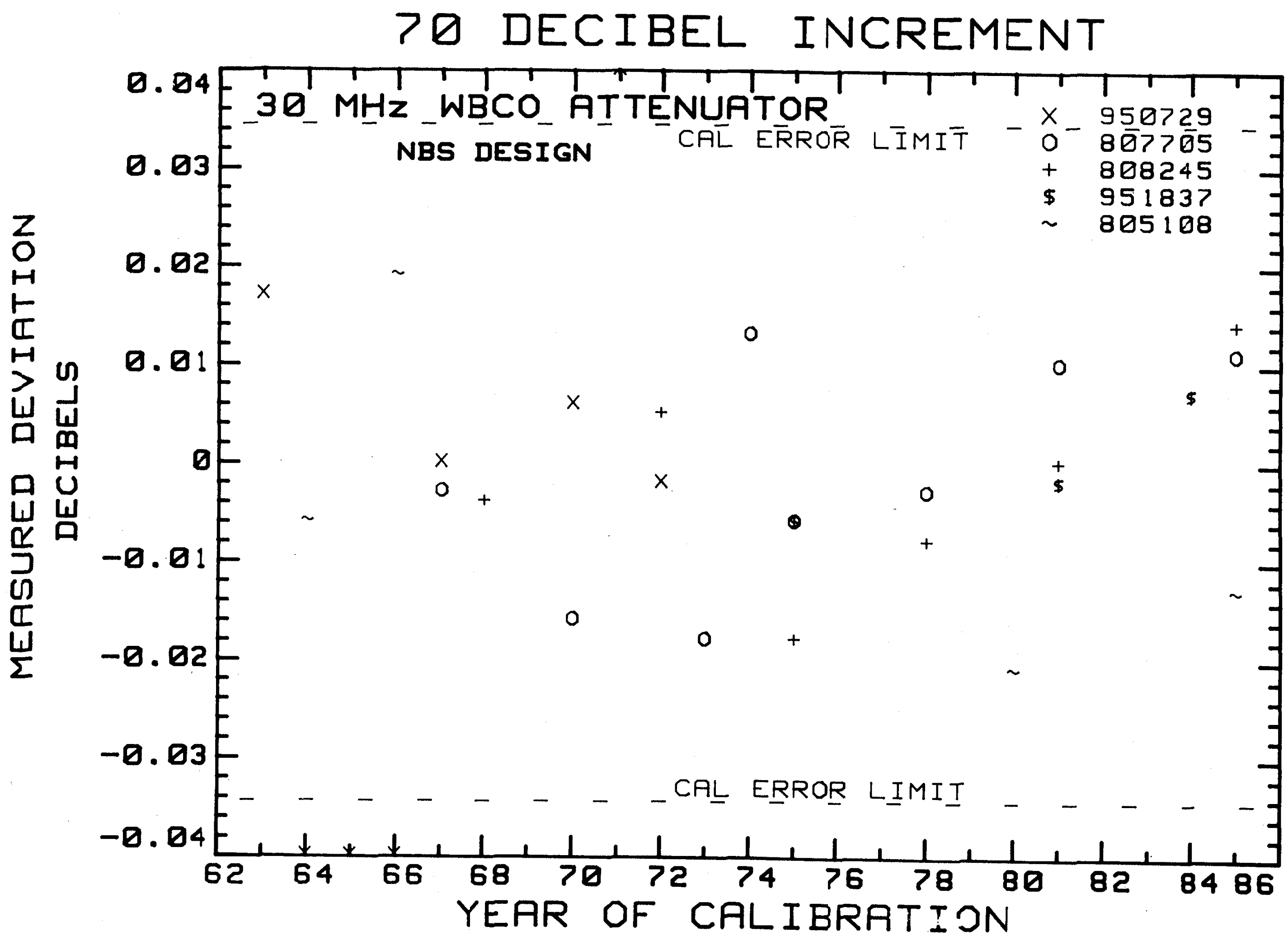

Figure 3.8. Calibration Results for NBS Design Variable WBCO Attenuators (70-dB increment), 1963 to 1985.

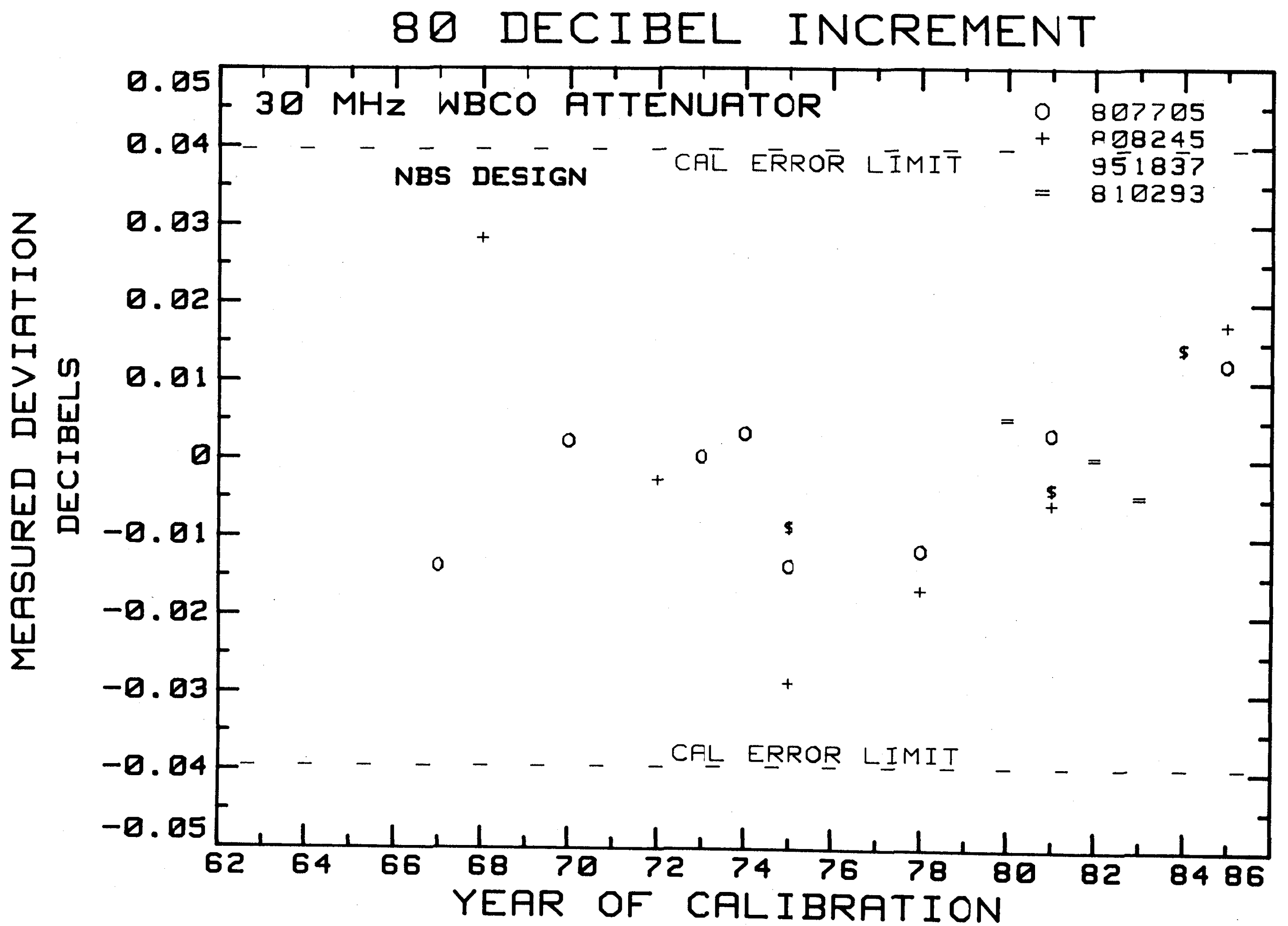

Figure 3.9. Calibration Results for NBS Design Variable WBCO Attenuators (80-dB increment), 1963 to 1985.

the corrections used are apparently adequate based on examination of NBS calibration results.

Twenty years of calibration history show an outlier at 70 dB in 1965 for test 806213. Since this was one of the first attenuators built by the manufacturer, and then was subsequently refurbished and has tracked almost perfectly for 19 years, we can assume that this outlier is a valid point.

An outlying value for 806547 at 10 dB in 1970 is probably a valid point since this attenuator shows a larger variation through the years than most of the others. Internal mechanical instability would cause this.

The remaining outlying values at 90 dB for 806623 and 100 dB for 808406 are also assumed to be valid and undoubtedly due to rf leakage within the devices.

Since these excessive deviations from nominal values are readily explained as due to the DUT and not due to the measurement system, NBS feels confident that the reported values are correct.

The resettability of the NBS 30 MHz standard attenuator, being based on an optical readout and scale, is superior in this respect to the attenuators grouped under 3.2.2. As a result, this calibration history strongly validates NBS claims to statistical control of our 30 MHz measurement system. The small degree of scatter evidenced at 90- and 100-dB increments adds confidence that the NBS system rf leakage is well controlled.

3.2.3.1 <u>Conclusions</u>:

1. Assigned uncertainty limits are valid.
2. The system is in excellent statistical control.

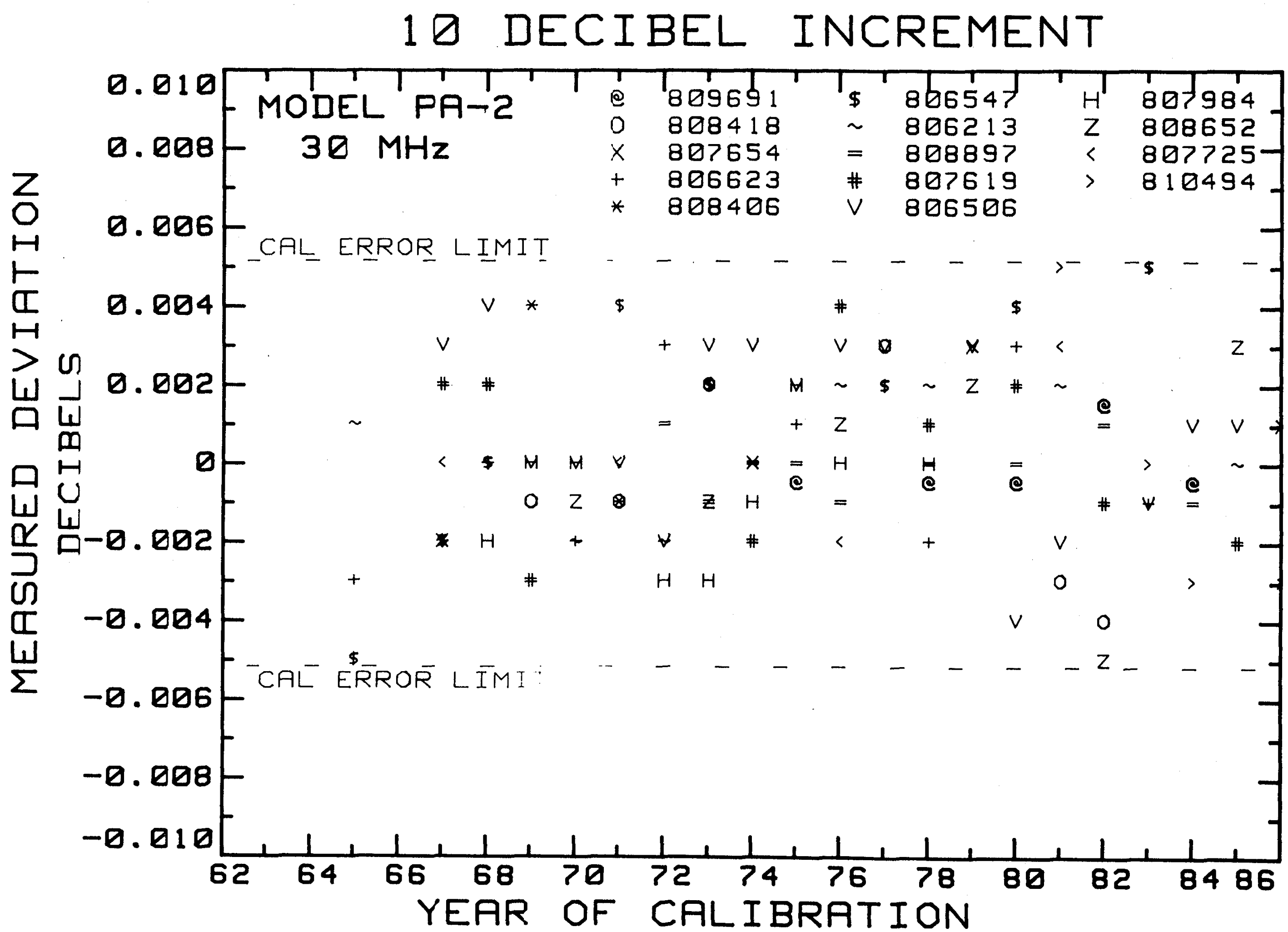

Figure 3.10. Calibration Results for Commercial Variable WBCO Attenuators (10-dB increment), 1965 to 1985.

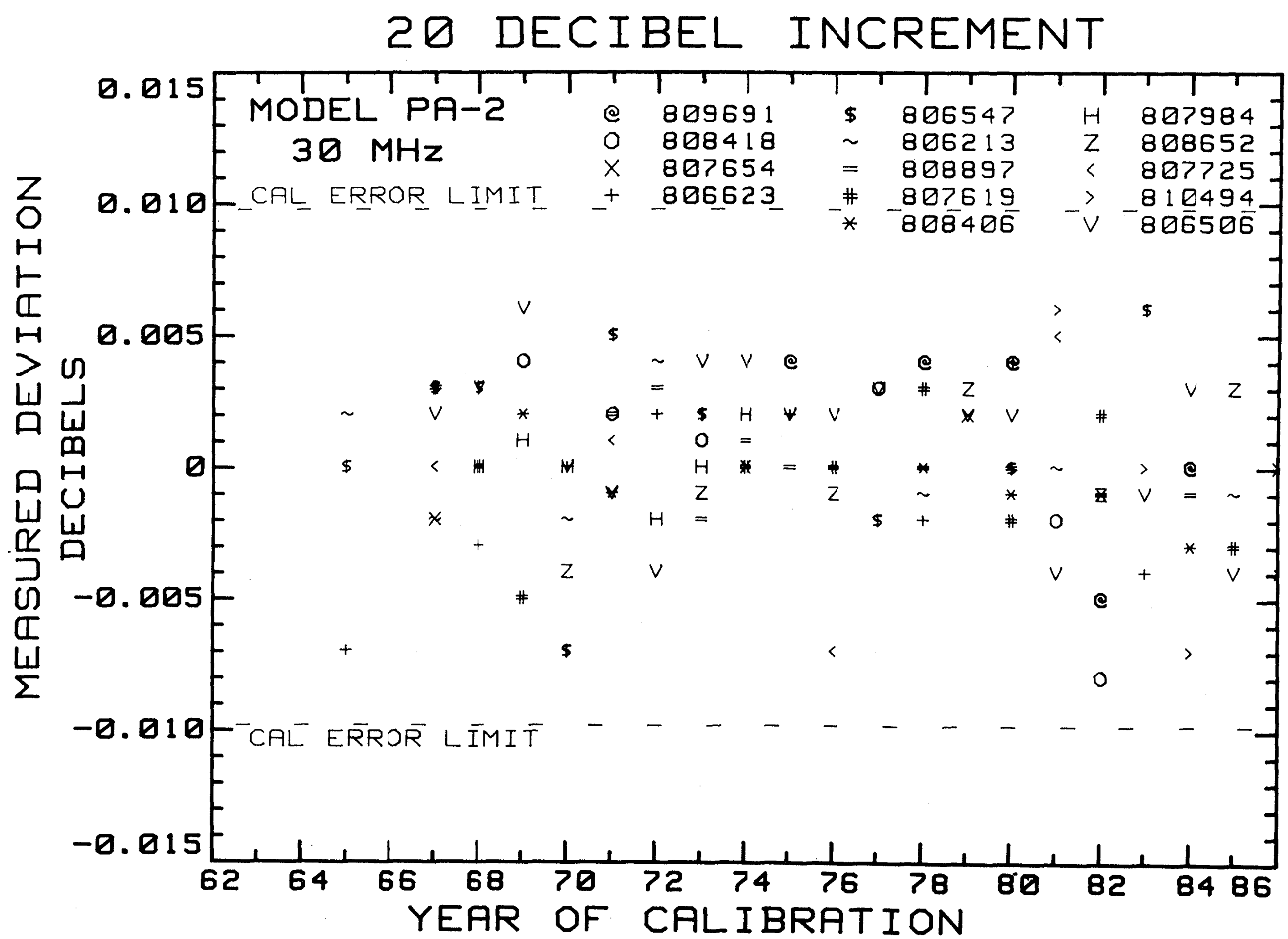

Figure 3.11. Calibration Results for Commercial Variable WBCO Attenuators (20-dB increment), 1965 to 1985.

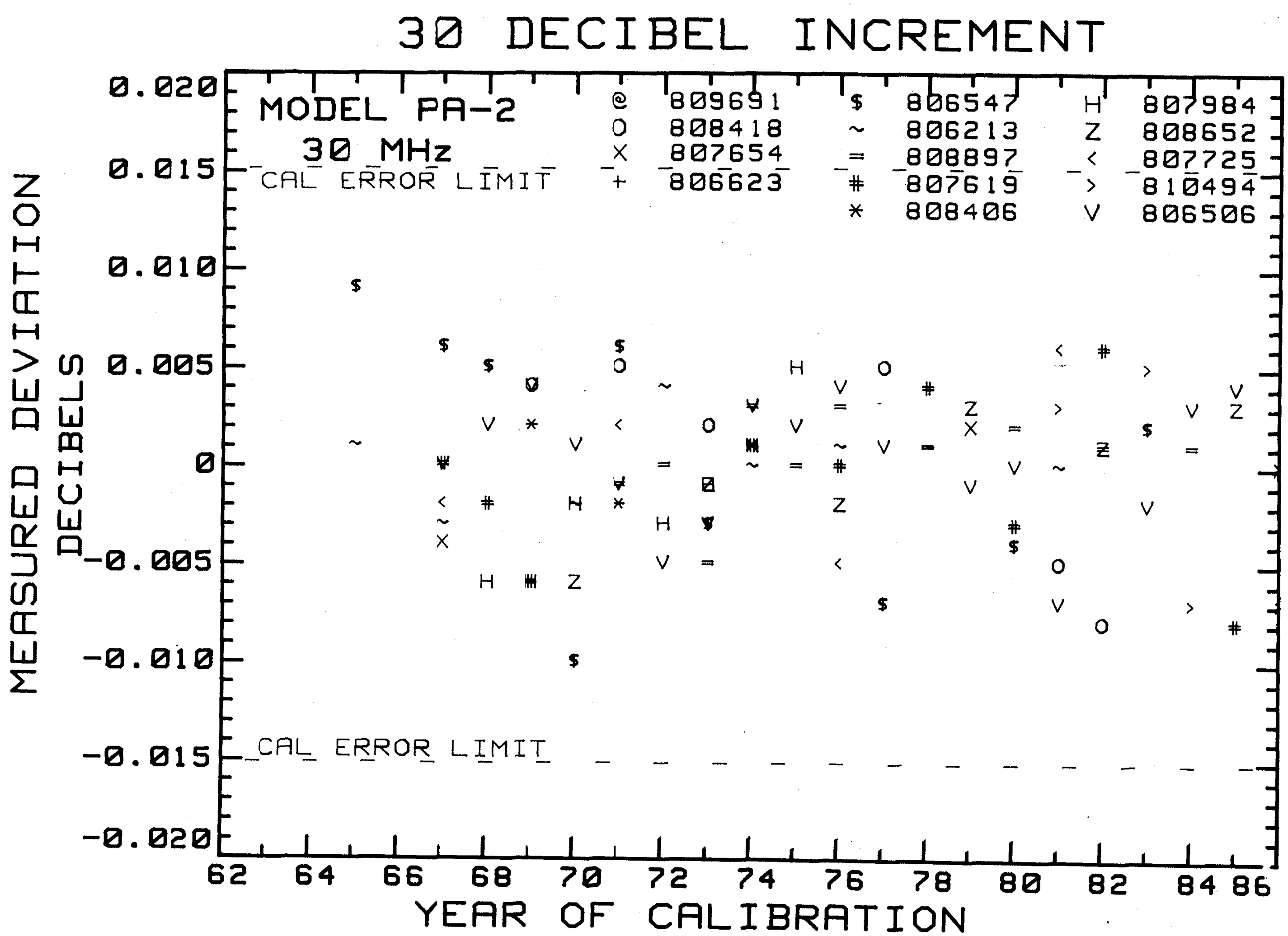

Figure 3.12. Calibration Results for Commercial Variable WBCO Attenuators (30-dB increment), 1965 to 1985.

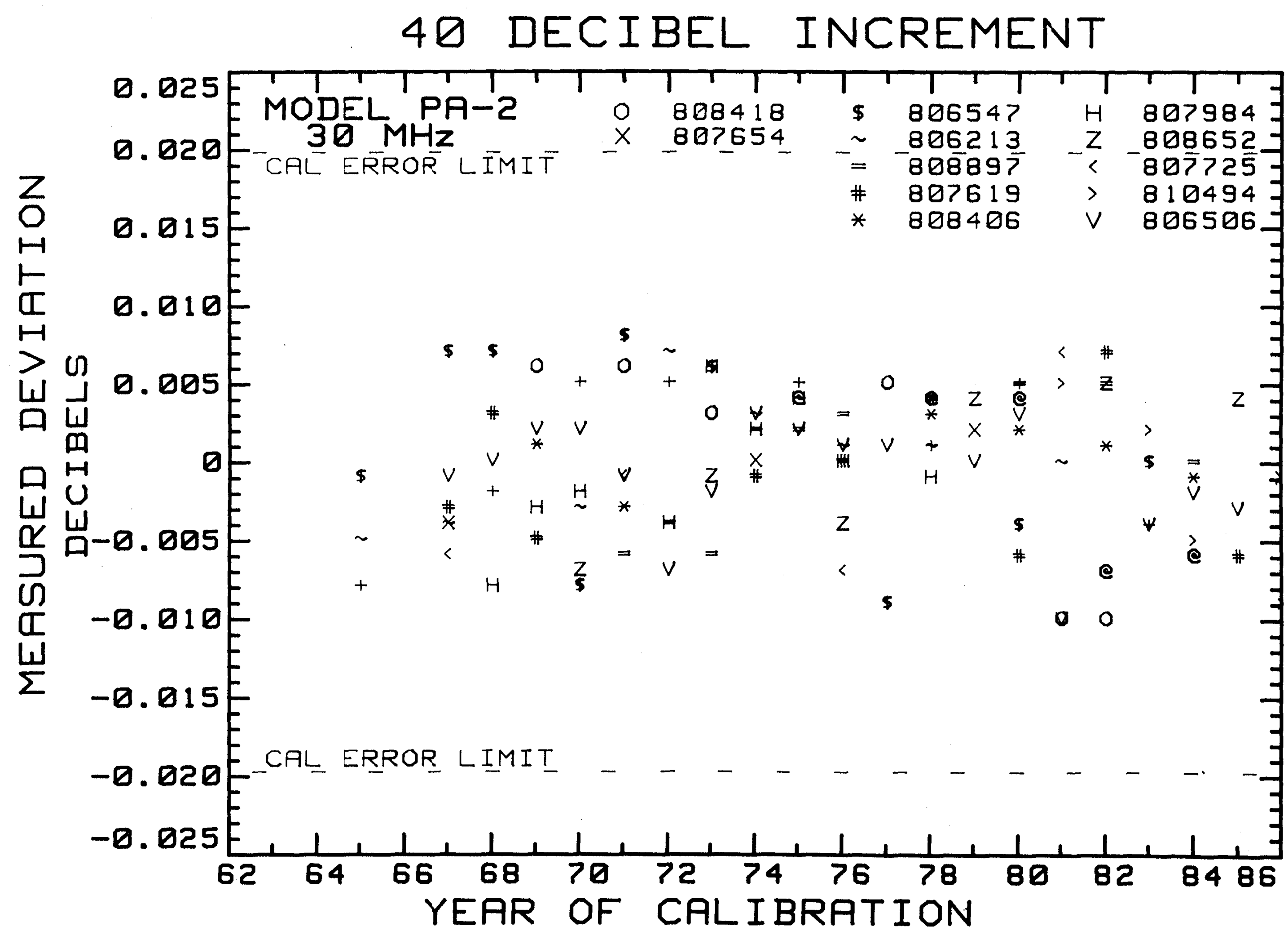

Figure 3.13. Calibration Results for Commercial Variable WBCO Attenuators (40-dB increment), 1965 to 1985.

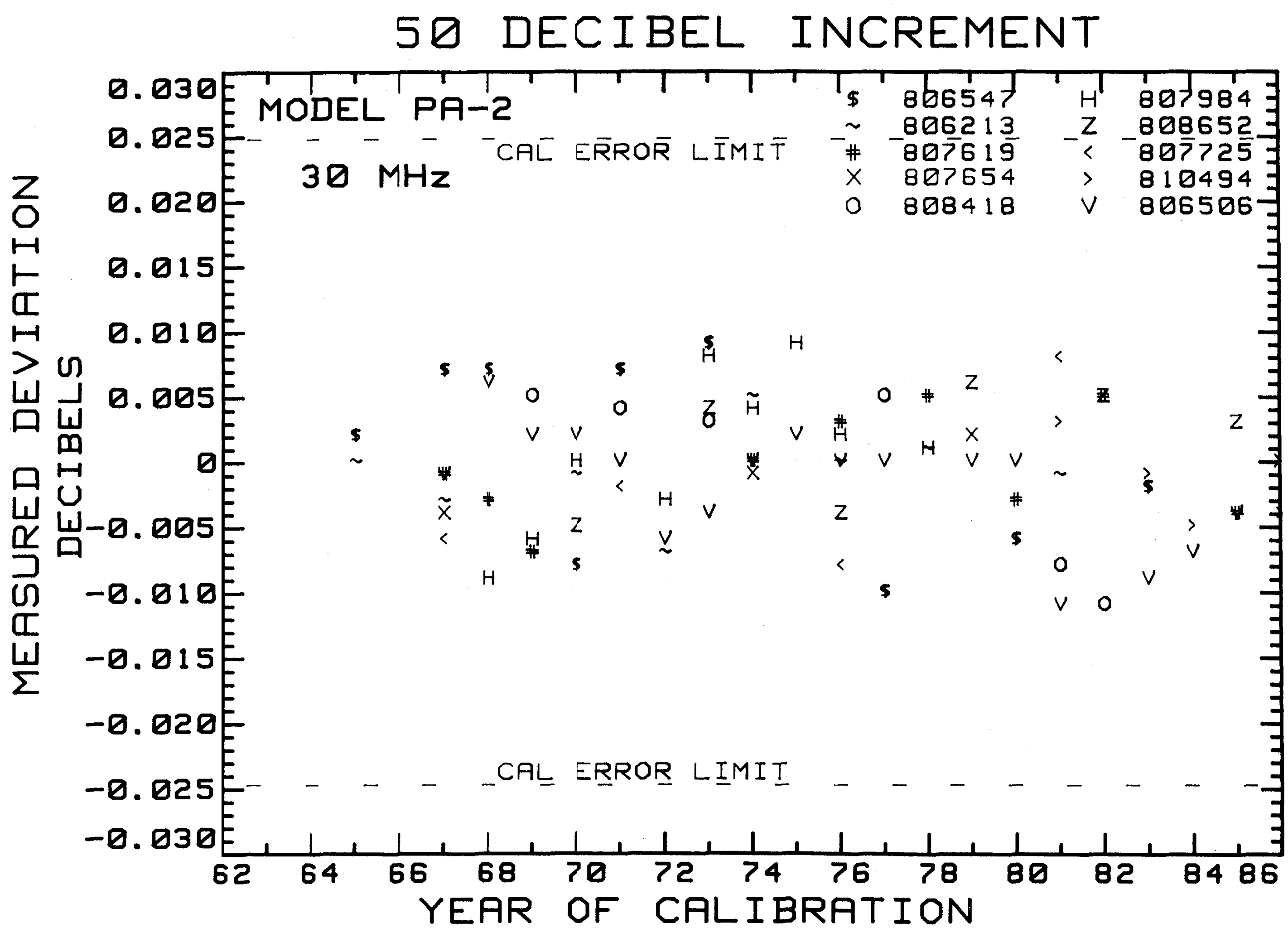

Figure 3.14. Calibration Results for Commercial Variable WBCO Attenuators (50-dB increment), 1965 to 1985.

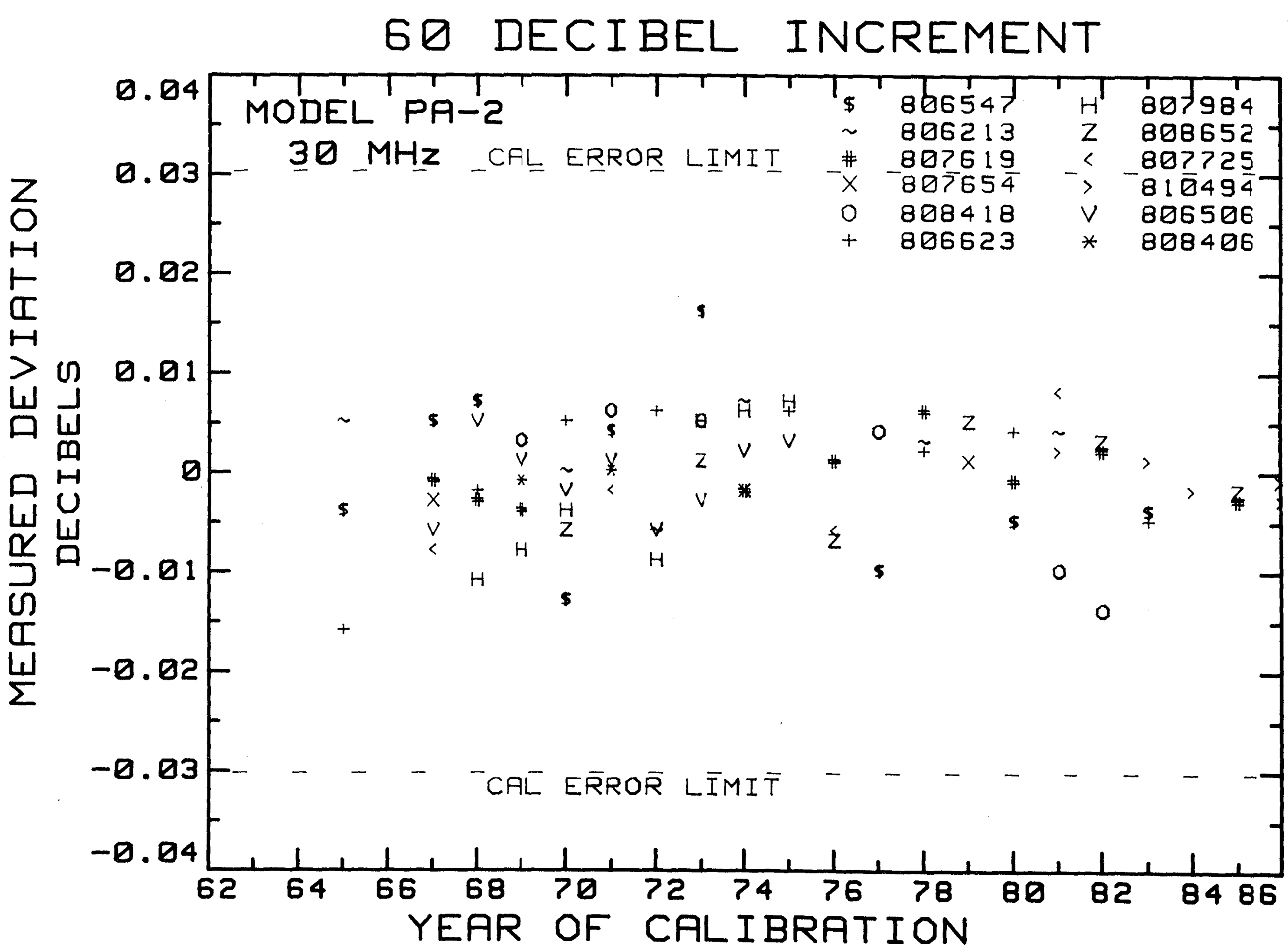

Figure 3.15. Calibration Results for Commercial Variable WBCO Attenuators (60-dB increment), 1965 to 1985.

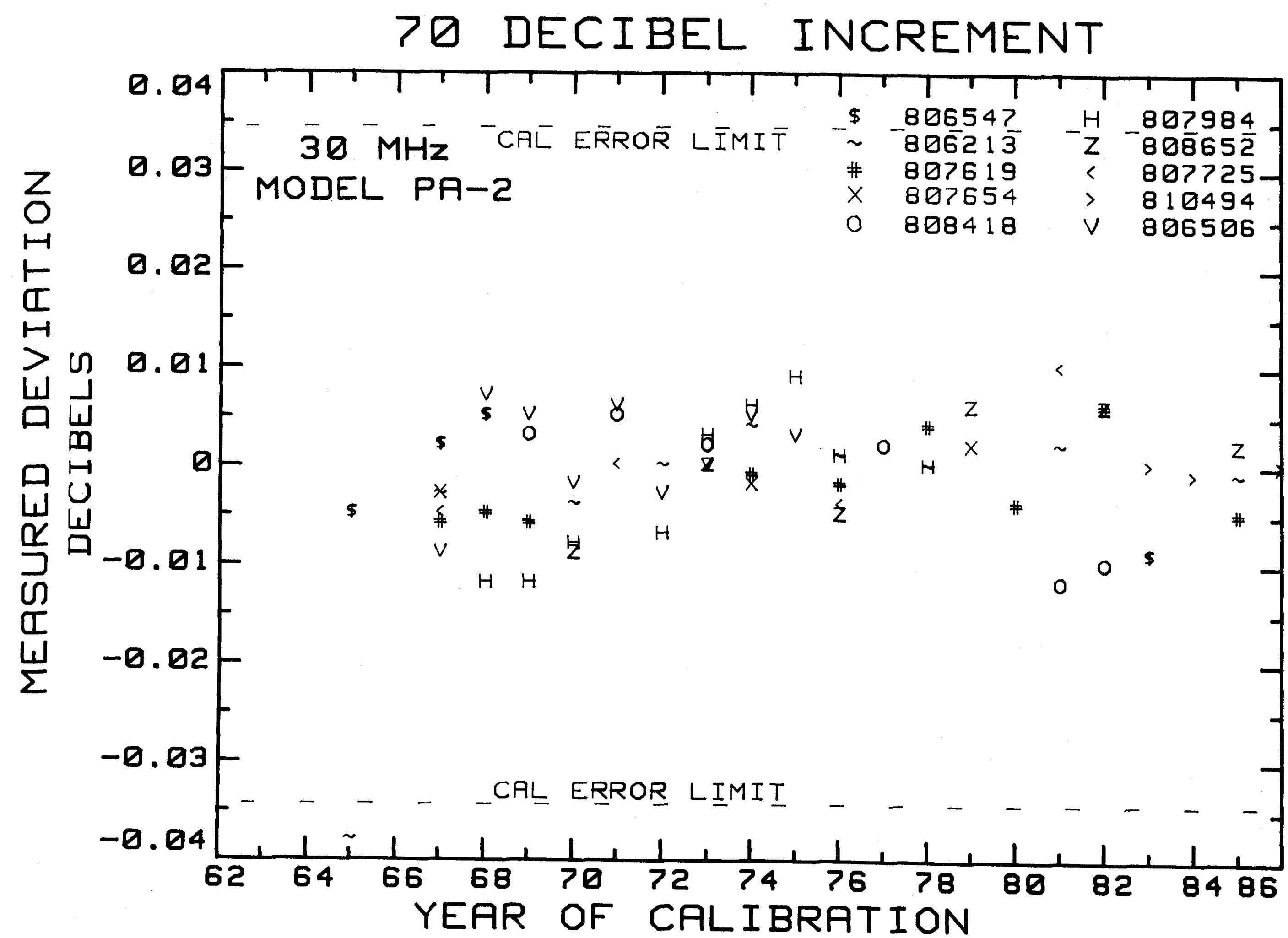

Figure 3.16. Calibration Results for Commercial Variable WBCO Attenuators (70-dB increment), 1965 to 1985.

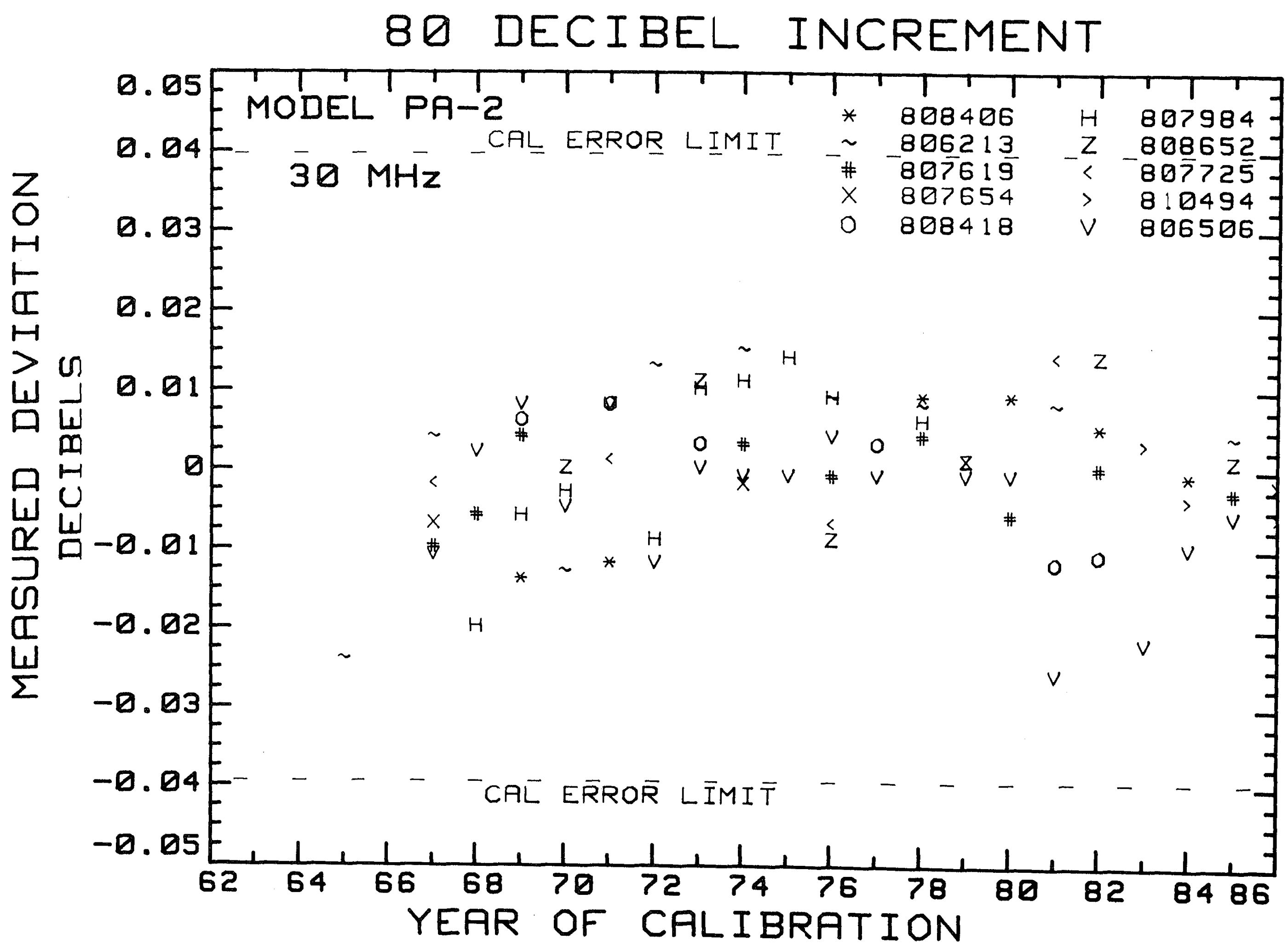

Figure 3.17. Calibration Results for Commercial Variable WBCO Attenuators (80-dB increment), 1965 to 1985.

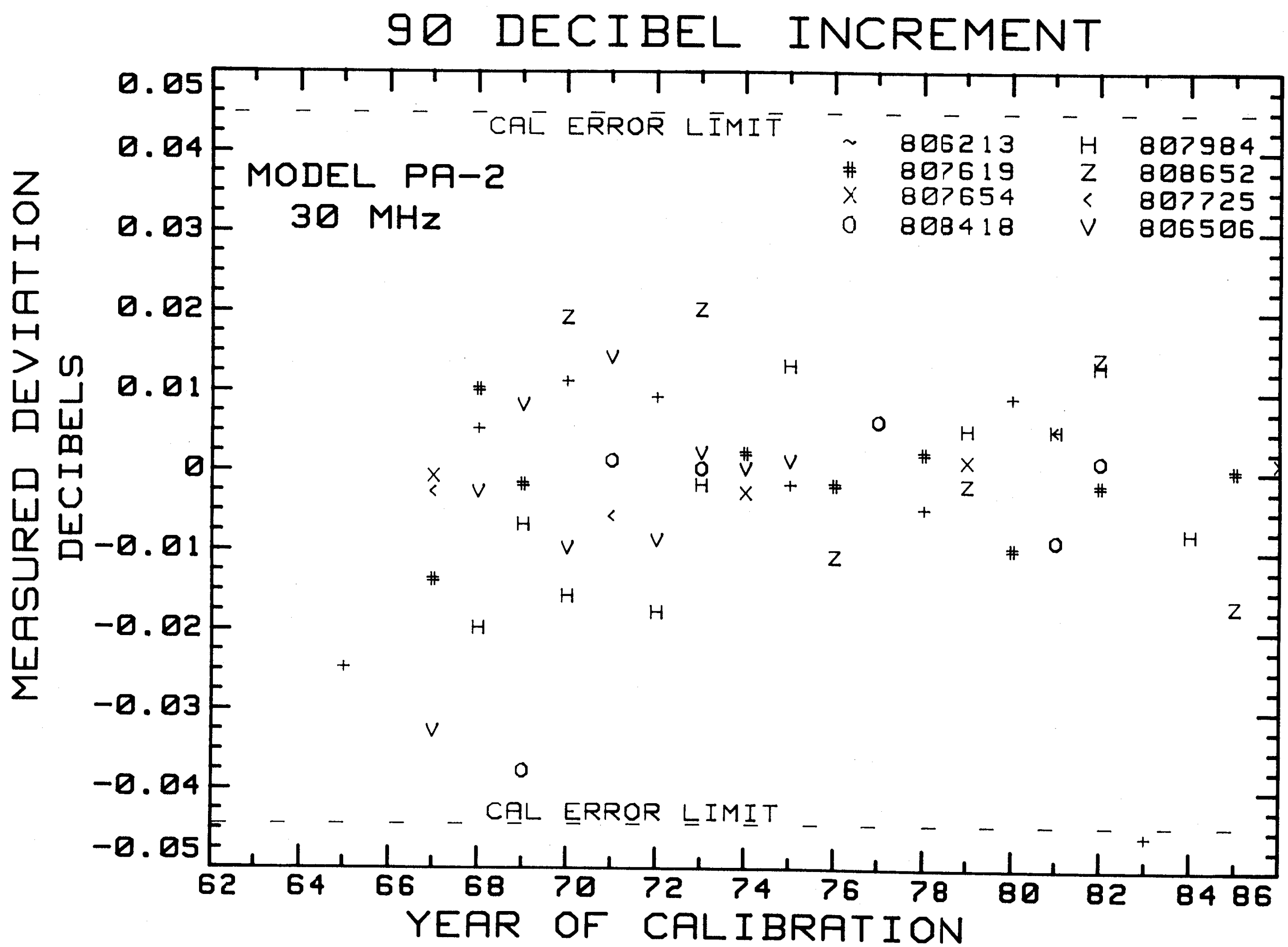

Figure 3.18. Calibration Results for Commercial Variable WBCO Attenuators (90-dB increment), 1965 to 1985.

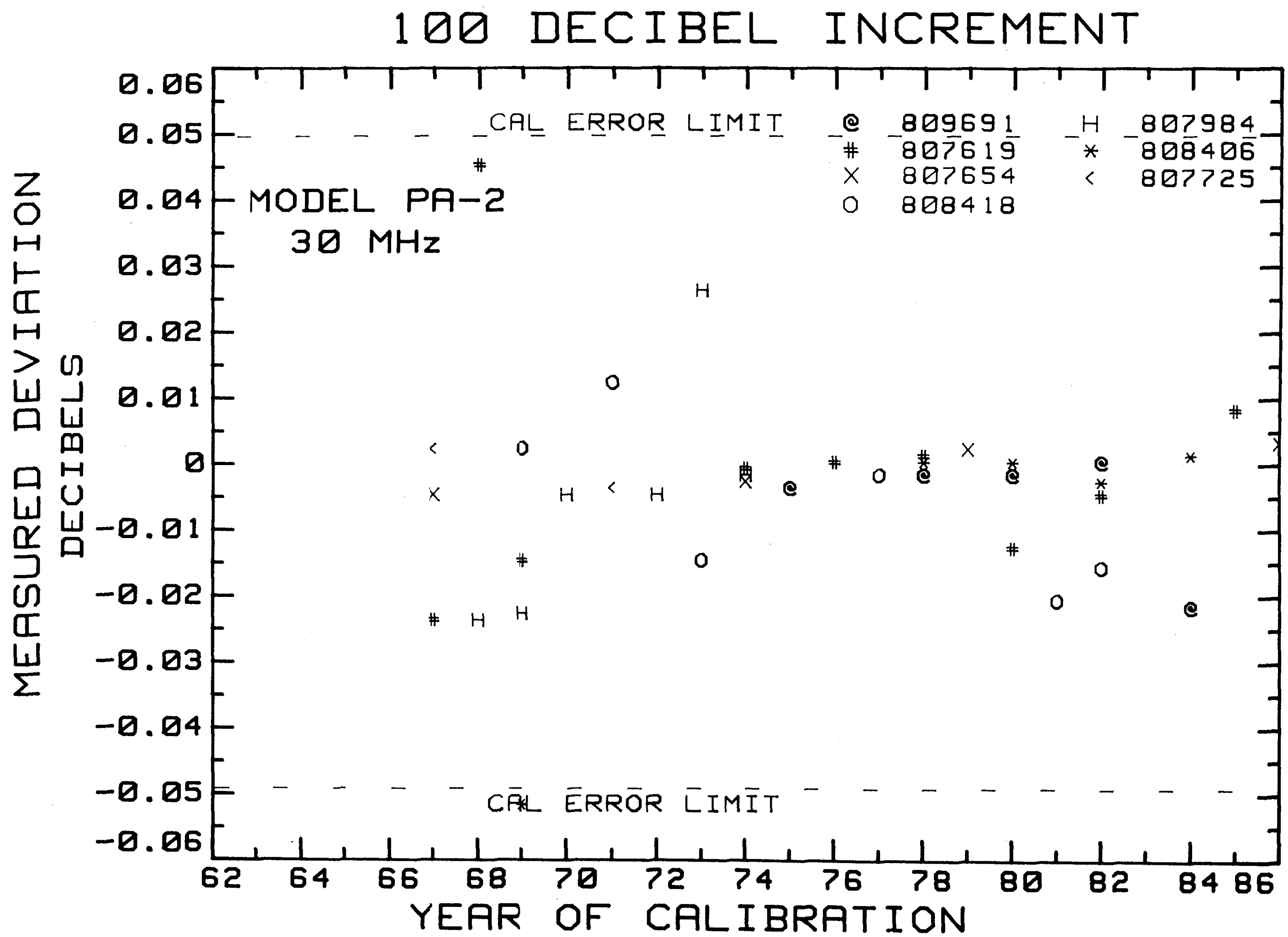

Figure 3.19. Calibration Results for Commercial Variable WBCO Attenuators (100-dB increment), 1967 to 1985.

3.3 Typical NBS System Phase Shift Calibration Results (Figures 3.20.1 through 3.21.5)

The following figures, 3.20.1 through 3.21.5, are based on an extremely limited data base which makes it difficult to draw conclusions about uncertainty estimates. The two devices, however, have been measured over a significant time span (18 years in one case) and appear to validate adequate system statistical control.

Figures 3.20.2, 3.20.3 and 3.21.2 through 3.21.5 show assigned error limits at each phase shift value reported. The uncertainty limits are indicated by vertical lines above and below the data points plotted in these figures. For both devices at each value measured, the assigned uncertainty bounds have been assigned conservatively and seem valid. Note that the 1975 repair of test unit 809499 shifted the measured values substantially but reduced their deviation from nominal values for subsequent calibrations.

3.3.1 Conclusions:

1. The phase shift measurement system is in statistical control.
2. The limited calibrations performed indicate the desirability of phasing out the phase shift service calibration on this system. Since NBS six-port measurement systems are capable of this measurement now and will provide this service when qualified, no further evaluation of the 30 MHz phase shift measurement system is planned.

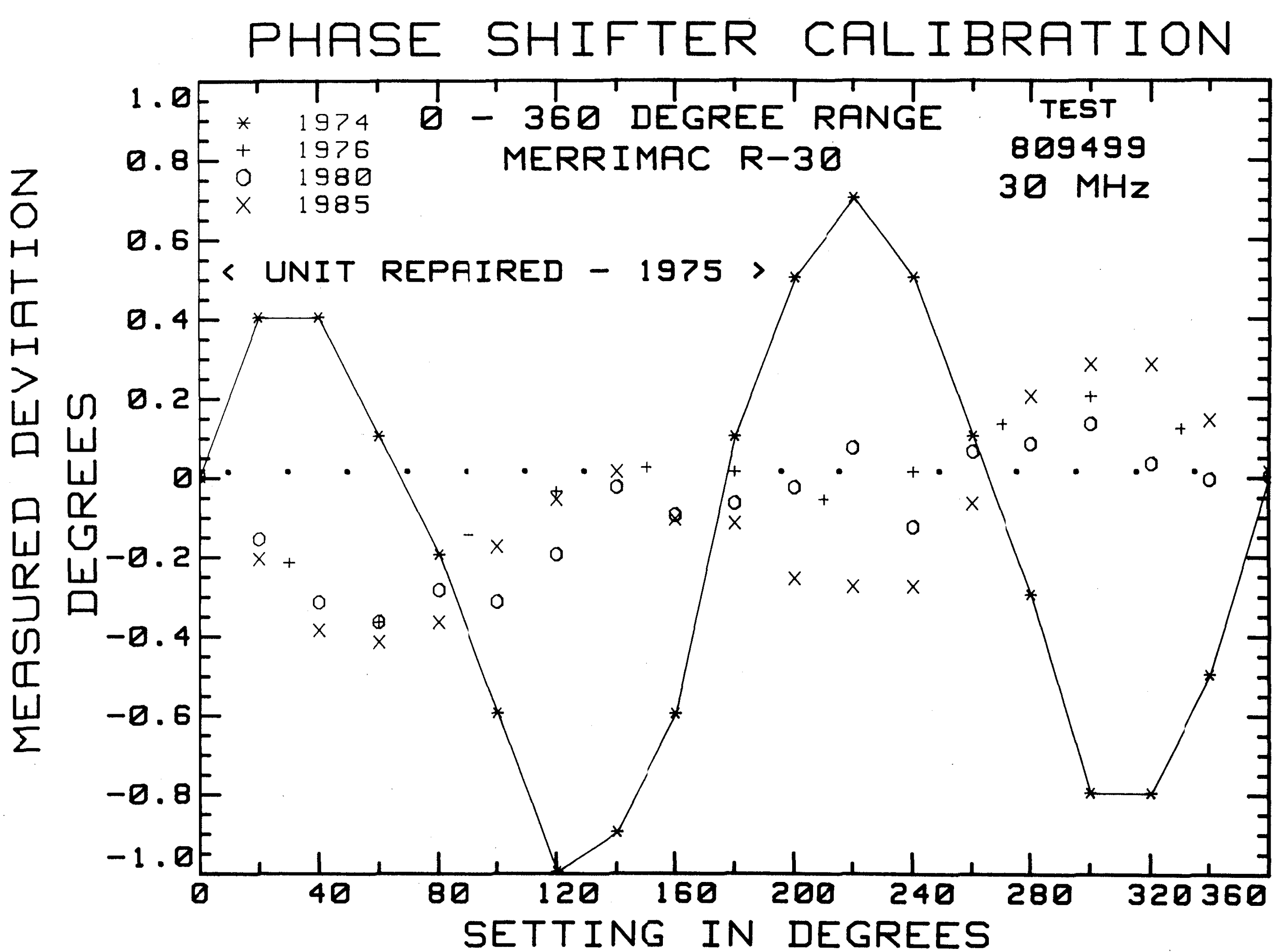

Figure 3.20.1. Calibration Results for Commercial Phase Shifter A.

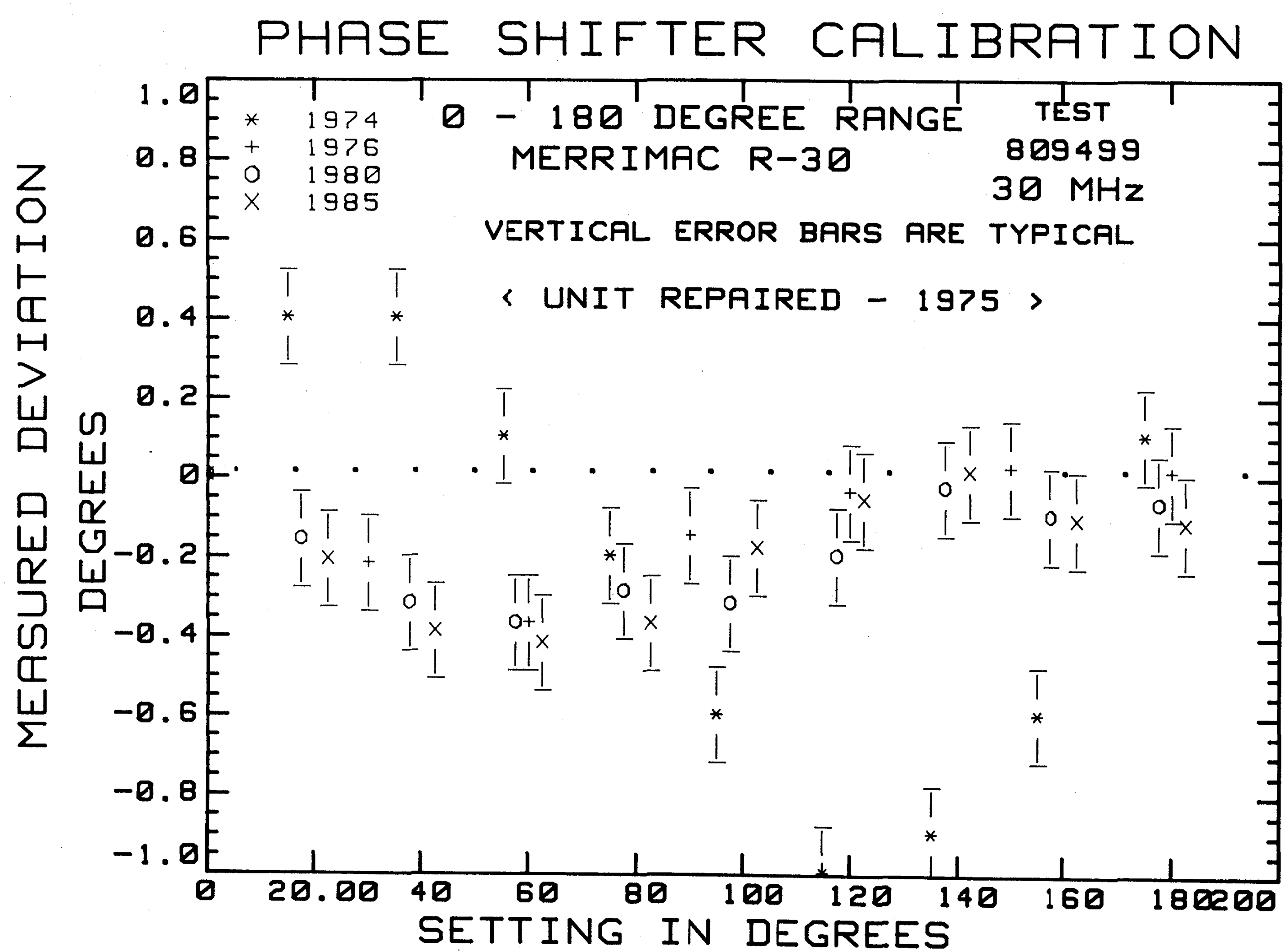

Figure 3.20.2. Calibration Results for Commercial Phase Shifter A.

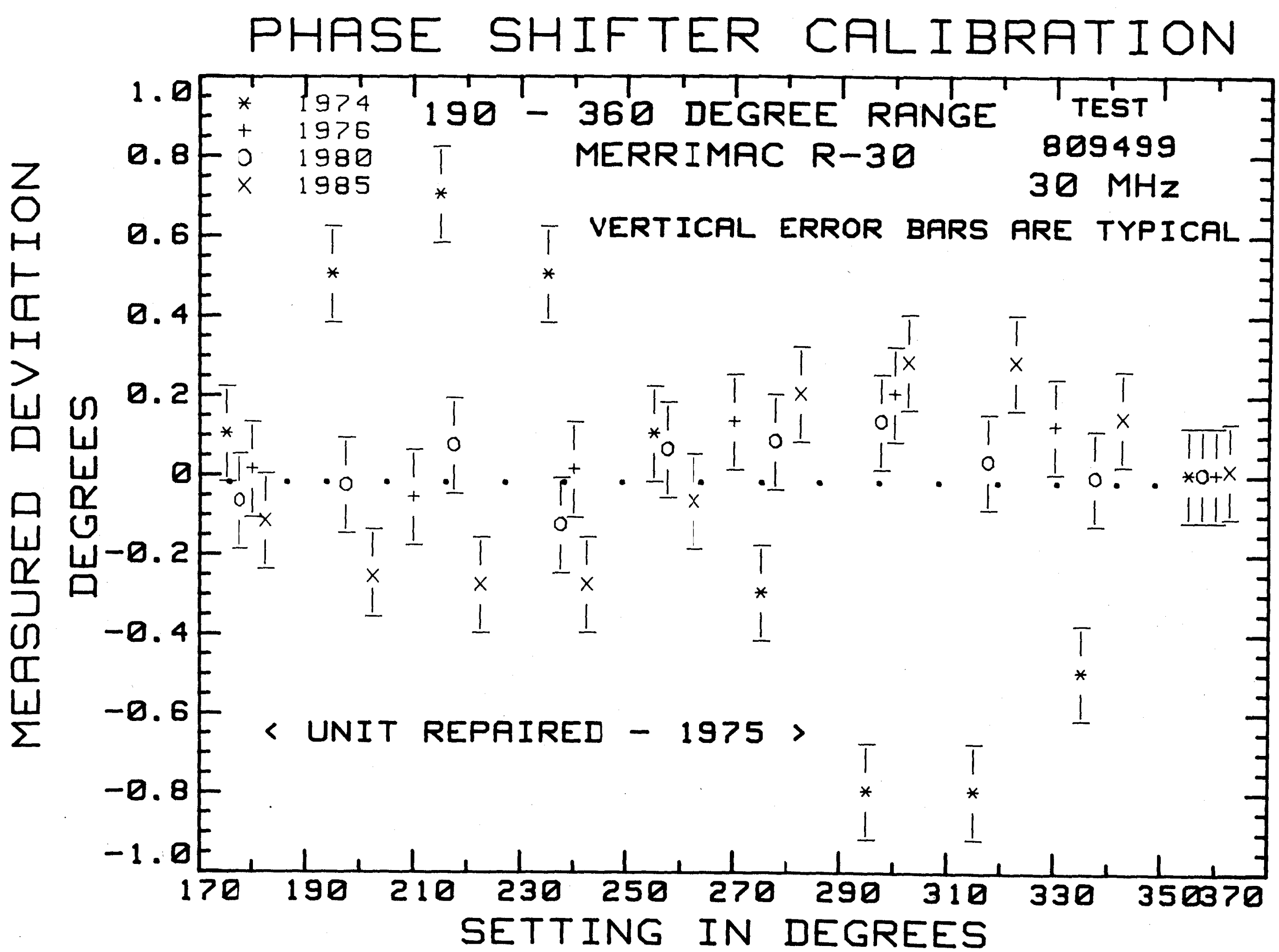

Figure 3.20.3. Calibration Results for Commercial Phase Shifter A.

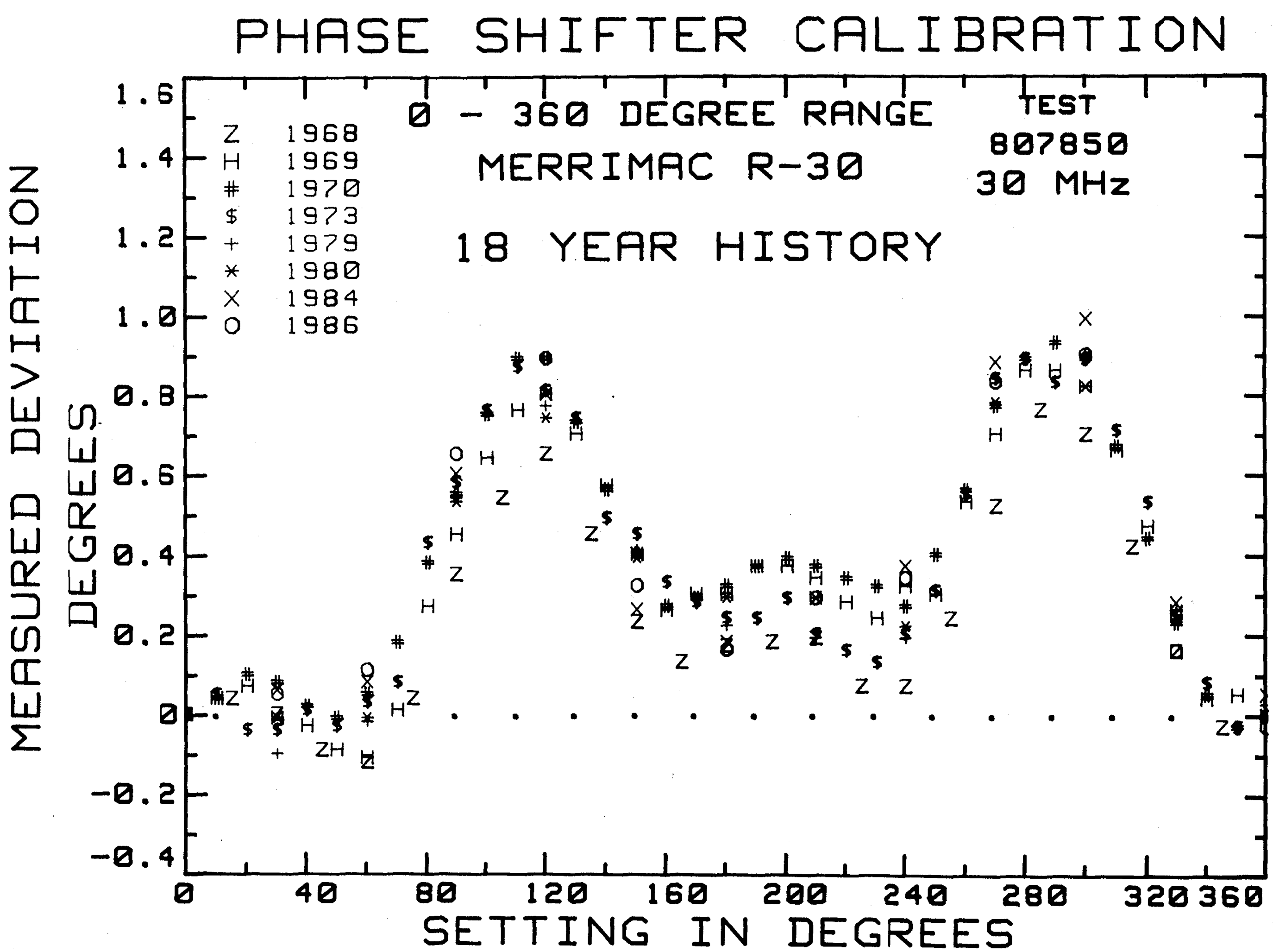

Figure 3.21.1. Calibration Results for Commercial Phase Shifter B.

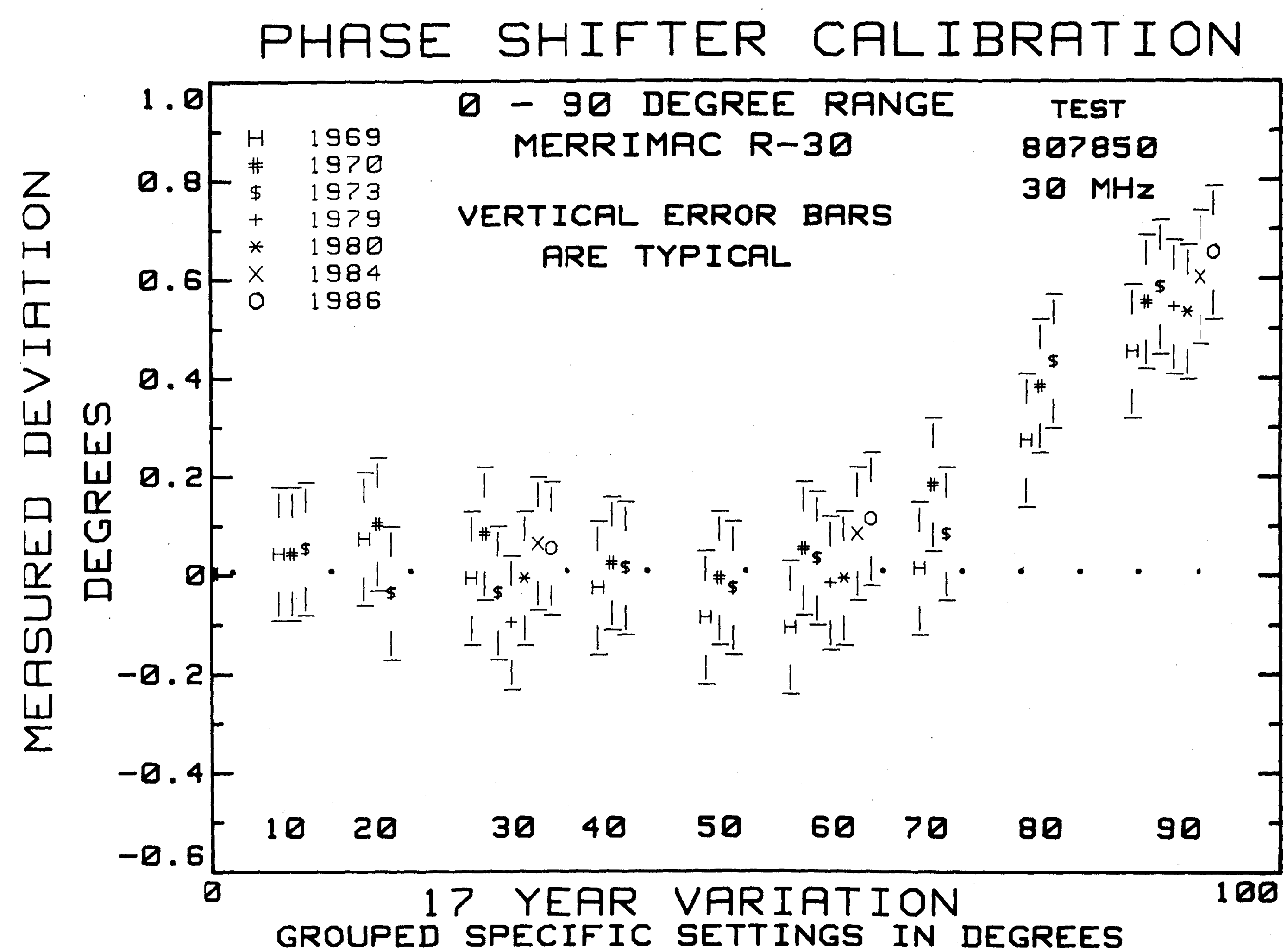

Figure 3.21.2. Calibration Results for Commercial Phase Shifter B.

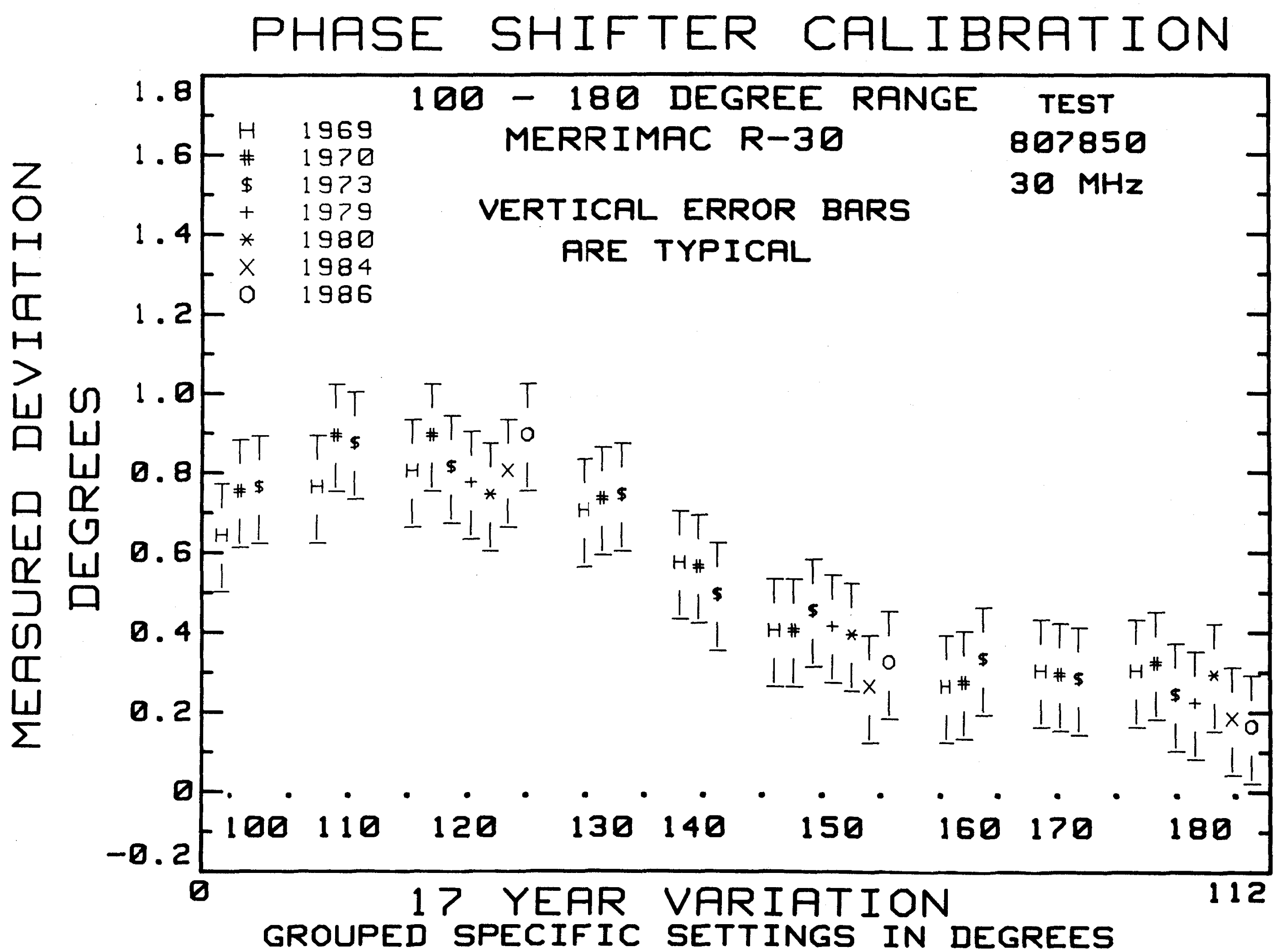

Figure 3.21.3. Calibration Results for Commercial Phase Shifter B.

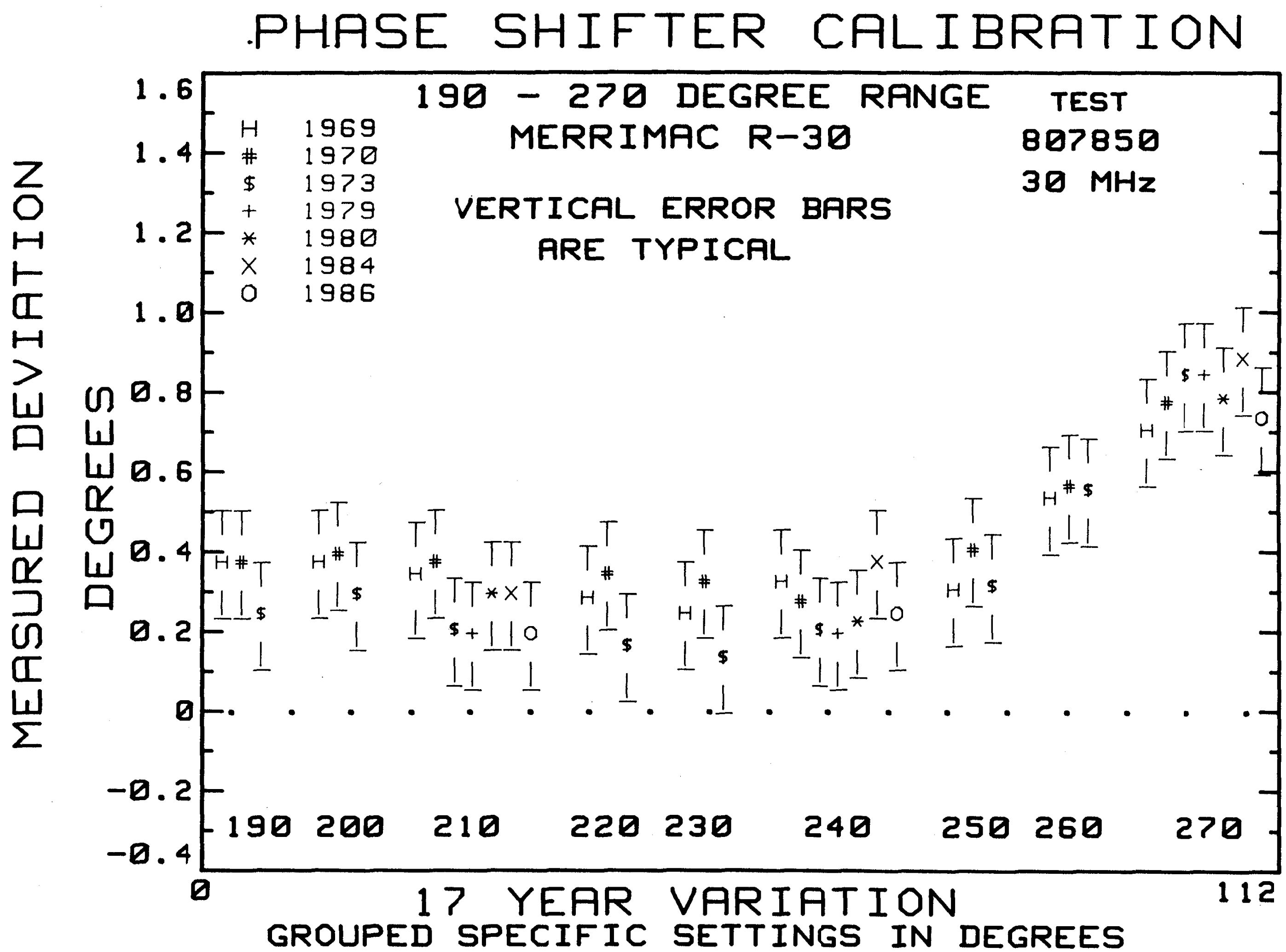

Figure 3.21.4. Calibration Results for Commercial Phase Shifter B.

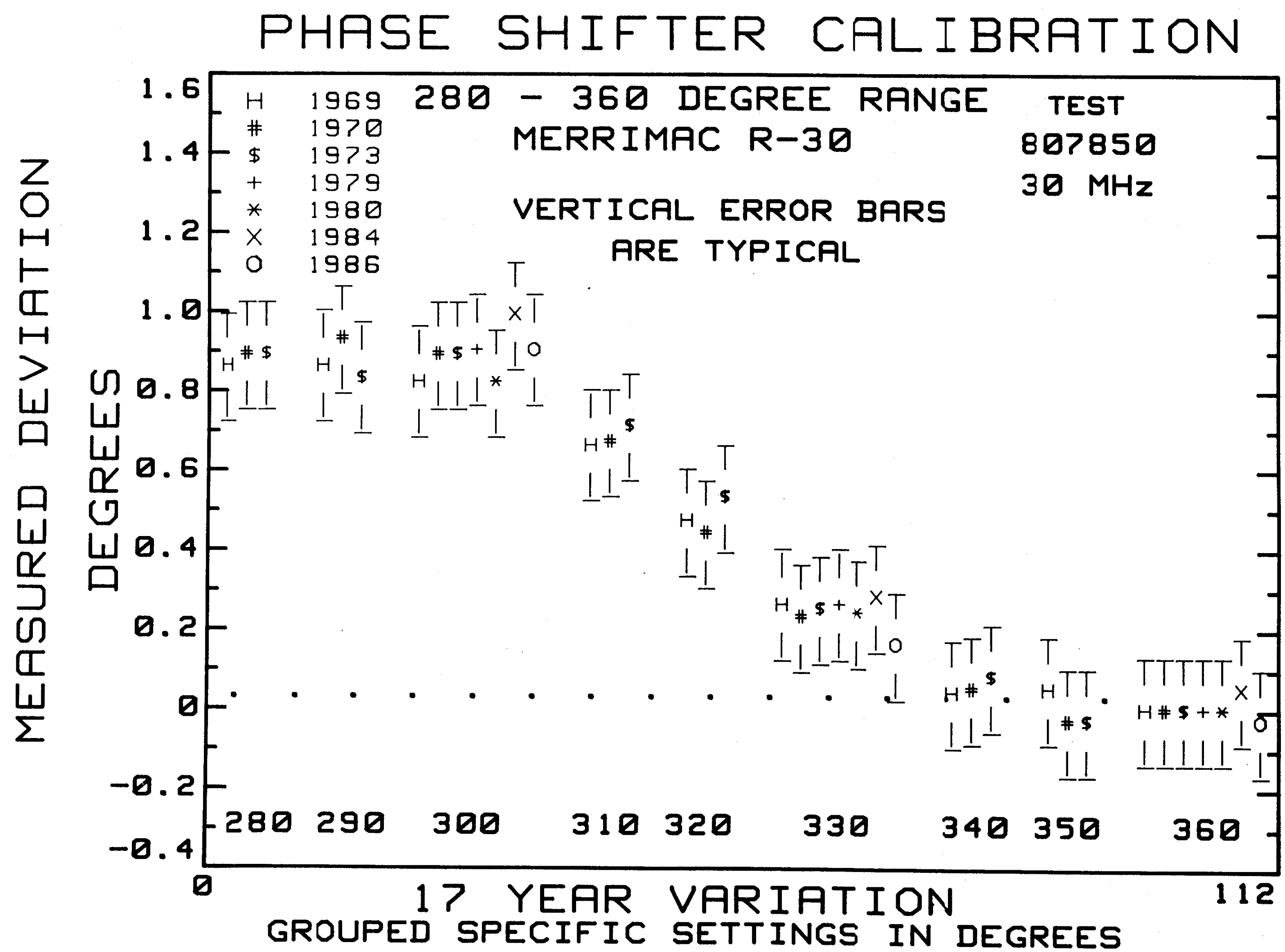

Figure 3.21.5. Calibration Results for Commercial Phase Shifter B.

3.4 Intercomparison of Attenuation Calibration Results

3.4.1 Comparison with NBS "SQUID" System (Figure 3.22)

A series of comparisons involving the measurement of a calibrated WBCO attenuator on a system based on a new concept, Superconducting Quantum Interference Device (SQUID), were carried out. This was done to lend confidence to the theoretical uncertainty analysis of the NBS attenuation measuring system.

The SQUID is a loop of superconducting metal closed by a weak point contact called a Josephson Junction, operating in a liquid helium bath. It converts variations in magnetic flux to periodic variations in impedance which are sensed at rf and microwave frequencies. This provides a convenient natural means of measuring electrical quantities such as voltage, current, power, and attenuation [13,14,15,16]. A system employing the SQUID for measuring attenuation was constructed at NBS and used for measuring a transfer standard WBCO attenuator.

The plot shown in figure 3.22 is taken from reference [14] and is typical of similar plots in the other references. It is apparent from observation of these results and examination of the references that a totally independent validation of NBS uncertainty bounds has been achieved. In addition, the comparison indicates that the uncertainty limits in this particular case are quite conservative. However, this is insufficient to allow the uncertainties to be arbitrarily reduced. The presence of rf leakage and its unpredictable effects preclude such action at this time. A specific development of uncertainty analysis will be required to validate reduction of present calibration uncertainties.

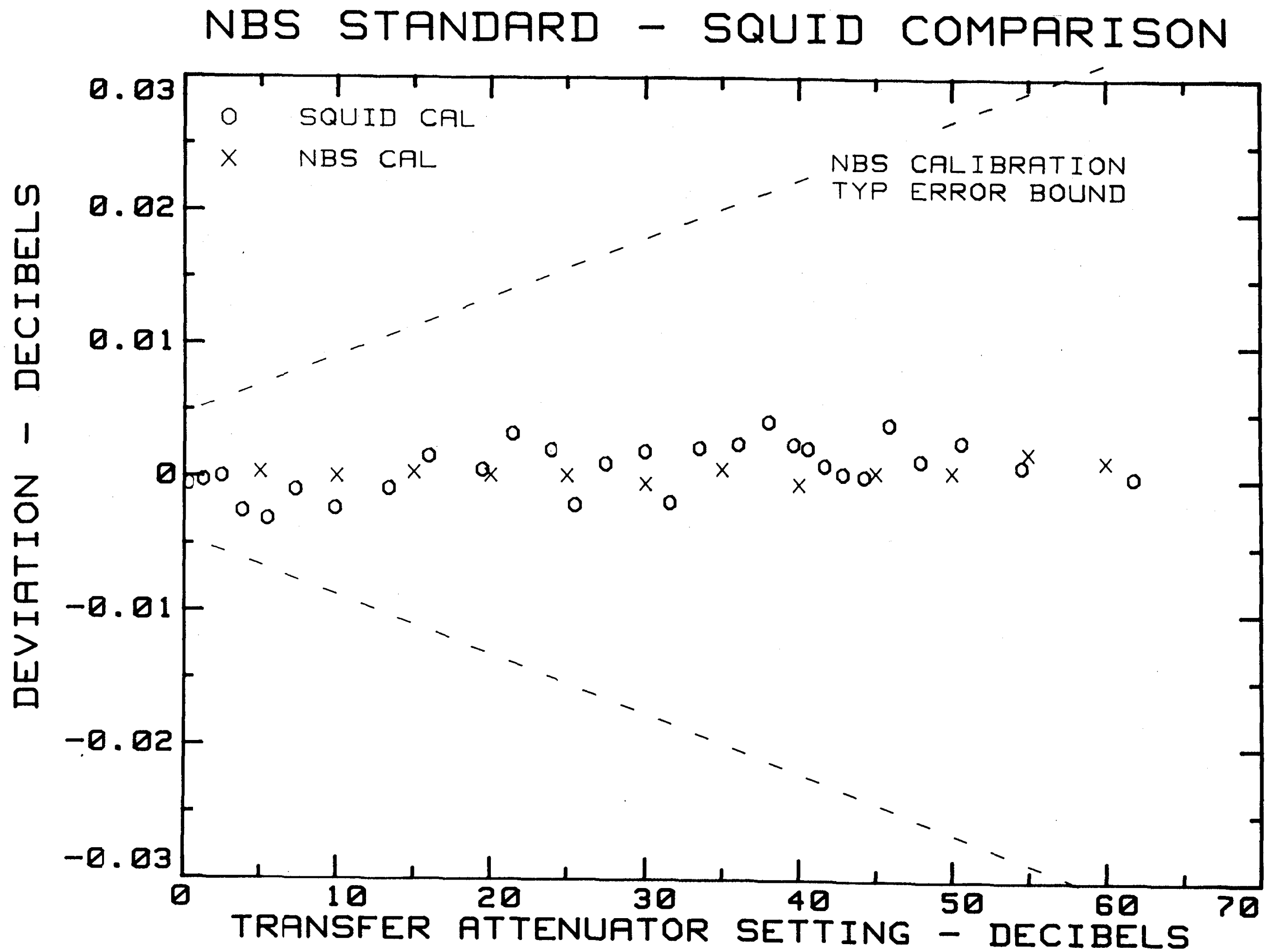

Figure 3.22. Comparison of Calibration Results for NBS Design WBCO Variable Attenuators (NBS 30 MHz System vs. NBS SQUID System).

3.4.1.1 Conclusions:

1. The present uncertainty budget is valid.
2. The absolute value of the attenuation rate is correct.

3.4.2 Comparison with NBS Six-Port System (Figures 3.23, 3.24)

3.4.2.1 Comparison Using the NBS Model SA-1 and the LF Six-Port ANA

To build confidence by further intercomparison, an NBS-designed Model SA-1 10-dB step attenuator was calibrated using the NBS 30 MHz primary attenuation standard and the NBS low frequency dual six-port system. The comparison was performed primarily to check the six-port, but a check on the NBS 30-MHz primary attenuation standard was also achieved.

The plot (figure 3.23) shows 40 measurements with the 30 MHz primary standard and 20 measurements with the six-port system. The averages differ by only 0.002 dB which is well within the estimated uncertainty bounds of both e transfer standard showed more occasion-to-occasion variability than normal but the consistency was adequate for a confidence check on both systems.

3.4.2.1.1 Conclusions:

1. The present uncertainty budget is valid.
2. The calculated attenuation rate is correct.

3.4.2.2 Comparison Using a Step Attenuator and the LF Six-Port ANA.

An additional comparison was performed using a step attenuator as a transfer standard at six fixed attenuation increments. This device exhibited excel-

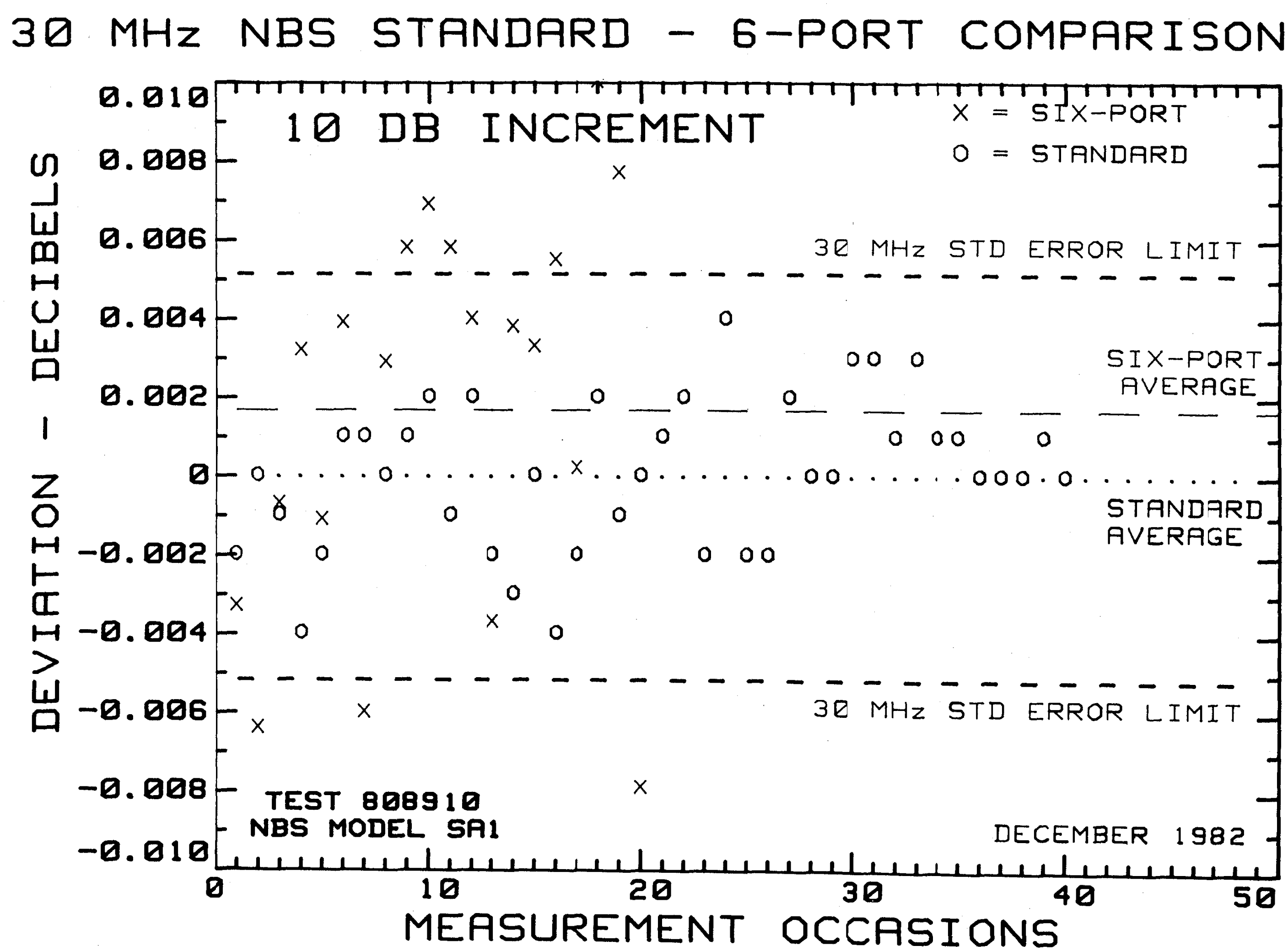

Figure 3.23. Comparison of Calibration Results for NBS Design WBCO 10 dB Step Attenuators (NBS 30 MHz System vs. NBS 6-Port ANA).

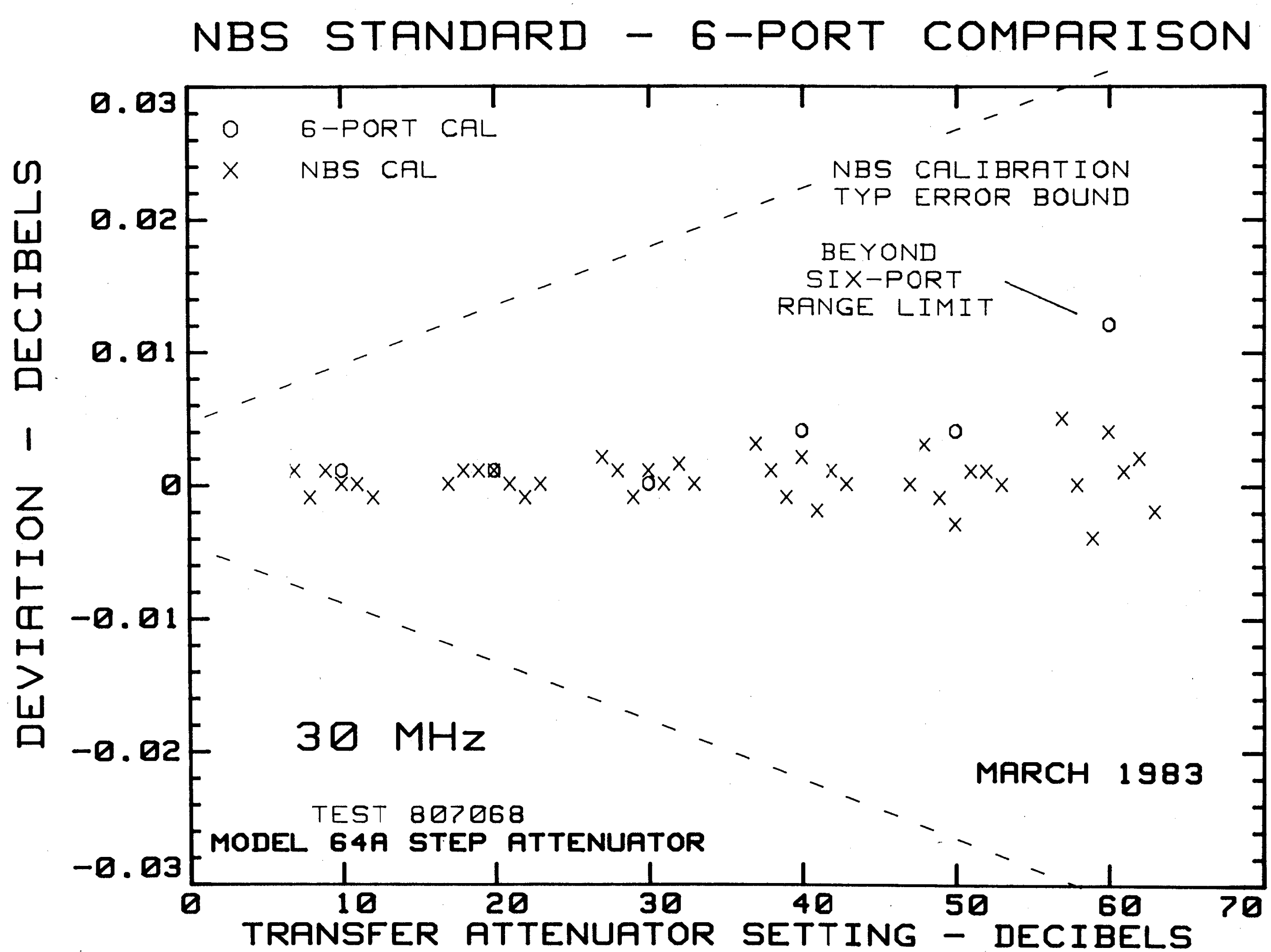

Figure 3.24. Comparison of Calibration Results for NBS Design WBCO Variable Attenuators (NBS 30 MHz System vs. NBS 6-Port ANA).

lent repeatability as shown in figure 3.24. Examination of the plot shows a significant deviation at 60 dB which is the current limit of the six-port range. This 60-dB point measured on the six-port, which is obviously in error, should be ignored in assessing the performance of the 30 MHz system.

3.4.2.2.1 Conclusions:

1. The uncertainty budget is valid but conservative.
2. The calculated attenuation rate is correct.

3.4.3 Comparison with International Laboratories

The results of an international comparison of several fixed attenuation standards are plotted in figures 3.25.1 through 3.25.5. This comparison spans four years and was reported in [17].

The participating laboratories were:

1. NML: Australia
2. NBS: National Bureau of Standards
3. NRC: Canada
4. ETL: Japan
5. NPL: Great Britain
6. FOA: Sweden
7. OMH: Hungary
8. PTB: West Germany

A study of the data shown on the five plots for the five fixed standards indicates two laboratories reported results with substantial bias. The values reported by NPL may be disregarded since they subsequently reported an error in computation which invalidates their results. The values reported by

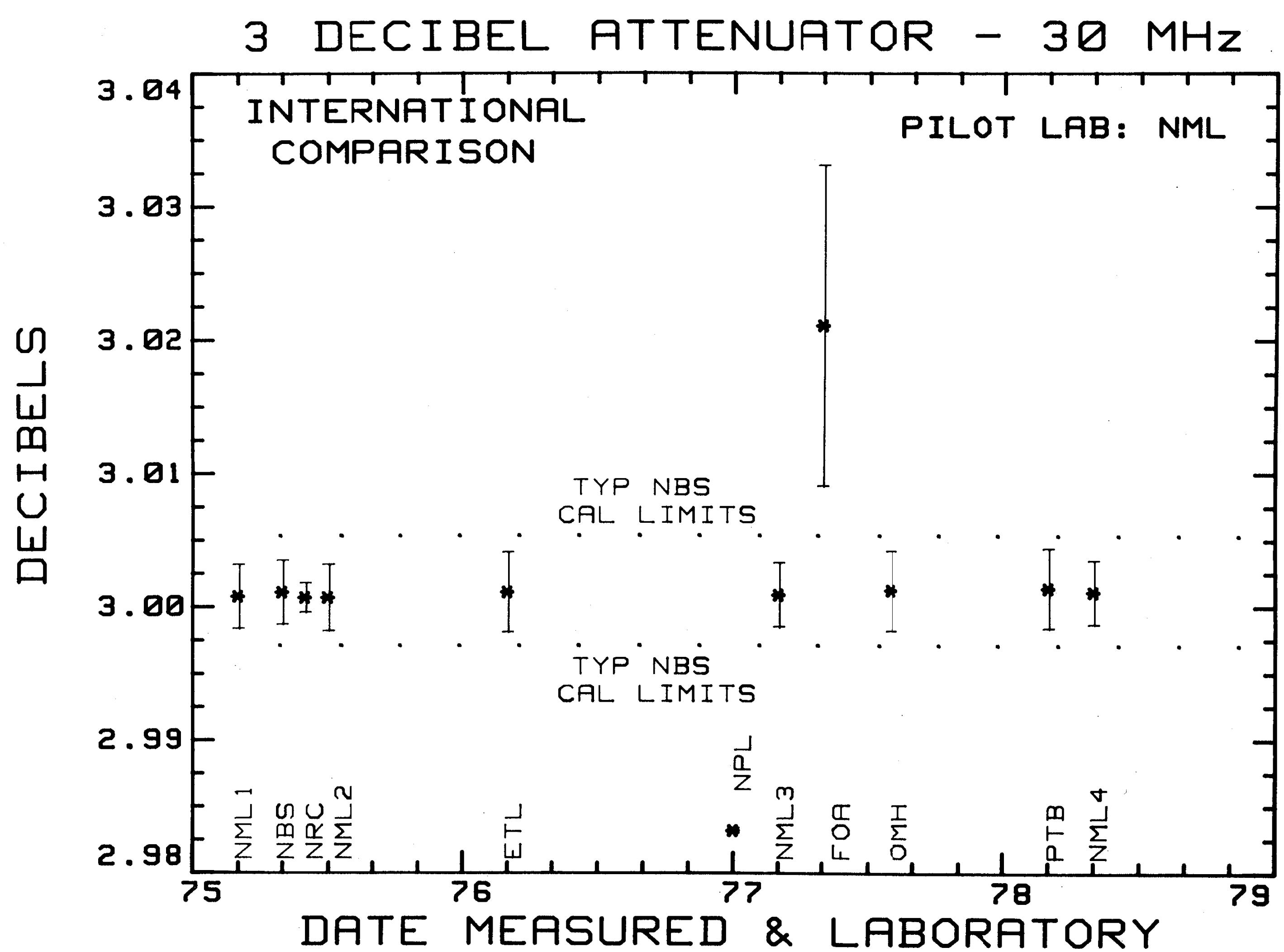

Figure 3.25.1. Calibration Results from International Laboratories for Commercial Fixed Coaxial Attenuator (3 dB).

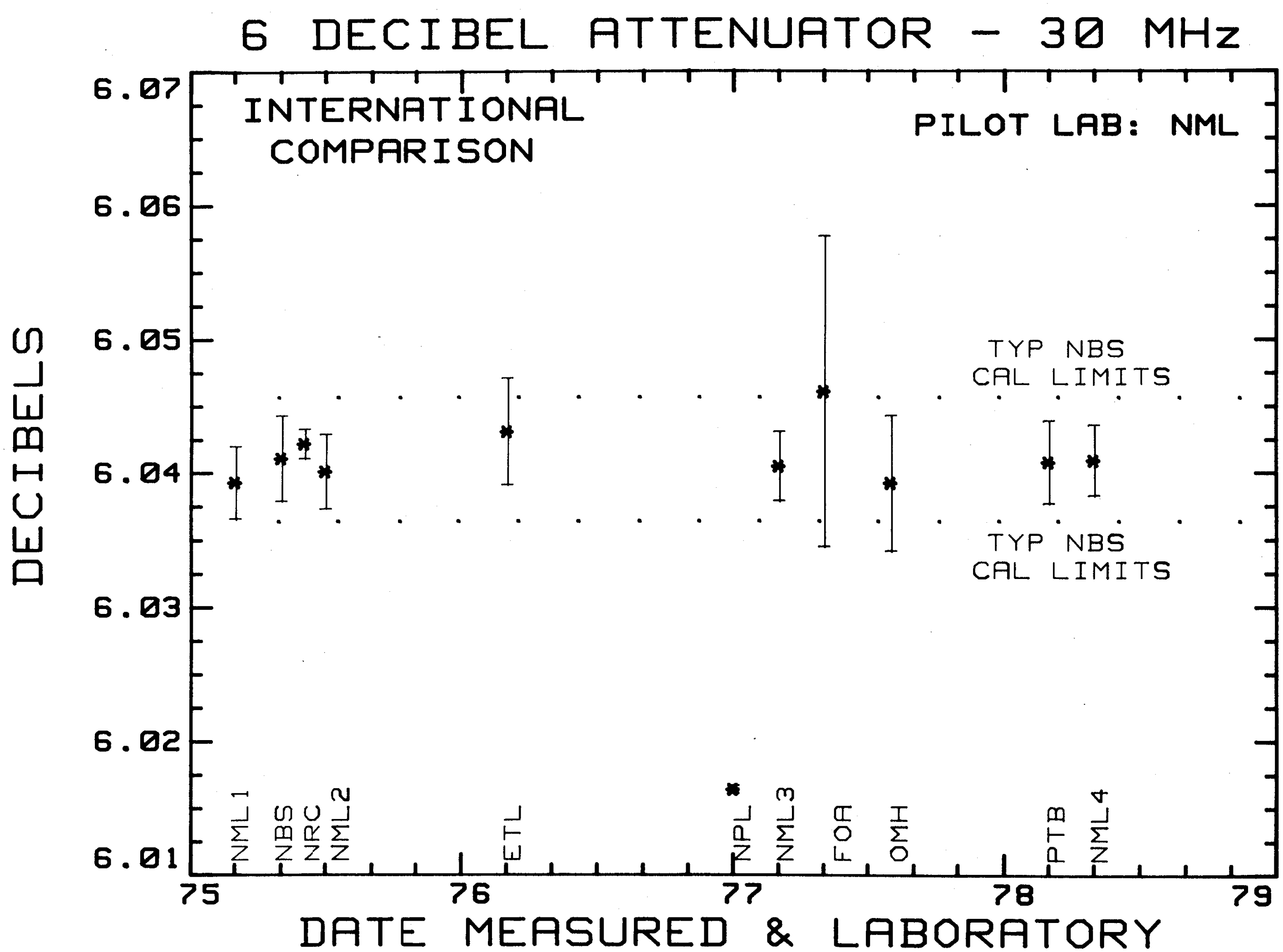

Figure 3.25.2. Calibration Results from International Laboratories for Commercial Fixed Coaxial Attenuator (6 dB).

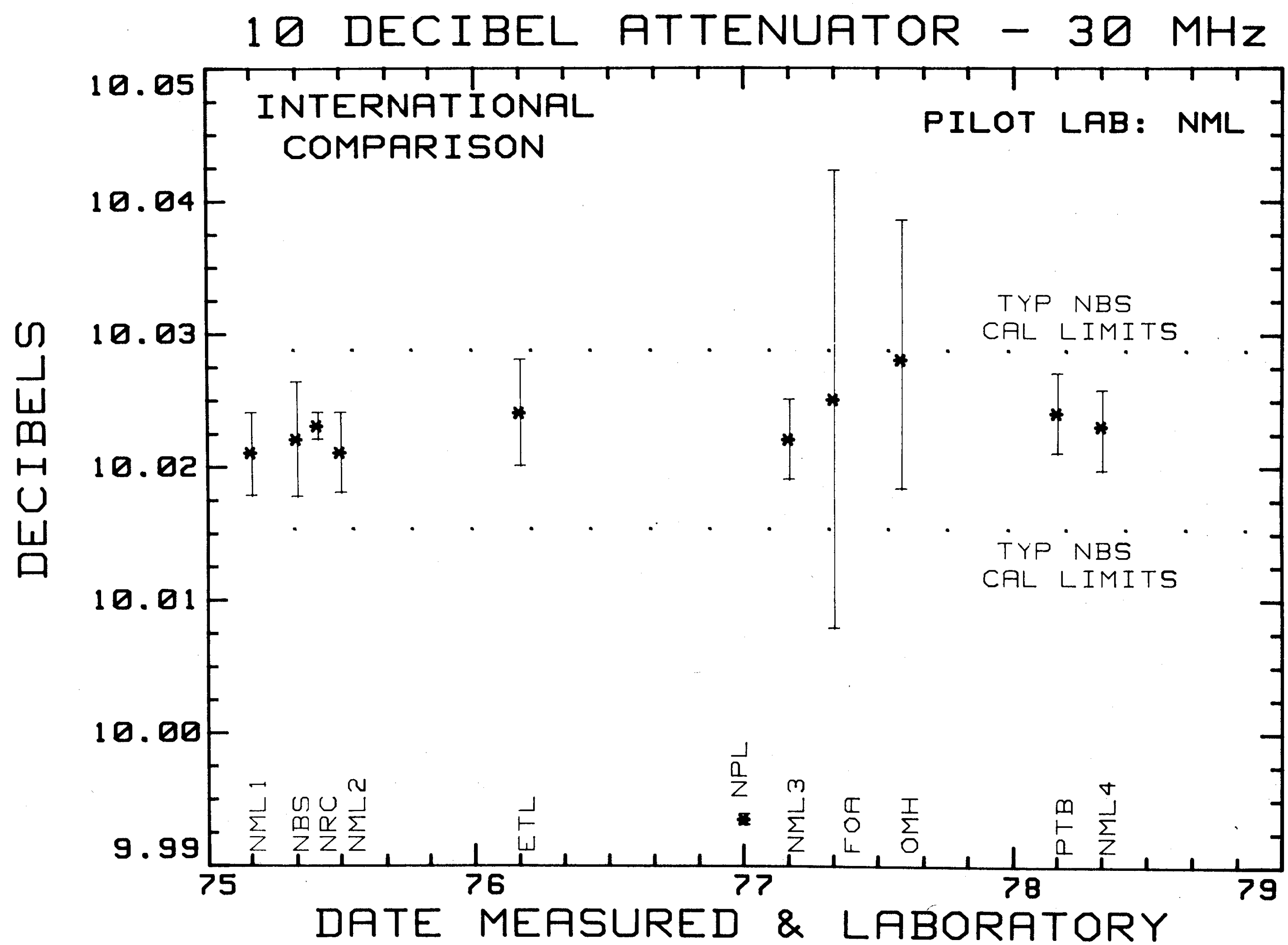

Figure 3.25.3. Calibration Results from International Laboratories for Commercial Fixed Coaxial Attenuator (10 dB).

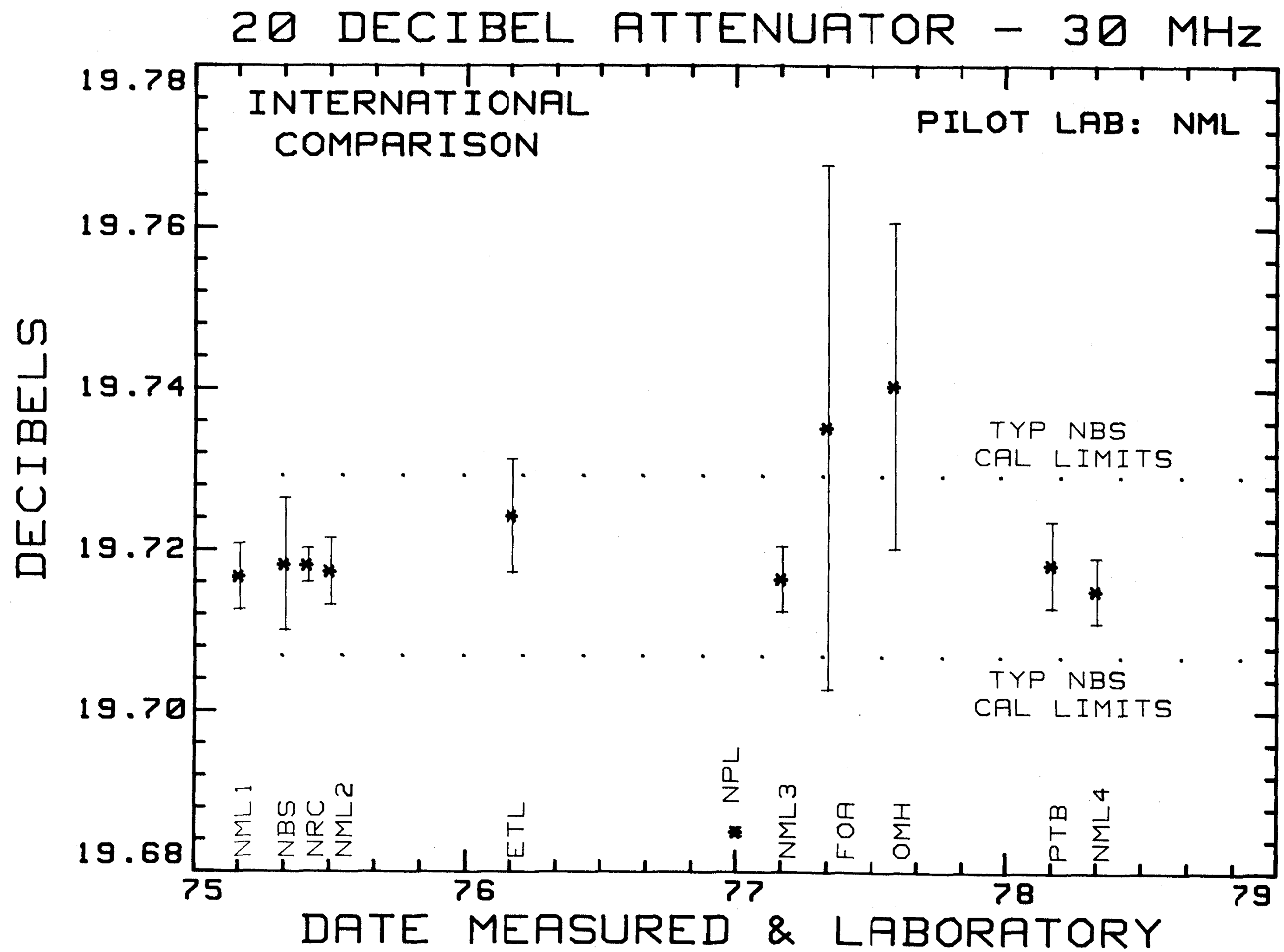

Figure 3.25.4. Calibration Results from International Laboratories for Commercial Fixed Coaxial Attenuator (20 dB).

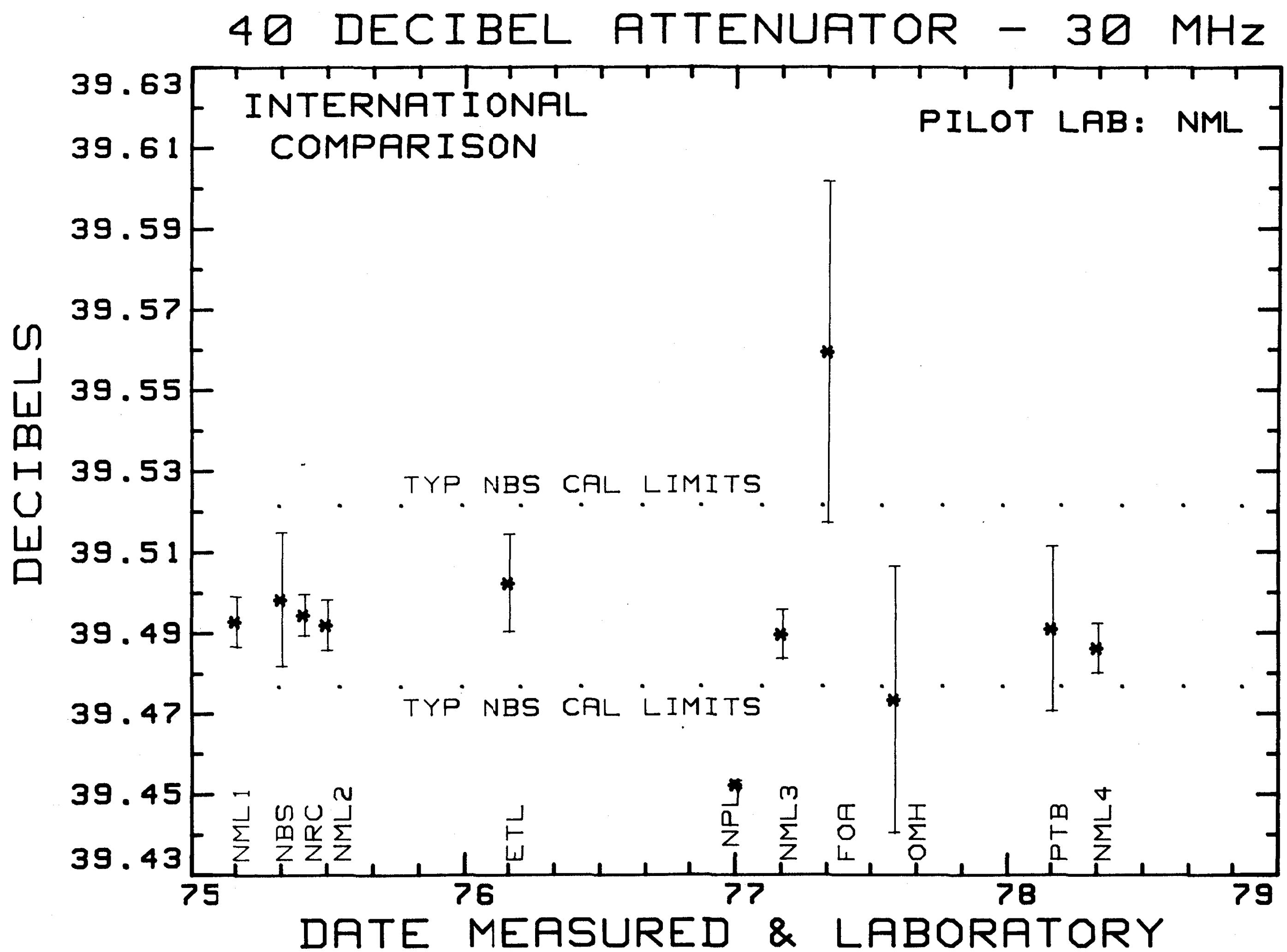

Figure 3.25.5. Calibration Results from International Laboratories for Commercial Fixed Coaxial Attenuator (40 dB).

Sweden include uncertainty budgets that are too large to be useful in examining the relationship of NBS to a mean value.

A decision has been made for purposes of this documentation to consider only the values reported by Australia, Canada, Japan, West Germany and NBS. Hungary was also eliminated because of the large uncertainty bounds associated with their reported values. Table 3.1 below lists the means of the values reported by the selected laboratories.

TABLE 3.1

Mean Values of Fixed Attenuation Standards Measured by Five International Laboratories Including NBS

Nominal Value of Standard dB	Mean of Selected Labs dB	NBS Deviation from Mean dB	Reported NBS Uncertainty dB
3	3.0009	0.0001	± 0.002
6	6.0409	0.0001	± 0.003
10	10.0225	-0.0005	± 0.004
20	19.7178	0.0002	± 0.008
40	39.4930	0.005	± 0.016

Examination of the results clearly lends confidence to both the absolute values reported by NBS and the associated uncertainty bounds.

3.4.3.1 Conclusions:

1. The NBS uncertainty budget is valid.
2. The calculated absolute attenuation rate is correct within the established uncertainty limits.

3.5 Measurement Quality Assurance

3.5.1 Summary of Consistency of 30 MHz System Measurements

Section 3.2 has a detailed multiple-year calibration history for three different basic attenuator designs. The results show a remarkable degree of measurement system control. The conclusions regarding the degree of control of the measurement process are particularly significant considering the evolution, repair and rebuilding of the 30 MHz system that has taken place over the past 22 years.

In addition to the affirmation of measurement control, the results also confirm the validity of the uncertainty analysis and the assigned measurement uncertainty. This is due to the measurements on attenuators with independently calculable values. Each device can be considered a separate check on the 30 MHz measurement system values.

3.5.2 Summary of Comparisons with NBS SQUID System

Section 3.4.1 describes the comparison plot shown in figure 3.22. This plot, and similar ones published in references 13 through 16, clearly validate the absolute attenuation rate calculated for the NBS 30 MHz primary standard of attenuation.

Although it appears that the typical calibration uncertainty limits normally assigned by NBS are conservative, such a conclusion would be erroneous.

The effect of rf leakage depends on where it occurs in the system, how it travels along exterior surfaces, where it recombines with the true signal to be measured and with what phase. These effects are impossible to assess with any confidence. An additional intangible factor is the effective source impedance of the leakage signal. If rf energy is emerging from a narrow gap in the system, this system will possess a very low source impedance. If the source impedance is sufficiently low it is extremely difficult to ground any of the surface-conducted energy or to prevent its reintroduction through small gaps into desired signal paths.

At this time we feel the present uncertainty budget is appropriate for all measured values, especially above 60 dB where leakage adds a significant uncertainty contribution. In the future, the uncertainty limits below 60 dB can be reduced by retrofitting a laser interferometer for displacement measurement as resources become available.

3.5.3 Summary of Comparisons with NBS Six-Port Systems

Section 3.4.2 describes comparison plots shown in figures 3.23 and 3.24. These plots of two different step attenuators were originally made to illustrate the performance of the NBS 10-1000 MHz dual six-port ANA system.

Figure 3.23 compares measurements made on an NBS designed 10-dB step attenuator based on the WBCO principle. The scatter of the observed data reflects a resettability problem with the Model SA-1 rather than random variations in the NBS primary standard. In a similar sense, the scatter of the six-port data probably reflects the same problem.

The significant conclusion to be drawn from figure 3.23 is the close agreement of the mean values. The two systems are totally different in principle; one is based on the decay of an evanescent mode and the other on a dual reflectometer. Both systems produced nearly identical results. The results clearly show that the NBS system is providing values within assigned uncertainty limits.

Figure 3.24 compares measurements made on a resistive step attenuator at six values of attenuation. The individual steps have been normalized to their nominal values (i.e., the 10-dB step actually measures 9.989 dB). The significance of the plot is the correspondence of values measured with two independent systems. As was concluded from figure 3.23, the NBS primary standard is providing measurements well within established uncertainty limits.

3.5.4 Summary of International Intercomparisons

Section 3.4.3 describes an extensive comparison of fixed attenuators by primary laboratories from seven countries in addition to the United States. Measured values for five fixed attenuators are plotted in figures 3.25.1 through 3.25.5. A table showing NBS deviation from an adjusted mean is also included to reflect the comfortable margin provided by the assigned NBS uncertainty bounds. It should be noted that these limits are tighter than normally assigned by NBS. This is due to a larger number of individual measurements above the normal quantity, thus reducing the standard deviation of the mean.

An analysis of these results offers the most conclusive evidence of all that the NBS system is providing measurements within our assigned uncertainty limits.

4.0 Conclusions - 30 MHz Attenuation Measurements

It has been proven that the NBS Attenuation Measurement System as documented in this text is operating under statistical control and is providing calibrations well within stated uncertainty limits.

It is also reasonable to conclude that assigned uncertainty limits could be reduced by hardware modification of the displacement measurement system. The development and marketing of improved 30 MHz WBCO attenuators in the United States and in Great Britain require that NBS undertake a modification program as soon as practical to maintain our assigned primary standards mission.

5.0 Conclusions - 30 MHz Phase Shift Measurements

The NBS Phase Shift Measurement capability has been sparingly used over the past 18 years. Even with a limited data base the uncertainty analysis appears to be conservative. The ability to use the concept of closure at 0 and 360 degrees further validates the assigned uncertainty limits (refer to Section 2.4.2).

As an example, the 1969 calibration of an R-30 resolver lacked closure by 0.76 deg based on measuring 12 separate 30-deg increments. This represents a deviation of 0.06 deg for each 30-deg increment. A comparison of this with the estimated uncertainty of 0.2 deg yields a fairly safe margin.

The lack of closure for test 807850 over 18 years averaged 0.3 deg for a deviation of 0.025 deg for each 30-deg increment. Inspection of figures 3.21.1 through 3.21.5 validates control of the measurement process over the 18 years. Figures 3.20.1 through 3.20.3 yield a similar conclusion for test 809499.

In summary, the phase shift measurement capability has reasonable assigned uncertainty limits and appears to be in good statistical control.

The limited data base for assessing measurement control, the limited use of this service and the lack of independent accuracy validation lead to the conclusion that phase shift measurements should be a special test service rather than a calibration service.

6.0 Summary of NBS 30 MHz Attenuation and Phase Shift Calibration System Uncertainties

TABLE 6.1

Summary of 30 MHz Attenuation and Phase Shift Calibration Uncertainties

Quantity/Device	Uncertainty
ATTENUATION:	
• International Comparisons and Primary Standards Laboratory Quality Devices	0.003 dB/10 dB
• Good Quality Calibration Standards with Low Rf Leakage	0.004 dB/10 dB
• Typical Commercial Fixed and Variable Attenuators	0.005 to 0.01 dB/10 dB
PHASE SHIFT:	
• Good Quality Phase Shifters with Low Rf Leakage and Nearly Constant Insertion Loss	0.2 deg per 36 deg
• Average Quality Phase Shifters	0.5 deg per 36 deg

7.0 References

[1] Uriano, G.A.; Garner, E.L.; Kirby, R.K.; Reed, W.P., eds. NBS calibration services users guide. 1986-1988 Edition. Natl. Bur. Stand. (U.S.) Spec. Publ. 250; 1986 July. 204 p.

[2] NBS calibration services users guide 1986-1988 edition fee schedule. Natl. Bur. Stand. (U.S.) Spec. Publ. 250 Appendix; 1986 July. 94 p.

[3] Beatty, R.W. Microwave attenuation measurements and standards. Natl. Bur. Stand. (U.S.) Monogr. 97; 1967 April. 45 p.

[4] IRE standards on antennas and waveguides: Definitions of terms (1959). Proc. IRE. 47,(4): 568-582; Standards 59 IRE 2.S1. 1959.

[5] IEEE standard specifications and test methods for fixed and variable attenuators, dc to 40 GHz. IEEE Stand. 474-1973. 24 p.

[6] Beatty, R.W. Effects of connectors and adapters on accurate attenuation measurements at microwave frequencies. IEEE Trans. Instr. 13: 272-284; 1964.

[7] Beatty, R.W. Insertion loss concepts. Proc. IEEE. 52(6): 663-671; 1964.

[8] Russell, D. H. High frequency calibrations systems. Notes from High-Frequency and Microwave Attenuation Seminar. March 1968.

[9] Russell, D.H.; Larson W. Rf attenuation. Proc. IEEE. 55(6): 942-959; 1967.

[10] Allred, C.M.; Cook, C.C. A precision rf attenuation calibration system. IRE Trans. Instr. I-9 (2): 268-274; 1960 September.

[11] Brown, J. Corrections to the attenuation constants of piston attenuators. Proc. IEE (London), 96 (III): 491-495; 1949 November.

[12] Stoltenberg, R.E. Rf null detector NBS/SND. Natl. Bur. Stand. (U.S.) NBSIR 73-302; 1973 June. 83 p.

[13] Kamper, R.A.; Simmonds, M.B.; Adair, R.T.; Hoer, C.A. Advances in the measurement of rf power and attenuation using SQUIDs. Natl. Bur. Stand. (U.S.) Tech. Note 661; 1974 September. 27 p.

[14] Adair, R.T.; Simmonds, M.B.; Kamper, R.A.; Hoer, C.A. Rf attenuation measurements using quantum interference in superconductors. IEEE Transactions on Instrumentation and Measurement. IM-23 (4): 375-381; 1974 December.

[15] Adair, R.T.; Frederick, N.V.; Sullivan, D.B. Rf attenuation measurement system using a SQUID. Natl. Bur. Stand. (U.S.) NBSIR 77-863; 1977 September. 146 p.

[16] Sullivan, D.B.; Adair, R.T.; Frederick, N.V. Rf instrumentation based on superconducting quantum interference. Proc. IEEE. 66(4): 454-463; 1978 April.

[17] Rapport de la 15e Session, Comité Consultatif d'Electricité; Bureau International des Poids et Mesures, Annexe E15, E81-E94, 1978.

8.0 Acknowledgments

The authors would like to express their sincere appreciation to the following people for their assistance in producing this document: L.F. Saulsbery for supervising the calibration services; Connie L. True for calibrating the sample devices under test and preparing the measurement results; Robert M. Judish for his help in properly reporting these measurement results; Edna M. Jones and J. Kathleen Hillen for preparing the sample calibration reports; Eleanor Livingston for technical editorial assistance; Shirley Deeg for handling the publication details; and Terry Yenser, Marlene Deutsch and Karen Forberg for preparing the manuscript.

We would also like to express our gratitude to the many technical staff members who assisted in the design, development, construction, and maintenance of this measurement system.

Furthermore, we would like to thank the technical readers M. Crawford, R. Lawton, and D. Vecchia for their valuable assistance in completing this document.

9.0 Appendices

9.1 Appendix A

Excerpt from Reference 5.

9.2 Appendix B

Complete copy of Reference 10.

9.3 Appendix C

Complete Copy of Reference 14.

9.4 Appendix D

Excerpts from Reference 17.

9.5 Appendix E

Drawings of System Components.

9.1 Appendix A

Excerpt from Reference 5.

IEEE Standard
Specifications and Test Methods for Fixed and Variable Attenuators, DC to 40 GHz

Including Trial-Use Sections on Insertion-Loss Repeatability and Characteristic Insertion Loss of a Noninsertable Two-Port

1. Purpose and Scope

This performance standard covers absorptive and reflective attenuators, both fixed as well as continuously variable or variable in fixed steps, both manual and programmable types. It does not cover electronic or solid-state-type attenuators.

This standard permits the user to select for a specification those minimum performance parameters which characterize an attenuator. A list of preferred test methods is included permitting verification of the attenuation characteristics.

Practical minimum performance limits are furnished for various applications. These are for guidance only and will improve with time.

2. Definition of Characteristic Insertion Loss

2.1 Interpretation of Characteristic Insertion Loss. An attenuator is ideally a linear network which may be in the form of a transmission line or waveguide component designed to reduce the input power by a predetermined ratio. The ratio of input to output power is commonly expressed in logarithmic terms such as decibels. The power output ratio as commonly used in the "characteristic insertion loss" relation is shown in Fig 1. The ratio specified is equal to the characteristic insertion loss since source and load are reflectionless. The term "attenuation" is used rather loosely and means "characteristic insertion loss" as defined in Fig 1. Attenuators include absorptive and reflective devices, having at least two ports.

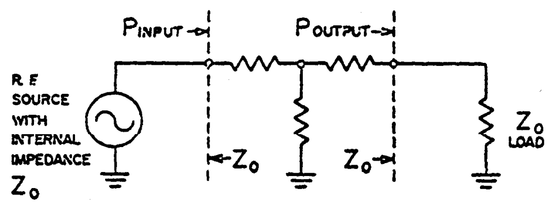

Fig 1
Definition of Characteristic Insertion Loss

P_{INPUT} = Incident power from Z_0 source
P_{OUTPUT} = Net power into Z_0 load
Characteristic insertion loss = $10 \log_{10} \dfrac{P_{INPUT}}{P_{OUTPUT}}$ (dB)

There are fixed attenuators, continuously variable, and step attenuators. Only Z_0 matched, two-port attenuators, designed for use in a Z_0 system, are treated in this standard.[1] They are reversible except when specially noted as, for example, for a high-power attenuator. All attenuators in this standard are passive, linear, resistive or reactive, nominally symmetrical in impedance.[1] Voltage-variable attenuators, including vacuum tube or solid-state types, are not covered in this standard.

To specify a variable attenuator, one must know its end use. If the device is used to extend the range of a power meter, one requires to know its terminal-to-terminal or total loss. This is described by the characteristic insertion loss. However, in most applications the variation above the mimimum loss is of major interest. One specifies then the

[1] Section 8, published for trial use, includes attenuators having different input and output impedance.

9.2 Appendix B

Complete Copy of Reference 10.

A PRECISION RF ATTENUATION CALIBRATION SYSTEM

BY

C. M. ALLRED AND C. C. COOK

Reprinted from IRE TRANSACTIONS
ON INSTRUMENTATION
Volume I-9, Number 2, September, 1960

PRINTED IN THE U.S.A.

A Precision RF Attenuation Calibration System*

C. M. ALLRED†, MEMBER, IRE, AND C. C. COOK†, MEMBER, IRE

Introduction

THE NEED for higher accuracy in attenuation measurements has kept pace with the advances in electronics. In an effort to meet the demands in this field, a precise and accurate system for the measurement of attenuation has been developed.

The system discussed operates at 30 Mc, but similar systems under construction are designed to operate at other frequencies. Choosing a single frequency of operation allows designs that increase the stability, extend the measuring range, lessen the problems of leakage, and enhance the over-all accuracy.

The System

Description of the System

Achieving a system with sensitivities of 0.001 db, accuracies of a few thousandths of a db, and a range exceeding 120 db requires careful design and special techniques. With such large ranges of attenuation to be measured, the monitor should be capable of voltage gains of 10^8 or more. Because of the stability problem of such a monitor and the desired sensitivity of 0.001 db, it was decided to operate in a two-channel system and use a null response. As is well known, the use of two-channel techniques greatly lessens the problems of level instability of the source and gain instability of the monitor. High sensitivity is also inherent in such systems. One may consider the increased complexity of the system and the necessity of making adjustment in both phase and magnitude as payment for the advantages. The block diagram of the system is shown in Fig. 1.

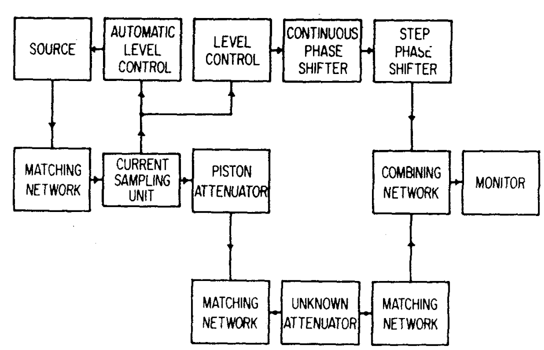

Fig. 1—Block diagram for attenuation measuring system.

The RF source is a 30-Mc crystal-controlled transmitter capable of 200 watts output with low residual modulation. The low resistive component of the piston attenuator launching coil is coupled to the 50-ohm source by a special impedance-matching network. The

* Received by the PGI, June 24, 1960. Presented at the 1960 Conference on Standards and Electronic Measurements as paper 6-2.
† National Bureau of Standards, Boulder, Colo.

current in the launching coil energizes the channel containing the phase shifter and also supplies the input to an automatic level control network connected to the source. This network is used to keep the current in the launching coil constant. The continuous precision phase shifter having low incidental level changes connects to a step adjustable phase shifter. The attenuator to be tested is inserted between matching networks in the channel containing the piston attenuator. The two channels are brought together in a special combining unit which presents correct impedances to the respective channels, minimizes interaction between the channels and has a low insertion loss. The system is completed by a high-gain monitor.

Measurements are made by adjusting both the standard attenuator and phase shifter until a null response is obtained. This is done with and without the attenuator under calibration in the system. The change in the standard attenuator and phase shifter readings gives the value of attenuation and phase shift of the unknown.

In its present form, the phase shifter has no accurate displacement measuring device and no attempt will be made to evaluate the phase measuring characteristics of the system.

Front and rear views of the complete system mounted in a console are shown in Figs. 2 and 3, respectively.

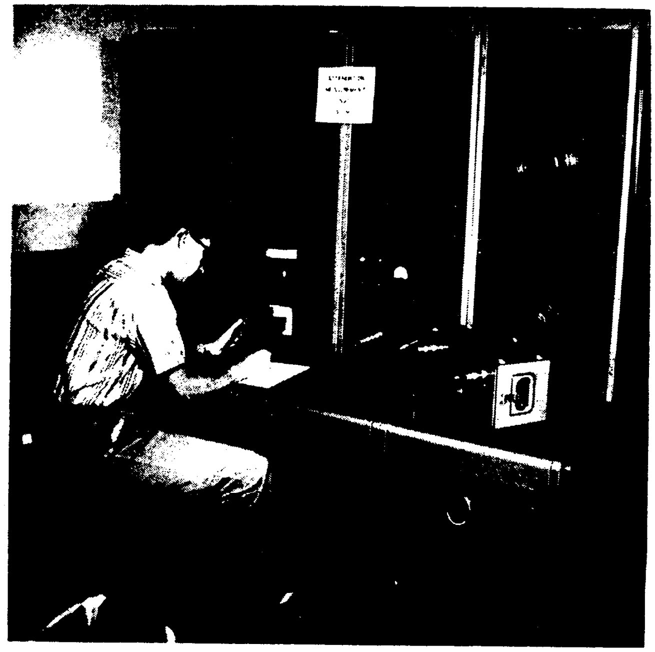

Fig. 2—Front view of attenuation measuring system.

Fig. 3—Rear view of attenuation measuring system.

Standard Attenuator

Properties: Piston attenuators are used quite extensively for precision attenuation measurements.[1-3] The major advantage of such attenuators is that the attenuation is determined (except for secondary effects) by the fundamental units, length and time (frequency). Another advantage is that close impedance matching is usually not a stringent requirement.

The attenuator has its disadvantages. It is essentially a nondissipative instrument and reflects varying amounts of energy rather than absorbing it as the attenuation is varied. As a result, the minimum insertion loss is quite high for linear operation and the terminal impedances are reactive. Usually, frequency sensitive networks are used for impedance matching. An additional problem occurs because of the permeability and finite conductivity of the material used for the waveguide. These cause a second-order effect on the attenuation constant. This requires a determination of the permeability and conductivity of the material used in the guide wall. Since the attenuation constant α is a slowly varying function of frequency, a single scale cannot be used over wide frequency ranges without correction. Only output signal ratios are measured; the relationship between input and output, if desired, must be determined by other means.

Theory: Fields existing within a uniform perfectly-conducting waveguide can be expressed as a linear combination of terms called modes. The field components for each mode are proportional to the quantity, $e^{-\gamma z+j\omega t}$, where the propagation constant γ is purely imaginary and is determined entirely by the guide dimensions and frequency.

Below a certain frequency, called the cutoff frequency, γ becomes purely real and the fields decay exponentially at a rate dependent upon the mode. To in-

[1] D. E. Harnett and N. P. Chase, "The design and testing of multirange receivers," Proc. IRE, vol. 23, pp. 578–593; June, 1935.
[2] R. E. Grantham and J. J. Freeman, "A standard of attenuation for microwave measurements," *Trans. AIEE*, vol. 67, pp. 535–537; June, 1948.
[3] C. G. Montgomery, "Technique of Microwave Measurements," M.I.T. Rad. Lab. Series, McGraw-Hill Book Co., Inc., New York, N. Y., vol. 11, ch. 11, pp. 679–719; 1947.

sure mode purity at high attenuation levels, the mode with the smallest decay rate is commonly used.

In the actual case, the permeability and finite conductivity of the guide walls and the properties of the medium within the guide add a small imaginary and real part to the above propagation constant.

A good approximate equation for the propagation constant of the TE_{11} mode is given by:[4,5]

$$\gamma = \frac{p_{11}}{a}\sqrt{1-\left(\frac{2\pi af}{p_{11}C}\right)^2 - \frac{1}{a\sqrt{\pi\mu f\sigma}}} \cdot \left[1 + j\left\{1 - \frac{1}{1 - \dfrac{1}{a\left[2-\left(\dfrac{2\pi af}{p_{11}C}\right)^2\right]\sqrt{\pi\mu f\sigma}}}\right\}\right]$$

where:

a = physical radius of guide

p_{11} = 1.8411838, a constant which is the first root of the first derivative of the first-order Bessel Function of the first kind

f = frequency

C = velocity of light in an unbounded medium having the electrical properties equal to that within the guide

μ = permeability of guide wall

MKS system of units are used throughout. With the operating frequency so far below the cutoff frequency, neglecting the effect of even moist air within the guide as compared to vacuum gives rise to an error less than 1 part in 10^7. (C for vacuum = 299793.0 ± 0.3 km/sec.[6])

Circular Waveguide: In the system described, circular waveguide was used with the excited field consisting of the TE_{11} mode. The displacement of the receiving coil relative to the launching coil is measured by a ruled scale and optical projector. The scale is accurate to 0.0001 inch in any 6 inches.

The guide is composed of brass and has an outside diameter of 3.9 inches and a length of 22.3 inches. The internal diameter of the guide was chosen so as to give an attenuation rate of 10 db per inch. This diameter was measured at 2-inch intervals along the guide. The average diameter was 3.19725 inches with a maximum variation of 0.00003 inch. The accuracy of the measurements are within ±50 millionths of an inch. These measurements were made at 68°F while the system is operated about 4°F above this temperature. The thermal coefficients of expansion of the stainless steel scale and the brass guide are approximately the same. If they were equal, temperature variations would have negligible effect. Assuming a conservative 5 parts per million (20 per cent) difference in their coefficients, a calculable error of 0.0001 db per 10 db could arise for the 4°F temperature variation. An uncertainty of 0.0001 inch in the diameter of the guide at 68°F adds an error of 0.0003 db per 10 db. The dc conductivity of the guide was found to be 1.35 ×10⁷ mhos per meter. From Chambers and Pippard[7] and Bussey,[8] it is conservative to say that the RF conductivity does not decrease more than 10 per cent from the bulk dc value. Assuming the RF conductivity has decreased from the dc value by 5 per cent, this value of conductivity will be fairly certain to ±5 per cent. Such an uncertainty gives rise to an error of 0.00026 db per 10 db.

The inside wall of the guide has a thin coating (5 to 10 microinches) of rhodium. This provides a hard surface for the silver sliding contacts of the piston to bear upon and prevents corrosion of the brass surface. The effective conductivity of the guide surface is insignificantly altered from that of the brass itself.

Input System

The input system of a piston attenuator is important, as it plays a major role in the over-all measurement range. The high initial insertion loss inherent in piston attenuators arises from lack of mode purity and the interaction of the output on the input when the coil separation is small. What is needed is an input system that launches the single TE_{11} mode with an intensity independent of the position of the output coil, or a system that launches the desired mode with such a strong intensity that the output coil need not come close to the input coil. Both approaches are simultaneously used. Barlow and Cullen[9] reduce the interaction effect by making the magnitude of the generator and load resistive impedances equal to the characteristic impedance of the attenuator. Weinschel, Sorger, and Hedrich[10] reduce the effect by considering the entire attenuator as a mutual inductive coupled tuned bandfilter and adjust the generator impedance for minimum deviation from linearity.

A different approach is used here. If one could achieve a current sheet with a spatial distribution in the transverse plane of the guide having the same form as the familiar electric field pattern of the TE_{11} mode, the desired evanescent mode would be launched in both directions from the current sheet. Furthermore, if the current sheet were constant (infinite impedance gener-

[4] J. Brown, "Corrections to the attenuation constants of piston attenuators," *Proc. IEE*, vol. 96, pt. 3, pp. 491–495; November, 1949.

[5] C. M. Allred, "Chart for the TE_{11} mode piston attenuator," *J. Res. NBS*, vol. 48, pp. 109–110; February, 1952.

[6] J. W. M. DuMond, "Present status of precise information on the universal physical constants. Has the time arrived for their adoption to replace our present arbitrary conventional standards?" IRE Trans. on Instrumentation, vol. I-7, pp. 136–175; December, 1958.

[7] R. G. Chambers and A. B. Pippard, "The Effect of Method of Preparation on the High-Frequency Surface Resistance of Metals," Inst. of Metals, London, Eng., Monograph No. 13, pp. 281–293; 1953.

[8] H. E. Bussey, "Standards and measurements of microwave skin depth-conductivity, surface impedance, and Q," this issue, p. 171.

[9] H. M. Barlow and A. L. Cullen, "Microwave Measurements," Constable and Co., Ltd., London, Eng., pp. 384–388; 1950.

[10] B. O. Weinschel, G. U. Sorger, and A. L. Hedrich, "Relative voltmeter for VHF/UHF signal generator attenuation calibration," IRE Trans. on Instrumentation, vol. I-8, pp. 22–31; March, 1959.

ators) and independent of the fields reflected from the pickup coil, the interaction effect would cease to exist. The above conditions are approached by constructing the launching coil after the above pattern (see Fig. 4). The constant current sheet feature is approached by sampling the launching current and keeping this current constant by means of negative feedback to the RF source.

The attenuator guide has been extended beyond the launching coil for a twofold purpose. The pickup coil must produce a reflected field since it absorbs energy. This reflected field passes through the launching coil with little interaction and is terminated by the guide extension. The field excited by the launching coil in the guide extension is also terminated.

The problem of matching the low resistive component (estimated to be between 0.01 and 0.1 ohm) of the launching coil is quite severe. This is accomplished by means of a special network utilizing small ceramic capacitors in a ladder arrangement. These capacitors have a high RF voltage and current rating; this permits operation of the matching network at inputs to 200 watts. A 100-watt input produces a current of the order of 35 amperes in the launching coil.

The launching unit is constructed of small stainless steel tubing and water is passed through the unit to prevent excessive heating of the guide which would change its dimensions.

Mode filters are also used, since the reactive impedance of the launching unit gives rise to some axial electric field.

Performance of the input system is discussed later along with the over-all system performance. A detailed report of such input systems is being prepared for publication.

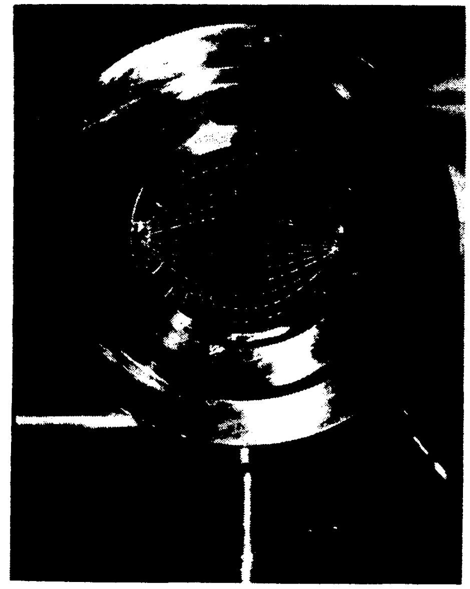

Fig. 4—Launching coil assembly similar to the one described.

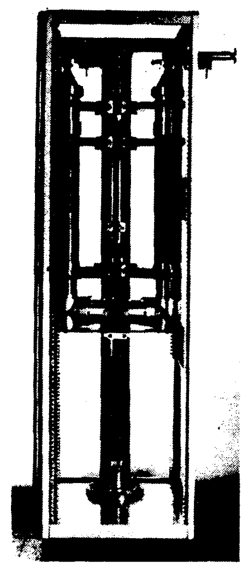

Fig. 5—Phase shifter.

Phase Shifter

A precision continuous phase shifter was needed which had level changes less than 0.001 db as the phase was varied. This placed the following restrictions on the phase shifter: the section of the phase shifter whose electrical length is varied must have a very uniform characteristic impedance, it must be terminated in this value of impedance, and the line must be sufficiently large to reduce the wall losses due to the finite conductivity of the metal.

The phase shifter is of the trombone type (see Fig. 5). This type consists of two stationary transmission lines connected together by a U-shaped transmission line which moves relative to the stationary section in a telescoping manner. Single-frequency operation permitted use of the simplified nonconstant impedance construction. The stationary sections of the phase shifter consist of precision coaxial lines which are terminated at both ends in their characteristic impedances. The moveable section is dimensionally stable but nonprecise. The undesirable level changes caused by imperfectly terminating the precision line are lessened if both ends are closely matched to the characteristic impedance of the line. A 10-db pad bracketed by impedance matching networks has been built into the center of the moving section. This provides isolation between the two halves of the trombone and the correct terminating impedances for the corresponding ends of the precision section. Additional pads and matching units are provided for terminating the other two ends.

The outer conductors of the precision section of the phase shifter are electroformed copper cylinders. A heavy silver plate with thin rhodium coating is on the inside walls. The inside diameters are 3.33 inches, outside diameters, 3.9 inches, and lengths, 22.3 inches. The center conductors are brass rods with silver plate and rhodium coating similar to that used on the outer conductors. The diameters are 1.44 inches. Maximum departure of the critical diameters from the mean value is 0.00035 inch. The maximum change in characteristic impedance at any point due to these diameter variations is less than 0.04 per cent. These are calculated variations and represent pairing the worst possible combinations of diameter measurements. The averaging effect of the smooth variations in the diameters would produce a much smaller variation in characteristic impedance.

The complete phase shifter was made operational by adjusting the four terminating matching networks until input and output impedance changes were very small as the moving section was varied. These changes were less than 0.01 ohm for both real and reactive components as measured on an RF bridge having high differential sensitivity.

The constancy of output level of the phase shifter was measured using crystal diode detectors in a very sensitive differential circuit. The maximum level variation was less than 0.0005 db. This occurred for a 33° phase shift. The phase shifter level change will be significantly less than this in the case of most piston attenuators and dissipative attenuators operating where the attenuation is essentially independent of frequency since the phase shift is usually small in these attenuators. In any case, corrections can be made.

The Combining Junction

The two channels are brought together by means of a special network. This network minimizes interaction between the two channels which would otherwise require excessive padding to maintain impedance match. The network[11] is based on the bridged-T circuit. Such a network, if ideal, completely isolates the two channels from each other, presents each channel with the correct matching impedances, and would have an insertion loss of only 3 db. The actual network has the following measured characteristics:

Isolation between inputs:	110 db
Input Impedance:	
Input 1	$50.4+j0$ ohms
Input 2	$50.9+j0$ ohms
Insertion Loss:	
Input 1 to output	4 db
Input 2 to output	4 db.

The combining junction with cover removed is shown in Fig. 6.

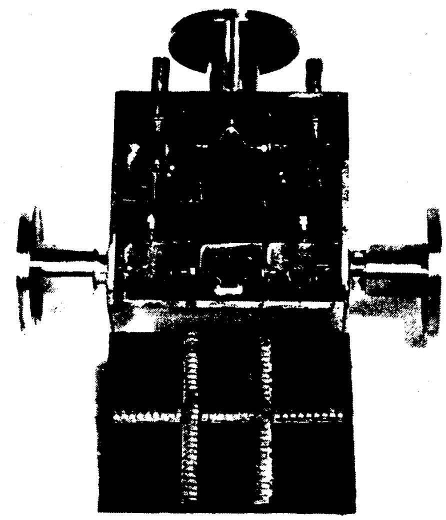

Fig. 6—Combining junction.

System Performance

The system is essentially a primary standard and therefore does not require calibration. In comparisons with other standards, agreement has been within the corresponding error limits. Tests to check the self-consistency of the system have been made by measuring a fixed value of attenuation at various initial positions of the attenuator, at different input power levels, and various initial positions of the phase shifter. The system is new and a few additions and modifications are yet to be made. The main addition will be a special low-noise stable monitor using phase detection designed to fit the system's special requirements. The present monitor is a slightly modified ordinary commercial communication receiver.

Sensitivity

The system has a sensitivity greater than 0.001 db at a level of 80 db below 1 volt output of the standard attenuator. In principle the sensitivity would increase by a factor of 10 for every 20-db increase in level. Instability of components and the fact that the signal is not strictly a pure single frequency sine wave prevent the sensitivity in a null system from completely achieving the ideal.

Stability

All components were constructed and mounted so as to give the system stability. For example, solid semi-flexible coaxial line is used throughout. The stability is indicated by the following calibration data of a commercial attenuator, Table I. The time sequence is from left to right and each row is a repeat of the attenuator settings. A lapse of about one hour occurred while data were being taken. This means that the time lapse between succcesive values in a given column represents roughly 12 minutes. All values are in db. Instabilities do occur sometimes, as indicated in the last two readings and a few components have had to be changed. Normally, quite a few readings can be taken before a drift of 0.001 db is noticed. As the difference between two readings gives the value of attenuation desired, the drift usually does not impair the accuracy significantly.

[11] C. M. Allred and C. C. Cook, "A multiple isolated-input network with common output," to be published in *J. Res. NBS.*

TABLE I
DATA SHOWING STABILITY OF SYSTEM

88.212	87.213	86.212	85.212	84.219	83.205
88.212	87.212	86.212	85.212	84.220	83.205
88.212	87.213	86.212	85.212	84.220	83.206
88.212	87.213	86.212	85.212	84.225	83.208

Linearity

The linearity of the attenuator at close coil separations is good but the point of departure from linearity (due to the interaction effect) could not be ascertained. The problem occurs because of heating effects in the pickup coil as the output level increases. This slow thermal drift occurs before any interaction effect is noticed.

The equivalent change in linearity produced by this high level thermal drift is about 0.006 db at the 3-volt level and is essentially absent at the 1-volt level.

A stable 10-db step of a dissipative attenuator was measured at various positions of the standard attenuator. The results are given in Fig. 7. The first point on the left, for example, gives the value of 9.971 for the nominal 10-db step of the dissipative attenuator when the standard attenuator is operated within the 23- to 33-db region. The 1-volt output level is at about the 33-db position. The first point deviates from the others because of the above-mentioned thermal drift in the pickup coil when operated at the 3-volt output level (23-db position). The last four points show deviations due to poor signal-to-noise ratio. When these data were taken, the temperature control system for the water flowing in the launching unit was not installed and the input end of the attenuator was a few degrees colder than the output end. A rough calculation of this effect is indicated by the dashed line and shows that, when in proper operation, the system will be more linear. There has been insufficient time to take new data.

Measuring Range

The data in Fig. 7 do not represent the range of the system, as additional padding had to be added to the attenuator channel at higher output levels (less attenuation) to permit nulling with the phase shifter leg. The last nine positions, however, represent roughly the level of the signal at the monitor. The last point, for example, is taken at 140 db below the 1-volt level. Thus the data on the graph represent a measurement range of 150 db. Each point was obtained by averaging 6 measurements. The standard deviations of the last five points were, respectively: 1.2, 1.6, 8.1, 6.2, and 30.3 thousandths of a db. The data include any nonreproducibility in the 10-db step of the dissipative attenuator.

Accuracy

The errors discussed do not include those due to mismatched impedances presented to the attenuator under calibration. There are situations where, because of high

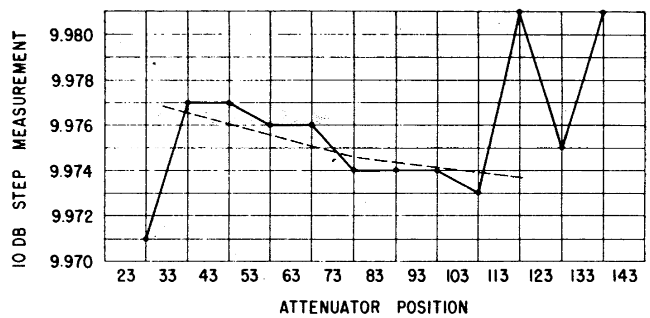

Fig. 7—Attenuator linearity test.

initial insertion loss, the measurement is essentially independent of impedance mismatch. Such cases occur in most piston attenuators and also in those dissipative attenuators having sufficient padding as an integral part of the attenuator.

The total system error, which is a function of the range of measurement, A, can be separated into its parts.

Let

$$E_t = E_m + E_g + E_\Phi + E_n$$

where

E_t = total system error.

E_m = error in measuring system. This can be subdivided into those errors due to the scale and those due to lack of resolution in the projection equipment.

Scale error = 0.001 db for $0 < A < 60$ db, 0.002 db for $60 < A < 120$, 0.003 for $120 < A < 180$ db.

Resolution error is somewhat less than 0.001 db for any value of A.

E_g = errors due to uncertainties in values of guide diameter, guide conductivity, and temperature effects. As indicated previously, this is well within 0.001 $A/10$ db.

E_Φ = errors due to level changes in the phase shifter. These are known sufficiently well to leave the uncertainties small compared to other errors.

E_n = errors due to the uncertainties caused by the random fluctuations of noise. If at large values of $A (A \geqq 100$ db) six measurements are averaged, the results of tests shown in Fig. 7 would indicate reasonably safe values of E_n to be:

$$\begin{aligned} E_n &= \pm 0.002 \text{ db for } 90 < A \leqq 100 \text{ db} \\ &= \pm 0.004 \text{ db for } 100 < A \leqq 110 \text{ db} \\ &= \pm 0.01 \text{ db for } 110 < A \leqq 120 \text{ db} \\ &= \pm 0.02 \text{ db for } 120 < A \leqq 130 \text{ db} \\ &= \pm 0.05 \text{ db for } 130 < A \leqq 140 \text{ db.} \end{aligned}$$

These could be reduced by averaging over a greater number of measurements. The above values of E_n are based on the assumption that the input signal level to the unknown attenuator (attenuation values, A) is 1 volt. If this is raised to 3 volts:

$$E_n' = \pm\ 0.03 \text{ db for } 130 < A \leqq 140 \text{ db}$$

$$E_n' = \pm\ 0.06 \text{ db for } 140 < A \leqq 150 \text{ db}$$

where E_n' includes the effect of noise and the thermal drift in the pickup coil.

The combination of these errors into a total error gives:

$$E_t = \pm \left(0.002 + 0.001 \frac{A}{10}\right) \text{ db for } 0 \leqq A \leqq 60 \text{ db}$$

$$E_t = \pm \left(0.003 + 0.001 \frac{A}{10}\right) \text{ db for } 60 < A \leqq 90 \text{ db}$$

$$E_t = \pm\ 0.015 \text{ db for } 90 < A \leqq 100 \text{ db}$$

$$E_t = \pm\ 0.018 \text{ db for } 100 < A \leqq 110 \text{ db}$$

$$E_t = \pm\ 0.025 \text{ db for } 110 < A \leqq 120 \text{ db}$$

$$E_t = \pm\ 0.037 \text{ db for } 120 < A \leqq 130 \text{ db}$$

$$E_t = \pm\ 0.068 \text{ db for } 130 < A \leqq 140 \text{ db.}$$

Again, if the 3 volt level is used instead of the 1 volt:

$$E_t = \pm\ 0.048 \text{ db for } 130 < A \leqq 140 \text{ db}$$

$$E_t = \pm\ 0.079 \text{ db for } 140 < A \leqq 150 \text{ db.}$$

ACKNOWLEDGMENT

Others have helped in various phases of this work and the authors gratefully acknowledge the contributions of the following: D. H. Russell, E. C. Wolzien, R. L. Peck, R. Barkhaus, R. Brunner, M. A. Mulligan, A. L. Schuster, P. A. Nichols, R. C. Darr, W. H. Long, and P. L. London.

9.3 Appendix C

Complete Copy of Reference 14.

RF Attenuation Measurements Using Quantum Interference in Superconductors

ROBERT T. ADAIR, MICHAEL BANCROFT SIMMONDS, ROBERT ANDREW KAMPER, CLETUS A. HOER

Reprinted by permission from IEEE TRANSACTIONS ON INSTRUMENTATION AND MEASUREMENT
Vol. IM-23, No. 4, December 1974, pp. 375-381

RF Attenuation Measurements Using Quantum Interference in Superconductors

ROBERT T. ADAIR, MICHAEL BANCROFT SIMMONDS, ROBERT ANDREW KAMPER, SENIOR MEMBER, IEEE, AND CLETUS A. HOER, MEMBER, IEEE

Abstract—**A unique portable system has been developed for measuring RF attenuation over a dynamic range of 62 dB at 30 MHz. A superconducting quantum interference device (SQUID) is the basis of the system. A SQUID is a loop of superconducting metal closed by a weak point contact called a Josephson junction, operating in liquid helium. It converts variations in magnetic flux to periodic variations in impedance which are sensed at microwave frequencies. This provides a convenient natural means of measuring electrical quantities such as voltage, current, power, and attenuation.**

I. INTRODUCTION

A TRANSDUCER that converts variations in magnetic flux into nearly perfect periodic variations in microwave impedance which are sensed as the change in the microwave reflection coefficient is known as a superconducting quantum interference device (SQUID). The period of a SQUID corresponds to one magnetic flux quantum (2.067854×10^{-15} Wb). This provides a convenient natural means of measuring attenuation.

These devices are very accurate over a wide dynamic range. Electrical quantities are measured by counting periods (flux quanta) in the response of a SQUID in the same manner that length can be measured by counting wavelengths of light emitted by a laser.

Under ideal conditions, if the SQUID input current I is an RF current, then the SQUID ouput response is the zero-order Bessel function of the *magnitude* of the RF input current.

Thus the output of the microwave readout circuit is proportional to $J_0(2\pi I/I_0)$ where I is the RF input current amplitude and I_0 is the current necessary to drive one quantum of magnetic flux into the SQUID. I_0 need not be known to make attenuation measurements. The values of the argument $2\pi I/I_0$ at the flux quanta nulls or zeros can be found in a table of Bessel functions. A single measurement system can be used to measure attenuation from dc to 1 GHz with accuracies comparable to existing conventional techniques. Several successful prototype measurement systems have been constructed at the National Bureau of Standards based on the SQUID [1].

The major advantages of this new technique for measuring RF attenuation include the following.

Manuscript received July 3, 1974; revised August 19, 1974. This paper is a contribution of the National Bureau of Standards and is not subject to copyright.

The authors are with the Institute for Basic Standards, National Bureau of Standards, Boulder, Colo.

1) The relative ease of construction of the system, e.g., the accuracy of the measurements does not depend on high precision machining of mechanical parts such as in waveguide below cutoff attenuators.

2) The system does not require a standard of attenuation. It requires only a table of Bessel functions to determine the exact change in attenuation between any two given flux quanta nulls.

3) This technique provides a broad frequency range of operation without tuning (0–1 GHz in one system).

4) The readout technique makes it relatively easy to automate measurements with this system.

II. SQUID DETAILS

A. *Principle of Operation*

The basic SQUID system configuration is shown in Fig. 1, where I_s represents the Josephson current and I represents the input current.

In addition to the usual leakage and displacement currents that flow through any metallic contact, a Josephson junction passes a component of current (the "Josephson current") which is controlled by conditions in the superconductors on either side of the junction. If the superconductors are connected together to form a loop closed by the junction, then the Josephson current I_s depends upon the magnetic flux ϕ linking the loop:

$$I_s = I_c \sin (2\pi\phi/\phi_0). \tag{1}$$

I_c depends only on the strength of the particular contact. The quantity ϕ_0 is a fundamental constant of nature known as the flux quantum

$$\phi_0 = h/2e = 2.0678538 \times 10^{-15}\ \mathrm{T\cdot m^2} \tag{2}$$

where h is Planck's constant and e is the charge on the electron.

This arrangement of a small superconducting loop closed by a Josephson junction is the basic form of the SQUID. Since this device is the heart of the whole system, we will analyze its properties a little further, following Silver and Zimmerman [2].

The total magnetic flux ϕ linking the loop is the sum of two terms

$$\phi = \phi_x + LI_s \tag{3}$$

where ϕ_x is the flux from some external source driving the device and L is the inductance of the loop. Strictly speaking, the current I_s in (3) is the total current (including leakage, etc.) flowing through the junction. However, SQUID's are usually designed so that the Josephson current (1) is the dominant term; thus we may obtain an approximate understanding of the action of the device by neglecting the other contributions to the current. We may therefore combine (1) and (3):

$$\phi = \phi_x + LI_c \sin (2\pi\phi/\phi_0) \qquad (4)$$

or, alternatively,

$$I_s = I_c \sin [2\pi(\phi_x + LI_s)/\phi_0]. \qquad (5)$$

Inspection of (5) shows that the current I_s has a periodic dependence on the external magnetic flux ϕ_x. If we add any whole multiple of ϕ_0 to ϕ_x, the sine function is unchanged and therefore the current I_s is unchanged also. Remembering that the EMF V around the loop is just $d\phi/dt$, we can see that the device presents a nonlinear impedance to alternating current which is also a periodic function of the applied magnetic flux ϕ_x.

The standard technique for using a SQUID as a sensor of magnetic flux is to monitor this variation in impedance by coupling the device inductively to a readout circuit operating at some convenient radio frequency, as shown in Fig. 1 [2]–[4]. (These references give the details of readout circuits operating at 30 MHz and the output signals that can be obtained). In any circuit with stable geometry the magnetic flux ϕ_x is proportional to the current I. The flux quantum is therefore a natural repeating unit with which to measure current. The periodic response of the impedance of the SQUID to variations of magnetic flux driven by the current I in this circuit is monitored by a microwave system which detects variations in the microwave reflection coefficient of the SQUID.

The basic response of a SQUID system to the current to be measured is displayed in Fig. 2. This is an oscilloscope display obtained with a slowly varying current I. Monitored in this way, the periodic response of the SQUID to magnetic flux has degenerated into a simple and remarkably pure sine function.

When the input current I is an RF current, the system records an average over a segment of Fig. 2. The width of the segment is determined by the amplitude of the RF current, and its location can be moved by simultaneously applying a dc bias current. As the amplitude of the RF current varies, this averaged response reflects the basic periodicity of the SQUID. This is shown in Fig. 3, which is an oscilloscope display obtained by applying a slow amplitude modulation to an RF current at 65 MHz applied to the SQUID. In the approximation, the basic response to current shown in Fig. 2 is a sine function $\sin (2\pi I/I_0)$, and the averaged response to RF current shown in Fig. 3 can be shown to be the zero-order Bessel junction $J_0(2\pi I/I_0)$ [1]. In both expressions I_0 is the current required to drive one quantum of magnetic flux into the SQUID. It may be determined with a single

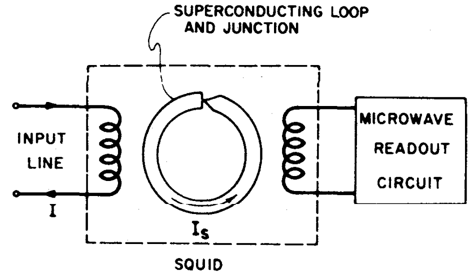

Fig. 1. Basic SQUID system, defining components and currents.

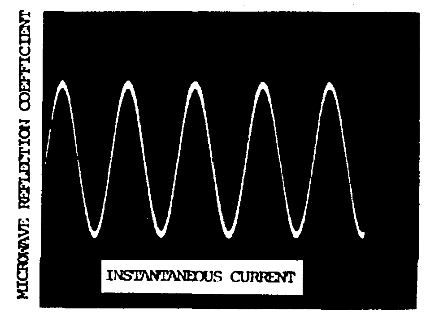

Fig. 2. Basic microwave reflection coefficient response to slow variations in input current I.

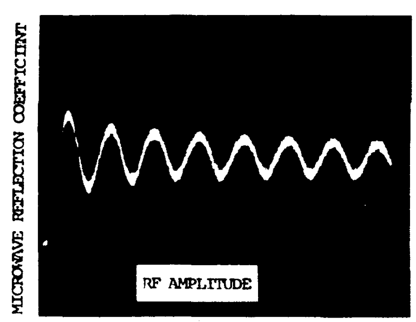

Fig. 3. Averaged microwave reflection coefficient response to a slowly modulated RF input current I.

measurement using dc. Notice that the frequency does not enter explicitly into these expressions.

B. Physical Configuration

Figs. 4 and 5 show a drawing and a photograph, respectively, of the L-band SQUID used in this work. It is a reentrant cavity that resonates at 1.2 GHz with a loaded Q of about 25. The coffin-like shape was chosen to facilitate packing multiple SQUID's into a confined space in a small cryostat. The microwave readout system contains L-band components connected via 50-Ω coaxial line. It is critically coupled to the cavity of the SQUID. The signal at 30 MHz to be measured is coupled in via a 3-turn coil terminated by a 50-Ω load connected directly to the SQUID. It requires 10 μA to induce a magnetic flux of one quantum. We chose this value of I_0 for a convenient power level for measuring attenuation; it can be adjusted over a range of about 20 dB by changing the number of

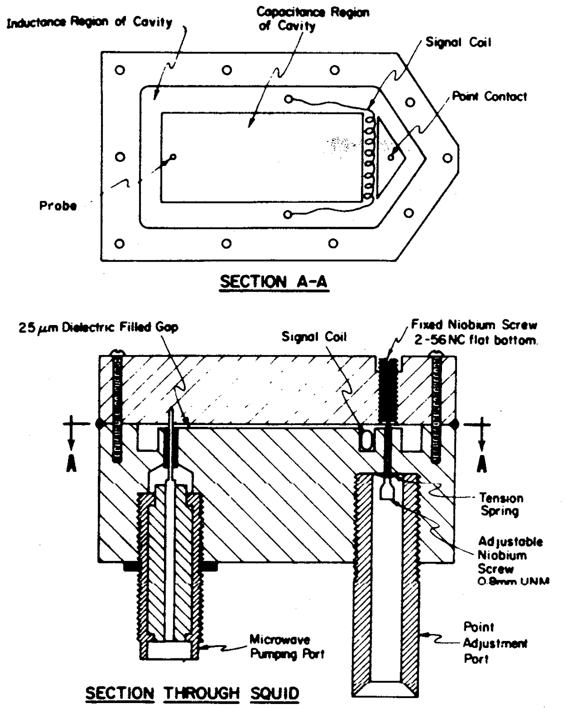

Fig. 4. Resonant L-band SQUID. This is a reentrant cavity with the point contact and the microwave coupling placed at points chosen to match impedances.

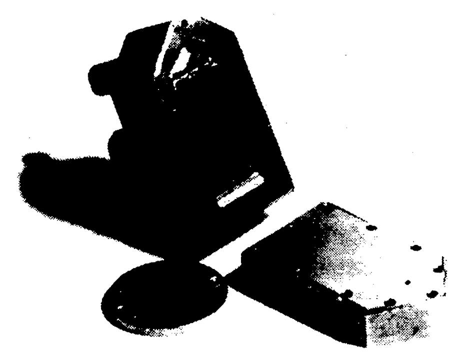

Fig. 5. Resonant L-band SQUID, showing RF input coupling coil and connection for microwave drive.

turns on the coil. This SQUID generates readout signals close to the theoretical optimum power (2 pW).

The two halves of this SQUID are made of solid Babbitt alloy (4.5-percent Sn, 10.5-percent Sb, and 85-percent Pb) for ease of fabrication. It is superconducting at approximately 8 K. The finished SQUID must resonate within the passband of the readout circuit at 1.2 GHz. This can be accomplished by trimming the metal parts or the dielectric spacer. This SQUID was machined by a computer-controlled milling machine.

The SQUID is assembled by bolting the two halves together. The joint is then sealed (electrically) with Rose's metal (50-percent Bi, 25-percent Pb, 25-percent Sn) applied with a soldering iron with no flux.

Three SMA connectors are soldered to the body of the SQUID with Rose's metal which is superconducting at approximately 8.5 K. Two of these are wired to the signal coil; while the third, which carries the L-band drive, is connected across the dielectric (polyimide plastic) gap to the opposite side of the cavity. This is most conveniently done by attaching a copper pin to the center conductor of the SMA connectors and pressing a matching socket into the lid of the SQUID. A suitable socket may easily be obtained by taking the center conductor out of a female SMA connector.

The point contact is between a sharp-tipped 0.8-mm UNM screw and a plated niobium foil, 1 mm by 2 mm by 0.02 mm, both plated with a Pt–W alloy, as illustrated in Fig. 6. The niobium foil is spot welded to a 2-56 NC niobium screw. This passes through the lid of the SQUID and should be held in place by a lock nut. The small 0.8-mm niobium screw passes through the main body of the SQUID. The far end is flattened to the shape of a screwdriver, which engages with a removable adjusting rod in a guide tube passing out through the top plate of the cryostat. A small leaf spring takes up the backlash of the screw when the drive is disconnected.

These junctions can survive electrostatic discharges 100 times greater than that which would burn out an uncoated (unplated) point contact of the same configuration. They behave electrically like an uncoated point contact with a shunt resistance of about 0.1 Ω. This does not noticeably degrade the readout signal obtainable from SQUID's at frequencies ranging from 30 MHz to 9 GHz. It brings the bonus of a tendency to increase the purity of the sine-functional form of the basic response shown in Fig. 1, thereby improving the convenience and accuracy of RF measurements with these devices [1].

III. MEASUREMENT SYSTEM

The system as shown in Fig. 7 can be used to measure variations in attenuation with no conventional calibration standard. A stable signal generator is connected to the SQUID through the variable attenuator under test,

The SQUID is inductively coupled to the center conductor of a 50-Ω coaxial line, which passes through the SQUID. Variations in the current flowing in this line cause variations in the magnetic flux linking the superconducting loop formed by the Josephson junction and the end of the cavity. Because of quantum mechanical interference, the microwave reflection coefficient of the device is sensitive to these variations in magnetic flux. For attenuation measurements, one end of the coaxial line is terminated with a 50-Ω load, and the other is connected to the RF system on which measurements are to be made.

Fig. 7 shows the basic layout of the components used to realize this system. The microwave system is driven by an L-band signal generator delivering a few nanowatts of power to the 20-dB directional coupler. The power level at the SQUID is therefore of order 10^{-11} W. The reflected microwave signal is amplified by a solid-state amplifier, with a gain of about 50 dB, and rectified by a crystal diode detector. This millivolt level signal is applied to the lock-in detector, where it is amplified to an operating

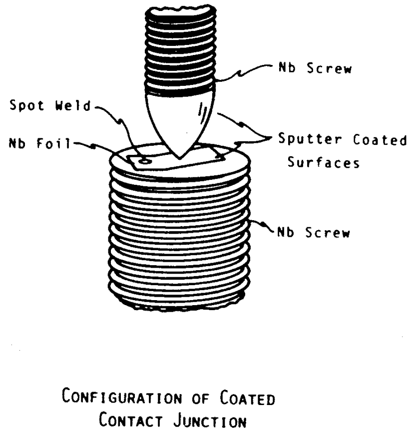

Fig. 6. Stabilized point contact. This is a spring-loaded contact between niobium parts plated with a Pt–W alloy.

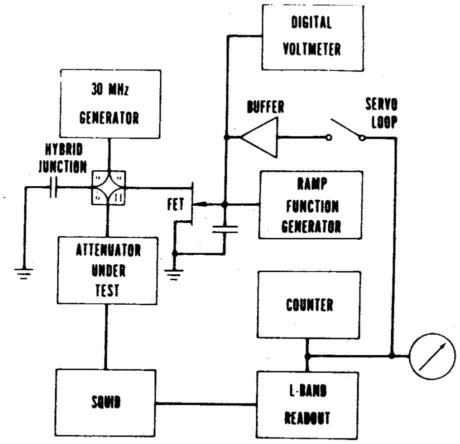

Fig. 8. System for automatic counting of nulls and interpolation between nulls.

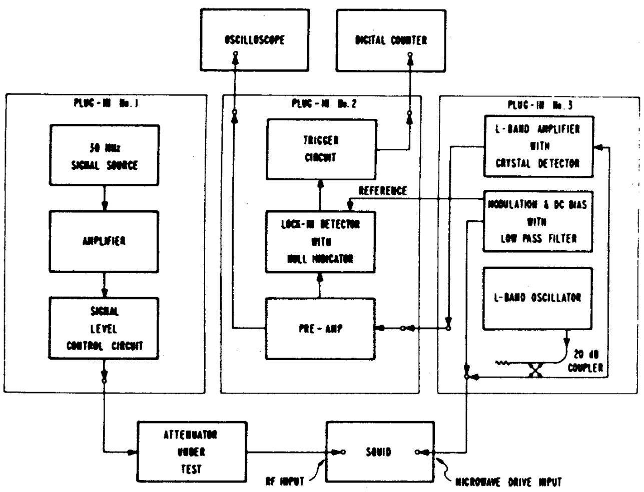

Fig. 7. Basic system for measuring RF attenuation showing modular packaging.

level of a few volts. An oscilloscope is used to monitor the dc bias and modulation levels in the SQUID. The modulation is a 1-kHz sine wave. Modulation and dc bias are applied to the SQUID via a low-pass filter connected to the RF line. This must pass the bias and modulation, but present at least 60 dB of attenuation to signals at 30 MHz. The high degree of attenuation is required to prevent crosstalk between the microwave and measuring channels: some of the low-frequency components are mounted in common boxes, which presents possible paths around the attenuator under test. Bias and modulation levels are of the order of 10^{-7} A at the SQUID.

The 30-MHz source is a crystal-controlled solid-state oscillator. An amplifier of comparable stability raises this level to the maximum permitted by the attenuator under test. All connections are made with semirigid coaxial line (with solid conductors) or double-shielded flexible coaxial line (with braided conductors). With this precaution and some care with connectors, leakage does not appear to be a significant problem.

The null indicator on the lock-in detector is used to locate the nulls of the response function $J_0(2\pi I/I_0)$ as the attenuator under test is adjusted. The system is set on a sequence of these nulls, and the reading of the attenuator dial is noted at each null. The dial readings are then compared with attenuation ratios calculated with a table of Bessel functions.

To eliminate the tedious task of counting the nulls visually by watching the null indicator, a semiautomatic system was devised for counting the nulls, as well as interpolating between them. This system is shown in Fig. 8. Nulls are counted by a counter, driven by the lock-in detector in the L-band readout system, as the incident power is slowly reduced from the working level to a very low level. The incident power is then restored to its working level and a servo loop is closed to lock it to the nearest null. The servo voltage is measured by a digital voltmeter, which can be calibrated against the corresponding small change in power level with sufficient accuracy for interpolation between nulls. The circuit for controlling the power level was developed after trying several commercial voltage-variable attenuators and modulators, which were rejected because of their high insertion loss and inconvenient control voltage characteristics. This circuit is also shown in Fig. 8. It consists of a well-balanced 180° hybrid junction with a field-effect transistor acting as a variable termination on one of the side ports.

When the gate of the transistor is held at ground potential, the two side arms of the hybrid junction are extremely unbalanced, so their reflections combine constructively and the device transmits power with less than 3-dB attenuation. When a large negative bias is applied to the gate of the transistor, its conductance is shut off and it presents an impedance consisting mainly of the capacitance between channel and gate. This is balanced by a small capacitor terminating the opposite port, so that the two signals cancel and the transmitted RF power is attenuated by 60 dB. At intermediate bias levels there is a convenient linear relationship between bias voltage and transmitted RF voltage over a large part of the range

Fig. 9. Complete 30-MHz attenuation measurement system including the attenuator under test.

of attenuation, enabling nulls in the response of the SQUID to be counted at a steady rate when the bias voltage on the gate of the transistor is varied as a simple linear function of time. Because of the high RF level (0.25 W), the transistor does draw significant gate current, which introduces harmonic distortion at intermediate bias levels. However, this does not appear to interfere with counting, and precise settings are always made with the gate at ground potential (i.e., the condition of maximum RF signal transmission). The servo loop to interpolate between nulls does not yet function satisfactorily, and refinement of the frequency response will be required to minimize the noise in the system before we will be able to evaluate the accuracy of interpolation.

The cryostat [5] is made of glass, with two copper radiation shields in the vacuum space between the inner and outer walls. These shields are attached to the inner wall near the neck, so that the escaping helium gas cools them. The interstices between them and the walls are filled with several layers of aluminized polyester film, for additional radiation baffles. No liquid nitrogen cooling jacket is required. Starting with a warm system, a day's running including the initial cool down requires about 2 l of liquid helium. Fig. 9 shows the complete compact system.

IV. ATTENUATION MEASUREMENTS

This system is capable of matching the accuracy of existing methods of measuring attenuation at 30 MHz such as the National Bureau of Standards (NBS) Calibration Service using a piston attenuator. However, achieving this accuracy requires careful attention to setting the optimum operating conditions.

The basic source of systematic error is a deviation in the response of the SQUID and its readout circuit to RF current from the simple form $J_0(2\pi I/I_0)$. This is caused by harmonic distortion of the simple sinusoidal response of the system to direct current. The complete distortion analysis is found in Section VI.

A routine has been developed for initial adjustment of the system to minimize systematic errors. A minicomputer has been programmed to analyze experimental data and list and plot the results of calibration runs.

The procedure for system setup is as follows.

1) Adjust the contact pressure at the Josephson junction until maximum signal occurs at a microwave power level not exceeding −80 dBm at the SQUID.

2) Adjust the dc bias level and make fine adjustments to the microwave power level until the reflected microwave signal appears exactly symmetrical on an oscilloscope display such as Fig. 2. Tests with a spectrum analyzer have shown that this has the effect of eliminating even-order (i.e., second, fourth, etc.) harmonic distortion.

3) With a digital ac voltmeter, observe the modulation depth which just nulls out the desired signal and set the modulation depth at exactly one-third of that level. This nulls out the effect of third harmonic distortion.

After using this procedure, the systematic errors in measurements with the system are usually less than ± 0.01 dB at the first null, less than ± 0.005 dB at the second null, less than ± 0.003 dB at the third null, and negligibly small (compared with random setting errors) thereafter. Errors exceeding these amounts can usually be traced either to external interference or to violation of one of the rules in the setup procedure. Random errors have been consistently less than ± 0.002 dB rms.

Measurements were extended to cover the first 900 nulls in the response of the SQUID system which provides a dynamic range of nearly 62 dB. The accuracy obtainable with the last 800 nulls appears to be as good as with the first 100. The tedium of counting was eliminated by using an electronic system to count from one measured setting to the next.

For the greatest accuracy, the first and second nulls in the response of the SQUID system can be ignored, at the sacrifice of 11 dB in dynamic range. The remaining 898 nulls would then cover a dynamic range of 50 dB with confidence that systematic errors are less than ± 0.002 dB.

The procedure for calibrating an attenuator is to note the readings on its dial corresponding to a sequence of nulls of the response of the SQUID. A simple computer program compares these readings with attenuation ratios calculated from a table of Bessel functions and prints out the deviations.

V. MEASUREMENT RESULTS

An NBS model VII piston attenuator was used for testing this SQUID system. This attenuator was first calibrated by the NBS Calibration Service and then used in a series of tests with the new SQUID system. With everything adjusted properly, the results illustrated in Fig. 10 were obtained. This is a plot of the deviation from actual attenuation versus dial setting for the piston attenuator, representing the results of the average of three separate calibration runs on each system. The dots represent measurements made with the SQUID, while the crosses at 5-dB intervals represent the information supplied by the NBS Calibration Service. The estimated limits of error of the NBS Calibration Service [6] are represented by divergent lines that are drawn symmetrically with respect to the abscissa for convenience. These

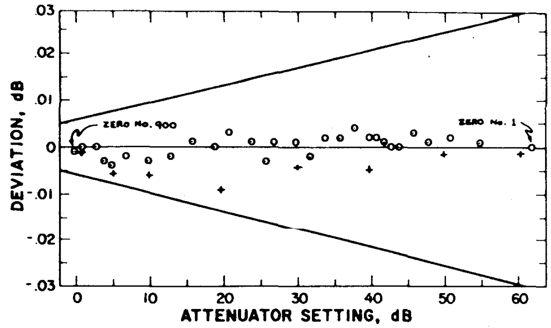

Fig. 10. Comparison of the calibration of a variable attenuator using the SQUID system (dots) with the NBS Calibration Service (crosses). The solid lines represent the estimated limits of error of the NBS Calibration Service.

lines illustrate the relationship between the measurement results and the error limits.

The average rms deviation of the first three measurements at each point taken by the NBS Calibration Service was ± 0.0011 dB. The rms deviation of the measurements taken with the SQUID from a smooth curve drawn through the calibration points was ± 0.0017 dB, the major contribution coming from the last two points at high attenuation. These correspond to the first and second nulls of the response of the SQUID, which are the most prone to errors due to harmonic distortion. On the other hand, the power level in the NBS calibrating system is raised at 50 dB to a higher level for measuring high attenuation. This is known to increase the systematic error in the range above 50 dB. Apart from these considerations based on previous knowledge of the idiosyncrasies of the two systems, the difference in scatter between the two sets of measurements is not statistically significant in such a small number of samples.

The most obvious feature of Fig. 10 is the large discrepancy between the estimated limits of the systematic error of the NBS calibration and the degree of agreement between the two entirely independent methods of measuring attenuation. Clearly, the estimated errors are very conservative, but so long as one accepts them it is difficult to say which system is testing which. We hope that after further careful comparison of measurements made by the two systems it will be possible to revise the estimate of errors and issue reports of calibration giving better justice to the quality of the measurements that are actually made.

VI. ANALYSIS OF SYSTEMATIC ERRORS

The measurements described are based on the assumption that the instantaneous response of the microwave system to current through the SQUID has the pure sinusoidal form expressed in (6),

$$P = P_0 + P_1 \cos(2\pi I/I_0) \qquad (6)$$

where P is the microwave power reflected from the SQUID. Let us now entertain the notion that this is not a perfectly accurate assumption [7].

First, we replace (6) by

$$P = P_0 + \sum_n P_n \cos(2\pi n I/I_0) \qquad (7)$$

to allow for harmonic distortion of the response. Next, we recognize that the current I has several components,

$$I = I_B + I_M \sin(2\pi f_M t) + I_1 \cos(2\pi f t). \qquad (8)$$

The first term is the dc bias, the second term is the modulation ($f_M = 1$ kHz), and the third term is the RF input to be measured ($f = 30$ MHz for the measurements reported in the previous section). Combining (7) and (8), and taking a time average over the excursions of the RF component I_1, we find that the amplitude V_M of the voltage presented to the lock-in detector at frequency f_M is

$$V_M = 2G \sum_n P_n \sin(2\pi n I_B/I_0) J_1(2\pi n I_M/I_0) J_0(2\pi n I_1/I_0) \qquad (9)$$

where G is the response of the microwave crystal rectifier (in volts per watt).

Inspection of (9) reveals that the effect of harmonic distortion of the basic response of the system [(7)] on the time-averaged response to RF current is to mix in some zeroth-order Bessel functions of multiple argument. The coefficients of these extra terms are functions of both the dc bias level and the depth of modulation, so we can manipulate them by a proper choice of these parameters. In practice we observe that the leading term P_2 appears to dominate the distortion, and this can be eliminated exactly by setting $I_B = 0.25 I_0$ and $I_M = 0.305 I_0$. The presence of this distortion can be detected immediately because it affects the odd and even null points differently. In particular, a small second harmonic distortion moves the odd and even null points by approximately equal amounts in opposite directions. This will become obvious on a plot similar to Fig. 10, since the odd and even null points will separate into distinct branches.

We always observe some distortion of this kind, and adjust the bias level and modulation depth to null it out. The results displayed in Fig. 10 give us confidence that when the odd and even nulls are consistent with each other this source of error is essentially eliminated.

The other prime source of systematic error lies in the relationship between the RF current to be measured and the magnetic flux to which the SQUID actually responds. This depends upon a geometrical factor, which may be perturbed by variations in the distribution of the electromagnetic field with changes in frequency and (to a much smaller extent) intensity. One major advantage of superconducting metals is that the penetration depth for electromagnetic fields is small ($\sim 10^{-7}$ m) and insensitive to frequency through the radio and microwave range. The penetration depth is also slightly sensitive to the intensity of the field, but this effect is negligible at the level of precision of most measurements at radio frequencies. At frequencies sufficiently high so that the linear dimensions of the SQUID become a significant fraction of the wavelength, it is necessary to consider the effect of standing waves on the distribution of the fields. This may become significant for measurements with swept frequency extending into the low microwave range. Corrections to a calibration performed with direct current are calculable and would be of the order of 1 percent at 1 GHz. These corrections do not affect measurements of attenuation conducted at a fixed frequency.

VII. CONCLUSIONS

We have shown that, over a dynamic range of 62 dB, a SQUID can be used to calibrate an attenuator in agreement with the NBS Calibration Service to within ±0.002 dB rms. The measurements were made at 30 MHz because the piston attenuator used as a transfer standard is a narrow-band device. The SQUID could be used equally well at any frequency from zero to over 1 GHz [8].

We believe that when this system is fully developed it will be a strong contender for the position of primary standard of attenuation. This work is continuing, with the aim of making further refinements and extensions of these systems.

ACKNOWLEDGMENT

The authors wish to thank their colleagues, N. V. Frederick, J. E. Zimmerman, and D. B. Sullivan for their contributions to this work.

REFERENCES

[1] R. A. Kamper, M. B. Simmonds, C. A. Hoer, and R. T. Adair, "Measurement of rf power and attenuation using superconducting quantum interference devices," Nat. Bur. Stand., Tech. Note 643, pp. 12–63, Aug. 1973.

[2] A. H. Silver and J. E. Zimmerman, "Quantum states and transitions in weakly connected superconducting rings," *Phys. Rev.*, vol. 157, no. 2, p. 317, 1967.

[3] J. E. Zimmerman, P. Thiene, and J. T. Harding, "Design and operation of stable rf-biased superconducting point-contact quantum devices and a note on the properties of perfectly clean metal contacts," *J. Appl. Phys.*, vol. 41, no. 4, p. 1572, 1970.

[4] D. B. Sullivan, "Superconducting quantum interference devices: An operational guide for rf-biased systems," Nat. Bur. Stand., Tech. Note 629, pp. 3–10, Nov. 1972.

[5] J. E. Zimmerman and J. D. Siegworth, "Portable helium dewars for use with superconducting magnetometers," *Cryogenics*, vol. 13, p. 158, 1973.

[6] "Calibration and test services of the National Bureau of Standards," Nat. Bur. Stand., Spec. Publ. 250, Dec. 1970.

[7] R. A. Kamper, M. B. Simmonds, R. T. Adair, and C. A. Hoer "Quantum mechanical measurement of RF attenuation," *Proc. 1972 Applied Superconductivity Conf.*, pp. 696–700.

[8] ——, "A new technique for RF measurements using superconductors," *Proc. IEEE* (Lett.), vol. 61, pp. 121–122, Jan. 1973.

9.4 Appendix D

Excerpts from Reference 17.

COMITÉ INTERNATIONAL DES POIDS ET MESURES

COMITÉ CONSULTATIF D'ÉLECTRICITÉ

15ᵉ SESSION – 1978
(13-14 septembre)

BUREAU INTERNATIONAL DES POIDS ET MESURES
Pavillon de Breteuil, F-92310 SÈVRES, France
Dépositaire : OFFILIB, 48 rue Gay-Lussac, F-75005 Paris

TABLEAU I

Etalon voyageur NML S60255

Numéro	Laboratoire	Date des mesures	Valeur mesurée (en dB)	Ecart-type de la moyenne (en dB)	Erreur systématique estimée (en dB)	Température (°C)	Méthode
1	NML	mars 1975	3,000 7	0,000 1	± 0,002 3	22	Affaiblisseur à onde évanescente, substitution parallèle.
2	NBS	mai 1975	3,001	0,000 4	± 0,002	23	Affaiblisseur à onde évanescente, substitution série.
3	NRC	juillet 1975	3,000 6	< 0,000 1	± 0,001	22	Diviseur inductif à 10 kHz, substitution série.
4	NML	juillet 1975	3,000 6	0,000 15	± 0,002 3	22	Affaiblisseur à onde évanescente, substitution parallèle.
5	ETL	mars 1976	3,001	0,001	± 0,002	22	-id.-
6	NPL	janvier 1977	2,983 1	0,000 05	± 0,000 16	24	Affaiblisseur à onde évanescente.
7	NML	mars 1977	3,000 78	0,000 02	± 0,002 3	22	Affaiblisseur à onde évanescente, substitution parallèle.
8	FOA	mai 1977	3,021	0,001 9	± 0,01	20,5	Affaiblisseur à onde évanescente.
9	OMH	Août 1977	3,001 15	0,000 03	± 0,003	22	Substitution audiofréquence à deux canaux et substitution parallèle à fréquence intermédiaire.
10	PTB	mars 1978	3,001 3	0,000 04	± 0,003	23	Mesure de puissance
11	NML	mai 1978	3,001 02	0,000 02	± 0,002 3	22	Affaiblisseur à onde évanescente, substitution parallèle.

TABLEAU II

Etalon voyageur NML S60256

Numéro	Laboratoire	Date des mesures	Valeur mesurée (en dB)	Ecart-type de la moyenne (en dB)	Erreur systématique estimée (en dB)	Température (°C)	Méthode
1	NML	mars 1975	6,039 2	0,000 1	± 0,002 6	22	Affaiblisseur à onde évanescente, substitution parallèle.
2	NBS	mai 1975	6,041	0,000 2	± 0,003	23	Affaiblisseur à onde évanescente, substitution série.
3	NRC	juillet 1975	6,042 1	< 0,000 1	± 0,001	22	Diviseur inductif à 10 kHz, substitution série.
4	NML	juillet 1975	6,040 0	0,000 15	± 0,002 6	22	Affaiblisseur à onde évanescente, substitution parallèle.
5	ETL	mars 1976	6,043	0,001	± 0,003	22	-id.-
6	NPL	janvier 1977	6,016 3	0,000 9	± 0,000 22	24	Affaiblisseur à onde évanescente.
7	NML	mars 1977	6,040 39	0,000 02	± 0,002 6	22	Affaiblisseur à onde évanescente, substitution parallèle.
8	FOA	mai 1977	6,046	0,001 6	± 0,01	20,5	Affaiblisseur à onde évanescente.
9	OMH	août 1977	6,039 14	0,000 05	± 0,005	22	Substitution audiofréquence à deux canaux et substitution parallèle à fréquence intermédiaire.
10	PTB	mars 1978	6,040 7	0,000 07	± 0,003	23	Mesure de puissance
11	NML	mai 1978	6,040 83	0,000 02	± 0,002 6	22	Affaiblisseur à onde évanescente, substitution parallèle.

TABLEAU III

Etalon voyageur NML S60257

Numéro	Laboratoire	Date des mesures	Valeur mesurée (en dB)	Ecart-type de la moyenne (en dB)	Erreur systématique estimée (en dB)	Température (°C)	Méthode
1	NML	mars 1975	10,020 9	0,000 1	± 0,003	22	Affaiblisseur à onde évanescente, substitution parallèle.
2	NBS	mai 1975	10,022	0,000 3	± 0,004	23	Affaiblisseur à onde évanescente, substitution série.
3	NRC	juillet 1975	10,022 7	< 0,000 1	± 0,001	22	Diviseur inductif à 10 kHz, substitution série.
4	NML	juillet 1975	10,021 3	0,000 23	± 0,003	22	Affaiblisseur à onde évanescente, substitution parallèle.
5	ETL	mars 1976	10,024	0,001	± 0,003	22	-id.-
6	NPL	janvier 1977	9,993 4	0,000 05	± 0,000 3	24	Affaiblisseur à onde évanescente.
7	NML	mars 1977	10,022 3	0,000 01	± 0,003	22	Affaiblisseur à onde évanescente, substitution parallèle.
8	FOA	mai 1977	10,025	0,002 2	± 0,015	20,5	Affaiblisseur à onde évanescente.
9	OMH	août 1977	10,028 4	0,000 1	± 0,01	22	Substitution audiofréquence à deux canaux et substitution parallèle à fréquence intermédiaire.
10	PTB	mars 1978	10,024 2	0,000 11	± 0,003	23	Mesure de puissance.
11	NML	mai 1978	10,022 7	0,000 02	± 0,003	22	Affaiblisseur à onde évanescente, substitution parallèle.

TABLEAU IV

Etalon voyageur NML S60258

Numéro	Laboratoire	Date des mesures	Valeur mesurée (en dB)	Ecart-type de la moyenne (en dB)	Erreur systématique estimée (en dB)	Température (°C)	Méthode
1	NML	mars 1975	19,716 5	0,000 1	± 0,004	22	Affaiblisseur à onde évanescente, substitution parallèle.
2	NBS	mai 1975	19,718	0,000 2	± 0,008	23	Affaiblisseur à onde évanescente, substitution série.
3	NRC	juillet 1975	19,717 9	< 0,000 1	± 0,002	22	Diviseur inductif à 10 kHz, substitution série.
4	NML	juillet 1975	19,717 1	0,000 15	± 0,004	22	Affaiblisseur à onde évanescente, substitution parallèle.
5	ETL	mars 1976	19,724	0,001	± 0,006	22	-id.-
6	NPL	janvier 1977	19,684 8	0,000 05	± 0,000 5	24	Affaiblisseur à onde évanescente.
7	NML	mars 1977	19,716 2	0,000 04	± 0,004	22	Affaiblisseur à onde évanescente, substitution parallèle.
8	FOA	mai 1977	19,735	0,002 5	± 0,03	20,5	Affaiblisseur à onde évanescente.
9	OMH	août 1977	19,740 2	0,000 2	± 0,02	22	Substitution audiofréquence à deux canaux et substitution parallèle à fréquence intermédiaire.
10	PTB	mars 1978	19,718 1	0,000 4	± 0,005	23	Mesure de puissance.
11	NML	mai 1978	19,714 9	0,000 07	± 0,004	22	Affaiblisseur à onde évanescente, substitution parallèle

TABLEAU V

Etalon voyageur NML S60259

Numéro	Laboratoire	Date des mesures	Valeur mesurée (en dB)	Ecart-type de la moyenne (en dB)	Erreur systématique estimée (en dB)	Température (°C)	Méthode
1	NML	mars 1975	39,492 5	0,000 2	± 0,006	22	Affaiblisseur à onde évanescente, substitution parallèle.
2	NBS	mai 1975	39,498	0,000 5	± 0,016	23	Affaiblisseur à onde évanescente, substitution série.
3	NRC	juillet 1975	39,494 1	< 0,000 1	± 0,005	22	Diviseur inductif à 10 kHz, substitution série.
4	NML	juillet 1975	39,491 6	0,000 23	± 0,006	22	Affaiblisseur à onde évanescente, substitution parallèle.
5	ETL	mars 1976	39,502	0,002	± 0,01	22	-id.-
6	NPL	janvier 1977	39,451 9	0,000 05	± 0,000 9	24,1	Affaiblisseur à onde évanescente.
7	NML	mars 1977	39,489 2	0,000 04	± 0,006	22	Affaiblisseur à onde évanescente, substitution parallèle
8	FOA	mai 1977	39,559	0,002 2	± 0,04	20,5	Affaiblisseur à onde évanescente.
9	OMH	août 1977	39,473	0,003	± 0,03	22	Substitution audiofréquence à deux canaux et substitution parallèle à fréquence intermédiaire.
10	PTB	mars 1978	39,490 6	0,000 35	± 0,02	23	Mesure de puissance.
11	NML	mai 1978	39,485 9	0,000 1	± 0,006	22	Affaiblisseur à onde évanescente, substitution parallèle.

9.5 Appendix E

Drawings of System Components.